Driver-passenger synchrony: The identification of synchrony in head orientation and movement

Lauren Ickenroth

TU Delft

Driver-passenger synchrony: The identification of synchrony in head orientation and movement

by

Lauren Ickenroth

to obtain the degree of Master of Science in Mechanical Engineering
at the Delft University of Technology,
to be defended on Friday October 29, 2021 at 14:00

Student number:	4340485	
Department:	Cognitive Robotics	
Thesis committee:	Dr. ir. J. C. F. de Winter,	TU Delft, supervisor
	Dr. P. Bazilinskyy,	TU Delft, supervisor
	Ir. T. Driessen,	TU Delft, supervisor
	Dr. ir. R. Happee	TU Delft

Acknowledgements

This master’s thesis marks the end of the most challenging year of my life so far. My ambition when I started this master's program two and a half years ago was to complete my graduation project at a prominent automotive company in Germany or England. Unfortunately, this was not possible due to COVID-19 and a difficult home situation. Graduating during COVID-19 was quite challenging for me. Graduating, which is already a very independent process, became a lonely process. Working together with other students is something that I have missed a lot during this project. But here we are, close to the finish. With hard work, this project, which often felt like a battle, is almost finished.

My supervisors and I came up with the idea for this master's thesis, which is on driver passenger synchrony. This thesis is based on real-world driving data from a previously conducted experiment at the TU Delft by Cabrall et al. (2018). The data from this study has provided a good starting point for the current study.

First, I would like to thank my supervisors, Joost de Winter, Pavlo Bazilinskyy and Tom Driessen. Without the assistance of my supervisors, the outcome of this research would not have been possible. I want to thank them for their guidance during this project. They were always available and responded quickly. Also, I would like to thank them for reading and re-reading my report and providing critical comments. Most of all, I would like to thank them for giving me space and freedom after the loss of my father.

Furthermore, I want to thank my family and friends for their support. Special thanks to my father, who taught me so much. Two years ago, I was informed that my father was seriously ill but with a good chance to recover. However, after one and a half years of fighting, his illness proved invincible. He would have been so proud that I had worked so hard to achieve our goal. Additionally, I want to thank my mother, who is always there for me—no one who understands better and knows me as well as she does. The last year she showed me that continuing in such a difficult time can be enough. Finally, I would like to thank my friend Reinier. Without him, I wouldn’t be here now. The support he has provided over the last year is priceless. He has always believed in me and gave me confidence that everything will work out.

After more than seven years of studying with a difficult final year I am ending this period of my life, and I am looking forward to a new fresh start.

Contents

Abstract

The presence of a passenger can affect driver safety positively or negatively. Therefore gaining a better understanding of the nature of this interaction with a passenger is crucial. Additionally, drivers and passengers acquire nearly identical visual information from the driving scene. As a result, synchronised behaviour may occur. The driver-passenger synchrony may provide additional information on driver-passenger interactions. This led to the aim of the current study: The identification of synchrony in head orientation and movement between drivers and passengers for various road types and cornering events. This study was based on real-world driving data. The head angle (orientation) and angular velocity (movement) of all three principal axes (pitch, roll, and yaw) were analysed for synchrony.

The following methods were applied for the identification of driver-passenger synchrony. The head angles of drivers and passengers were detected using OpenFace 2.0, a video-based pose estimation method. Second, the windowed cross-lagged correlation (WCLC), a linear approach for synchrony identification, was applied. Next, two distinct facets of synchrony were measured. The first facet was determining the frequency of synchrony derived by the peak-picking algorithm developed by Altmann (2013). The frequency of synchrony was summarised as the percentage of synchrony that occurred over the measured road segment. The second facet of synchrony studied was the strength of synchrony with the help of the peak-picking algorithm developed by Boker et al. (2002). This peak-picking algorithm searches for the maximum peak correlation at every window of the WCLC. Then all maximum peak correlations were averaged into a single mean peak correlation per road segment or cornering event. Since behavioural synchrony could appear by chance, the results of the peak-picking algorithms were compared to pseudosynchrony. The first hypothesis states that it is possible to distinguish detected synchrony from pseudosynchrony of driver's and passenger's head angle and angular velocity. Secondly, it is hypothesised that more synchrony is detected in the urban road type than outside built-up areas- and highway road types.

The results showed that differentiation between the detected synchrony and pseudosynchrony could be made for the analysis on the total route for almost all head angles and angular velocity for the frequency- and strength of synchrony. Furthermore, the analysis on the different road types, revealed that the identified synchrony could be differentiated from pseudosynchrony for almost all urban road segments. The findings on the other road types were mixed. It can be concluded from these research results that synchronisation has been identified for the urban road type. The road types where the detected synchrony was not significantly different from pseudosynchrony could indicate that there was no synchrony present or that the applied methods were unable to capture the driver-passenger synchrony. Synchrony identification in cornering events revealed no observable patterns. As a result, no conclusions on the cornering events could be formed. The second hypothesis could only be tested for one condition, since the identified synchrony could not be differentiated from pseudosynchrony for all the required road types for the second hypothesis. The result showed no significant difference between the urban road type compared to the built-up areas and highway road types for the pitch–angular velocity.

According to this study, drivers and passengers exhibited synchronisation in their head orientations and movements along particular road segments. However, more research is needed to truly comprehend the synchronised behaviour of drivers and passengers. A good place to start is for a study that looks into the relation between synchronous behaviour and the impact on driver safety as a result of the passenger's presence.

Introduction

Driver distraction reduces road safety and is the cause of many accidents [1]. Former research revealed that the most common cause of driving distraction is the interaction with a passenger [2], [3]. The interaction between humans has been thoroughly studied. An essential factor of social interaction is synchrony [4]. Mayo and Gordon [5] cited interpersonal synchrony as "the spontaneous rhythmic and temporal coordination of actions, emotions, thoughts and physiological processes between two or more participants". The timing of behaviour, movement and speech is critical for achieving interpersonal synchrony. There are various interpretations of synchrony. Behavioural synchrony can consist of identical or similar behaviour. But also complementary behaviour, such as turn-taking when talking, can be seen as synchronous behaviour [5]. Several factors influence synchrony, for instance, the environment. Former research shows that when two humans are exposed to similar visual information, spontaneous phase synchrony, unintentional in-phase coordinated behaviour can emerge [6]. Since drivers and passengers interact and experience the same visual information from the driving scene, synchronous behaviour could emerge.

A passenger in the vehicle can directly affect the driver by interacting with the driver and indirectly due to social norms and expectations conveyed by the presence of a passenger. However, this passenger presence could positively impact safety depending on several factors, such as the passenger warning the driver of impending dangers [7]. Factors indicating whether the passenger influences the driver positively or negatively are the relationship between driver and passenger, gender, peer pressure, age and driving conditions [7], [8]. Investigation of single-vehicle accidents showed adult drivers are positively influenced by the presence of passengers, while on the other hand, young drivers are negatively affected by their presence [9], [10]. Driving safety improved when a young driver was accompanied by a passenger with driving experience, who provided comments regarding safety. This effect remained when driving alone afterwards [11]. Chandrasekaran et al. [12] showed that driving-inexperienced passengers modulated their conversation less than driving-experienced passengers.

Former studies found a difference between drivers' and passengers' head movements during driving. Drivers' head tilts are related to the road's curvature, while inactive passengers' head tilt correlates inversely with the lateral forces [13]. Another study conducted in a driving simulator has shown that there could be a difference in behaviour between aware and unaware passengers [14]. Unaware passengers were assigned to perform a secondary spatial cognitive task by the experiments. In contrast, aware passengers learned about the situation through arrows; for instance, up indicated accelerating. These aware passengers also performed a think-aloud task to facilitate their cognitive processing. Results show that the head's mean side rotation rate while cornering was similar between drivers and aware passengers [14]. Cabrall et al. [15] researched the eye measure eccentricity (mean percentage distance from the centre gaze point) for differentiation between drivers and passengers. Results indicate a higher eccentricity measure for passengers than drivers. The measurement duration and the inclusion of vehicle speed improved the differentiation between driver and passenger based on the eccentricity measure [15]. Former studies of Zikovitz and Harris [13], Schewe et al. [14] and Cabrall et al. [15] concentrated on finding differences between drivers and passengers. In short, a knowledge gap is discovered for synchronous head movements between driver and passenger in the same environment.

Humans are in control of driving a vehicle. In the future, this may change due to the introduction of advanced driving assistance systems (ADAS). This will change the driver's role from an active controller to a supervisor, and eventually, to a passenger [16]. Therefore, research to identify the changes

due to vehicle automation on the driver state and behaviour is necessary. Examples of these changes are; increased use of in-vehicle infotainment systems [17]-[19], reduced vigilance due to monitoring, mode awareness, changes in attention allocation, reduced situation awareness, over-reliance and complacency toward the systems and misuse [16]. The driver state and behaviour can be extracted by multiple measurement techniques, for instance, physiological, performance-based and subjective measures [20], [21]. In real-world driving experiments focused on automated driving, physiological measures are best suited. Eye- and head tracking measures are examples of physiological measures that can be non-intrusive and are direct [22]. These measures are commonly used in Driver Monitoring Systems (DMS). The function of a DMS is stated by Hayley et al. [23] as: ' … collect observable information about the operator to make real-time assessment of their capacity to perform the driving task'.

Pose estimation

Previous studies that analysed synchrony during conversations between dyads focussed on head movements regularly [24]-[26]. Several techniques, such as motion tracking devices, image processing techniques, and physiological sensors, are prominent in the literature for capturing head motion between dyads [26]. An image processing technique, more specifically, a video-based tracking approach, seems promising to gain information of the head pose of drivers and passengers. Since this approach is non-intrusive and only a single camera is sufficient, this is feasible for the implementation in DMS. Schoenherr et al. [27], Moulder et al. [28], Ramseyer and Tschacher [29], Feniger-Schaal et al. [30] and Paulick et al. [31] used a video-based tracking method - frame differencing technique called Motion Energy Analysis (MEA). This frame-differencing approach captures the human body in a plane or region. The frame-differencing technique is robust and implemented in various research contexts, such as casual chatting, clinical counselling, and specific collaborative tasks [29], [30], [32]. MEA does not include information about the direction and form of the movement, only the size. Another example of a video-based tracking method is a pose-estimation algorithm. Only one former study of Fujiwara and Yokomitsu [33] implemented a pose-estimation technique (OpenPose) for synchrony analysis between dyads. The OpenPose algorithm produces a real-time pose estimation (e.g., head, hand, face etc.) [34]. A promising pose-estimation algorithm for eye-and head detection is OpenFace 2.0. OpenFace 2.0 is a facial behaviour toolbox that detects facial landmarks (e.g., facial action units, head pose and eye-gaze) and contains a high detection rate compared to former head detection algorithms [34], [35]. This technique uses computer vision and deep learning to estimate the coordinates of the face. The result of the pose-estimation algorithm is a time series with information about the facial action units, head pose and eye-gaze of the detected face.

Measurement of synchrony

In this study, synchrony is defined as well-coordinated, or well-timed interaction. The measurement of synchrony is challenging since there are various methods available, leading to different results [28]. A couple of examples of these methods are correlations, regressions, structural equation models, recurrence quantification analyses, spectral analyses and human raters. The most apparent method, human rating, has low reliability [27]. Additionally, human raters should be trained to ensure all raters assess in a similar construct. This takes time. Automated synchrony identification could prove economical and reliable. However, the parameter settings are essential to generate meaningful results for synchrony detection [27], since both the method and the input parameters strongly affect the outcome. To date, there is still no agreement on which parameter values produce the best outcomes [28]. In behavioural sciences that focus on synchrony between two dyads, correlation- and regressive time series analysis methods are mostly applied [27], [36]. These approaches are based on linear relationships between dyads. Therefore, stationarity is required. This entails a stable frequency or repetitive pattern throughout the time series. The method used to identify synchrony should capture what happens during

synchrony. It should also allow for a slight time delay. The windowed cross-lagged correlation (WCLC) and windowed cross-lagged regression (WCLR) fulfil these requirements. Since the WCLR was developed for cyclic and auto-correlated time-series and is computational more expensive, the WCLC is promising for behavioural synchrony [27].

Windowed Cross-Lagged Correlation

WCLC is the most used method to quantify synchrony between dyads [37] and is regularly applied for head movement analysis regarding synchrony in former studies [24], [25], [38]. The WCLC analysis is a well-ordered method for capturing dynamic changes in synchrony. The WCLC estimates the peak Pearson product-moment correlation and the associated time lag at the peak correlation between two time series signals. The signal is divided into smaller overlapping windows instead of calculating the correlation coefficient over the whole time series. The lag captures the slight differences in pace between two individuals' responses to one another. This method assumes that there is local stationarity (2 seconds) [39]. This indicates that the statistical properties, e.g. mean, standard deviation, autocorrelation and cross-correlation, remain stationary or stable over a timespan of two seconds. Finding the best parameter configuration for the application of WCLC is challenging. Choosing the best window size is a reliability-sensitivity trade-off [38]. It is recommended to have a sample size of at least 65 observations for a high correlation, while for a weaker correlation, a sample size up to 250 observations is advised [39]. A larger window size reduces the sensitivity, while a small window size reduces the reliability of the results. The linear time series analysis methods, where WCLC is one of, can measure different facets of synchrony, for instance the strength- and the frequency of synchrony over the total interaction [36]. The different facets of synchrony are measured by different peak-picking algorithms.

Peak-picking

The WCLC is supported by a peak-picking algorithm. A peak is the maximum cross-correlation. The peak-picking algorithm analyses patterns of change in peak cross-correlation between two time series. This is accomplished by the identification of correlation peaks and their associated time lag. Since synchrony fluctuates over time, the correlation and the associated time lag changes as well. These changes are identified by the peak-picking algorithms. Also, the time series what lead the synchronisation is revealed by the peak-picking algorithm. Boker et al. [38] introduced the first peak-picking algorithm. An alternative peak-picking algorithm was released by Altmann [40]. These peak-picking algorithms are fundamentally different. The algorithm of Boker et al. implies the occurrence of synchrony over the entire duration of the interaction, with only the strength of the synchrony varying. Therefore, this algorithm aims to quantify the strength of synchrony over a specific time window. The peak-picking algorithm proposed by Altmann assumes the existence of synchronisation intervals. The frequency of synchrony can be determined due to detection of synchrony intervals, what is also known as an on and off pattern. Therefore, the peak-picking algorithm of Altmann can be implemented to identify the frequency of synchrony in a specific bandwidth. The algorithm of Boker can be used to obtain information about the strength of synchrony over total duration of the interaction.

Pseudosynchrony

Another challenge researchers face when investigating synchrony, is the occurrence of spurious synchrony between two individuals that were not engaged with one another. The spurious synchrony, also known as pseudosynchrony, occurs because humans are in a constant state of motion [28]. Therefore, it is essential to distinguish the detected synchrony from pseudosynchrony to assess synchrony in any communication context, since pseudosynchrony may be present due to random coincidence [32]. The synchrony identified by the peak-picking algorithms should be compared to pseudosynchrony values to confirm that the detected synchrony did not appear by chance. To create

pseudosynchrony, a surrogate data stream is produced by destroying the quality of interest, synchrony, while keeping all other attributes of the data streams, such as the mean value, intact. Another name is a bootstrap method for the comparison of the detected synchrony to pseudosynchrony or surrogate data [41]. Ramseyer and Tschacher explained in their study that to implement surrogate data for group analysis, it is recommended to generate one hundred or more surrogate data streams per sample and derived the mean value [32].

Research Aim

The present study aimed the identification of synchrony in head orientation and movement between drivers and passengers for various road types and cornering events. Since the detection of synchrony during driving is a new area of research, analysis on different facets of synchrony was executed to study the frequency- and strength of synchrony over the total duration and the various segments of an interaction. This study was based on real-world driving data. Video-based pose estimation, windowed cross-lagged correlation analysis, two different peak-picking algorithms, and chance control were implemented. The head angle was intrinsically linked to the driver's field of view and focus of attention [42], [43]. The principle axes of the head, pitch, roll and yaw were taken for investigation of head orientation and movements of drivers and passengers. The output of the peak-picking algorithms was compared to synchrony that may be expected by chance, pseudosynchrony. First, the frequency of synchrony in head angle and head angular velocity for drivers and passengers were compared to the pseudosynchrony for different road segments and cornering events. Secondly, the strength of synchrony between drivers and passengers for different road segments and cornering events were analysed and compared to pseudosynchrony. Lastly, the results for the different road types were compared. The first hypothesis states that it is possible to distinguish between the detected synchrony and pseudosynchrony of drivers and passengers for both the frequency- and strength of synchrony. The second hypothesis states that more synchrony is detected in the urban road type than outside built-up areas and highway road types.

Methods

Dataset

For the identification of driver passenger synchrony, real-world driving data was used. This real-world driving data was obtained from a former naturalistic driving experiment of Cabrall et al. [15], [44]. The participants were 16 pairs (78% male, 22% female, mean age = 27.3, SD age = 2.4) recruited from the Delft University of Technology and had a normal or corrected-to-normal vision. All participants obtained their initial driver's license at least more than one year prior to the experiment. The experiment was carried out in a 2014 Toyota Prius Hybrid passenger vehicle with an automatic transmission and without advanced driving assistance systems. Each participant was involved in two trips. One trip the participant sat in the driver's seat and one trip in the passenger's seat, leading to a total of 32 trips. The drivers did not receive any instructions, except to drive safely and as they usually would. The passengers started without any instructions for the first part of the trip. In segment 5 (Figure 1), the passengers received an instruction paper asking them to pay attention and behave with their eyes as if they were driving. No restrictions were given regarding conversation, the use of electronic devices, e.g.

The vehicle was instrumented with additional equipment including GPS and measuring tools for steering and pedal inputs, to collect data about the vehicle state and the control input at 25 Hz. Also, the vehicle contained facecams for assessing driver behaviour. The facecams are cameras inside that were directed at the driver and passenger. The generated videos had a sampling rate of 30 Hz. The drivers and

passengers wore UV shielded eye-tracking glasses from SensoMotoric Instruments (SMI) during the experiments. The glasses recorded eye measures sampled at 60 Hz.

From the total of 32 trips, 24 trips were included in the analysis. The excluded trips are trip 7 due to a detour, trip 9 since no facecam videos of the driver and passenger were available, and trip number 32 due to an error in the recording of the facecam video of the driver. Trips 11, 12, 13, 22 and 27 were eliminated due to too many missing values in the data produced by the head detection algorithm. The detection algorithm OpenFace 2.0 experienced difficulties detecting the head during large, fast movements due to the eye tracking glasses participants wore. Since the remaining trips contained a limited amount of missing data spread over the whole duration of the trip, it was considered sufficient for this study.

Route

The driving route covered mixed types of roads and various driving situations (e.g., traffic, signage, road geometry) (Figure 1). The total length of one trip was about 20.0 km and took approximately 30 minutes on average.

To analyse the impact of the different road types and cornering events on the synchrony between driver and passengers, various road segments and cornering events are introduced. These segments differentiate between the mixed types of roads. Segments 1 and 9 are urban segments with cornering events A, N, B, M, C, L, D and K. The corner events E, and, J are the transition from urban area to outside built-up areas. The road type of segments 2 and 8 are outside built-up areas. Next, entering and exiting the highway, segments 3 and 7, with cornering events I and F. The highway is annotated by the segments 4 and 6. The last road segment is segment 5, the turnaround point with cornering events G and H, is called exit and entry highway. Figure 1 shows an overview of the different road segments and cornering events. Table 1 shows an overview of the distance of each segment, the mean time duration of each segment and the percentage of time of each road segment in relation to the total route. Table 2 shows the average duration of each corner.

	Distance (m)	Duration (s)	Percentage of time (%)
Total route	20543	1842	100
Part 1: Pre task	9261	811	44.0
Part 2: Post task	9853	889	48.3
Segment 1: Urban	2044	286	15.5
Segment 2: Outside built-up areas	3178	354	19.2
Segment 3: Entry highway	179	16	0.9
Segment 4: Highway	3246	164	8.4
Segment 5: Exit and entry highway	1429	142	7.7
Segment 6: Highway	3456	143	7.8
Segment 7: Exit highway	386	30	1.6
Segment 8: Outside built-up areas	3867	419	22.7
Segment 9: Urban	2143	297	16.4

Table 1. Overview of average distance (m), average duration (s) and the average percentage of time (%) of each road segment compared to the total time.

	Duration (s)
A	19.7
B	23.4
C	12.3
D	24.6
E	12.0
F	11.5
G	15.5
H	45.7
I	8.07
J	20.4
K	18.5
L	12.9
M	22.9
N	15.2

Table 2. Overview average duration (s) of each cornering event.

The road segments were determined by analysing the route of the trip. The distinguishment of the segments in the data were implemented by deriving the travelled distance of the start of each segment. This method proved to be more accurate than the application of GPS for the current data. First, the start positions of the road segments were defined with road signs and characteristics that were visible at the side windows of the vehicle in the facecam videos of one trip. Thereafter, the distance travelled at those points was derived via the recorded vehicle speed. The distance travelled was then kept identical for all trips. Since some drivers may drive at a different corner radius, the distance travelled leads to a slight

deviation in the segment starting point. However, for the differentiation of the road segments this level of accuracy is considered sufficient and will not affect results.

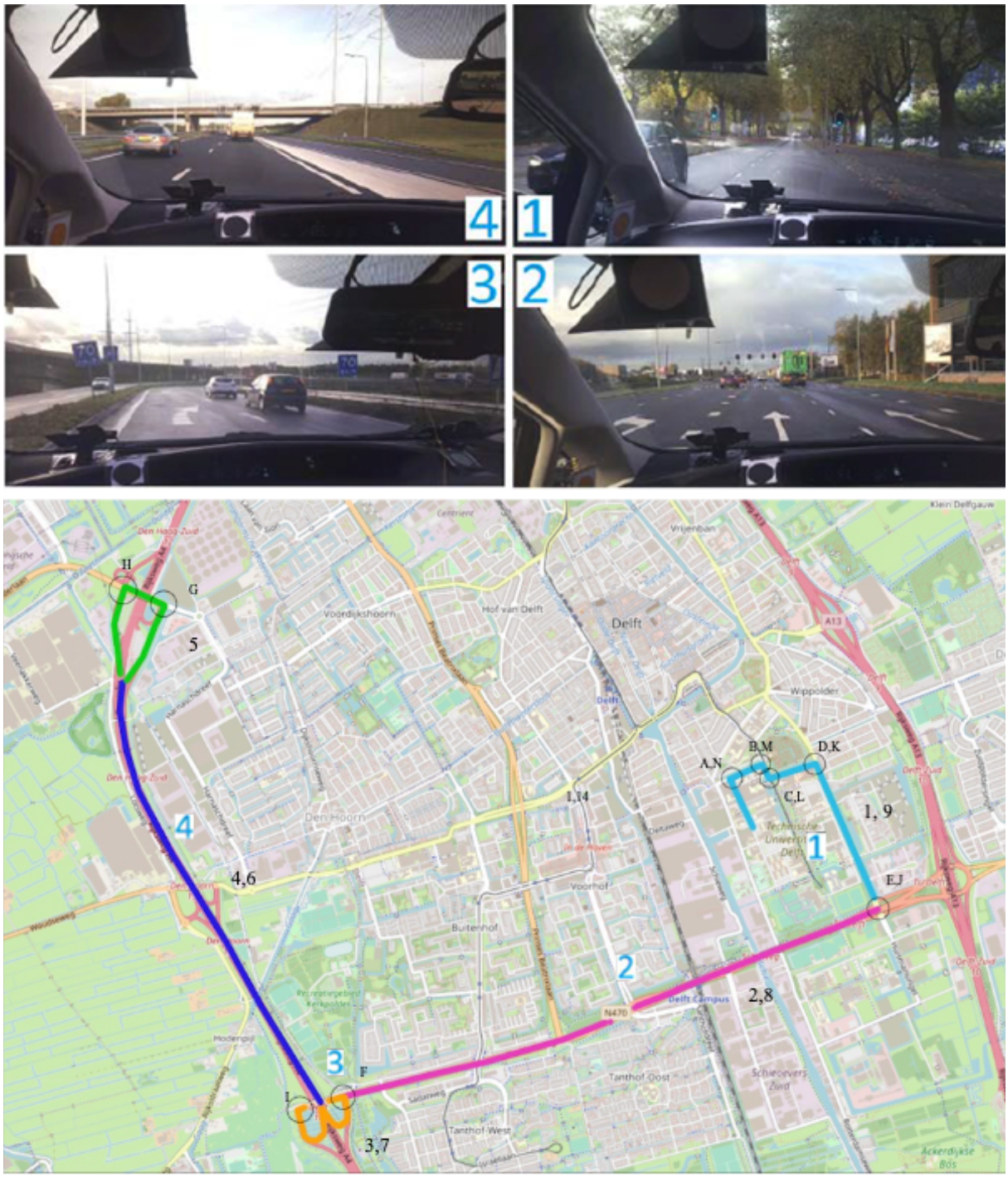

Figure 1. Top: Various route scenes; 1: urban, 2: outside built-up areas, 3: entry highway, 4: highway. The location at the route is annotated by a blue number in bottom figure [45]. Bottom: The driving route of the real-world experiment divided into road segments. The different road types are marked in different colours, light blue: urban, pink: outside built-up areas, orange: entry/exit from the highway, dark blue: highway, green: entry/exit from the highway. The black numbers annotate the road segments, and the corners are circled and annotated by a letter.

Identifying synchrony

The synchrony of head orientation and movement between drivers and passengers was analysed as follows: (I) automatic detection of the head pose, (II) data filtering, (III) syncing data, (IV) creation

surrogate data, (V) application windowed cross-lagged correlation, (VI) identification frequency of synchrony (VII) identification strength of synchrony, and (VIII) statistical analysis.

I. Automatic detection of the head pose

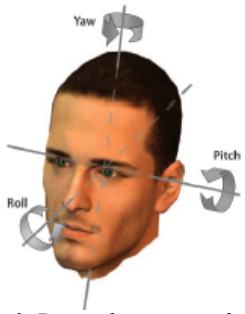

Figure 2. Principles axes pitch, roll and yaw [44].

First, the video-based pose-estimation OpenFace 2.0 algorithm was applied to provide the principle axes of the head of the driver and the passenger. These principle axes are angles are pitch, roll and yaw. These head pose angles are essential for driver attention monitoring, and therefore all three were analysed [45]. Besides the head pose, the head angular velocity was also explored. The angular velocity contains information about the activity of the head. The angular velocity of the head is derived from the head orientation. Figure 3 shows the values of the head angle and angular velocity of pitch, roll and yaw for trip 5, for a 10-second time window of road segment 1 - urban.

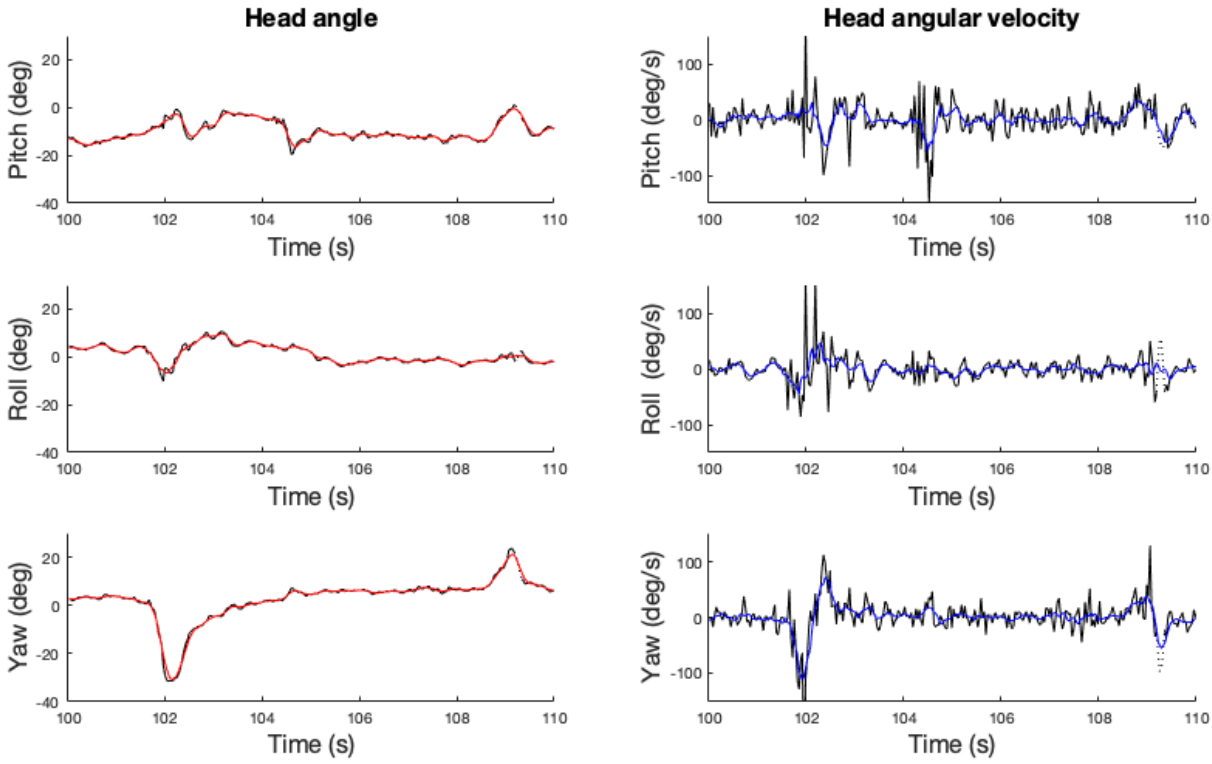

Figure 3. The head angles (left) and head angular velocities (right) in the road segment 1 - urban for the driver of trip number 5. Black line: raw signal detected by the OpenFace 2.0 algorithm, black dotted line: interpolated signal, red line (head angle): smoothed signal, blue line (head angular velocity): derivative smoothed signal head angle.

An important feature for running OpenFace 2.0 was the detection of multiple faces, since the experimenters at the backseats of the vehicle were visibility in the facecams. Although face detection algorithms have improved the last years, the OpenFace 2.0 algorithms experienced difficulties in head detection in some cases. This could have been caused by the fact that large eye trackers were installed on the participant's faces, occluding facial landmarks as eyes and eyebrows. This led to false positives and missing data. False positives were detected values of the correct participant but with incorrect proportions of the head resulting in incorrect head angles. The false positive values were removed from the data (Appendix A). Since, for most trips, the data gaps were small, a spline method for interpolating

these gaps was applied. For five trips, the percentage of missing data after head detection and removing the false positive was more than 20% for the driver and/or passenger data (Appendix B). These five trips, (trip numbers; 11, 12, 13, 22 and 27), were excluded from analysis.

II. Data filtering

The detected head angle by the OpenFace algorithm contained noise. Applying a moving average filter keeps most variations in the detected data but it removes the high frequency noise. The moving average sample length was determined based on literature, most papers analysing movement synchrony use a moving average filter with a length of 400 milliseconds to 1 second for filtering movement signals [28], [33], [46], [47]. To reduce the amount of noise in the collected data a moving average filter was applied with a length of 8 samples (0.267 seconds) on the signal containing the head angle. Then the signal was differentiated to derive a filtered angular velocity signal. Figure 3 shows the detected, interpolated and smoothed signals of the head orientation and movement for pitch, roll and yaw for the driver of a random trip for a small time window in segment 1. The results of the filtering method for other segments and the passengers' role are included in Appendix C.

III. Syncing data

Next, the time series data of the driver and passenger of each trip was synced to the car data. A method based on vibrations created by Fridman et al. was implemented to sync these data streams [48]. First, the dense optical flow from the facecam video was derived by the Farneback algorithm. The dense optical flow detected fluctuations (vibrations) in the y-direction of the videos. The next step was finding the maximum cross-correlation between the dense optical flow derived from the video and the body acceleration of the vehicle in Z-direction. The maximum correlation identified the lag between the two signals, after which we could correct for this lag, synchronising the two streams. Appendix D contains more information on the applied syncing method.

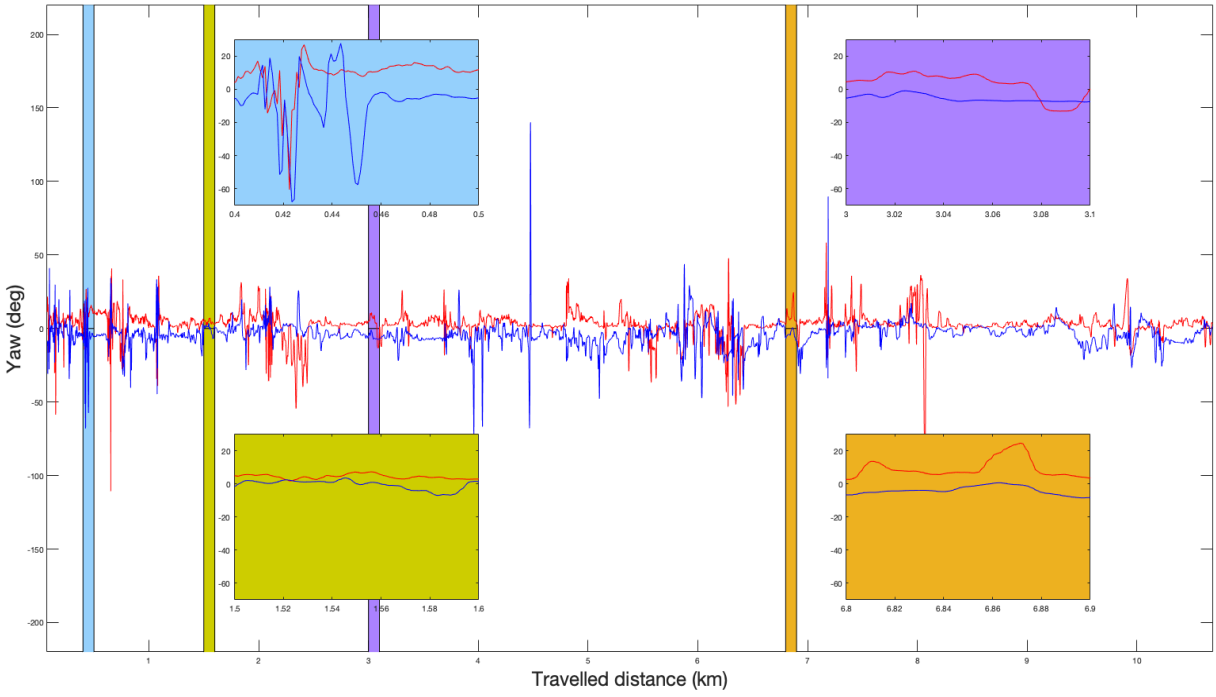

Figure 4. Head angle yaw for the driver (red line) and passenger (blue line) for the first half of the trip 1. Blue box: road segment 1 – urban including a cornering events, green box: road segment 1– urban without a cornering events, purple box: road segment 2 – outside built-up areas without a cornering event and the orange box: road segment 4 – highway without a cornering event.

IV. Creation surrogate data

Many methods of testing and quantifying nonverbal synchrony showed a level of synchrony, even when the two time series are not correlated, e.g. data of research participants that show no interaction [28]. Therefore, it is necessary to differentiate between detected – and pseudosynchrony to verify synchrony is not detected by chance. Different methods could be used to generate surrogate data. Since we were assessing synchrony over longer time intervals, data sliding was the best fit method for surrogate data generation for this application [28]. The method of data sliding does not destroy as much time dependency as, for example, data shuffling. For data sliding, a single cut was created at a random point between 50-70% of the first data stream. The data past this point was removed from the end of the time series and appended at the beginning. An important note is that the placement of the cut should not be too close to the start or the end of the time series, hence the cut in the range of 50-70% of the signal. The second data stream remains unchanged. Next, the pseudosynchrony was calculated identically to the synchrony of the original signal. In the study of Ramseyer and Tschacher, it was stated to generate one hundred pseudosynchrony streams per sample and derive the mean value for a group analysis [32]. Since the number of trips is twenty-four, the total sample size of the group is relatively small. Therefore, the method of Ramseyer and Tschacher was applied. This strengthens the application of pseudosynchrony.

V. Application Windowed Cross-Lagged Correlation (WCLC)

The WCLC was calculated using the formulas (1) and (2) [38]. Suppose we take a segment of the time series of the head orientation from the driver, define this vector X. The exact length segment of the time series of the head orientation of the passenger is described as vector Y. The size of the window is denoted by w_{max}, and τ indicates the time lag. The time lag should be between the minimum and maximum time lag.

$$W_x = \begin{cases} \{x_i, x_{i+1}, x_{i+2}, \dots\ x_{i+w_{max}}\} & if\ \tau \leq 0 \\ \{x_{i-\tau}, x_{i+1-\tau}, x_{i+2-\tau}, \dots\ x_{i+w_{max}-\tau}\} & if\ \tau > 0 \end{cases} \qquad (1)$$

$$W_y = \begin{cases} \{y_{i+\tau}, y_{i+1+\tau}, y_{i+2+\tau}, \dots\ y_{i+w_{max+\tau}}\} & if\ \tau \leq 0 \\ \{y_i, y_{i+1}, y_{i+2}, \dots\ y_{i+w_{max}}\} & if\ \tau > 0 \end{cases}$$

$$r(W_x, W_y) = \frac{1}{w_{max}} \sum_{i=1}^{w_{max}} \frac{(W_{x_i} - \mu(W_x))(W_{y_i} - \mu(W_y))}{sd(W_x) sd(W_y)} \qquad (2)$$

The sampling frequency of the head angle estimation was 30 Hz. The WCLC was calculated for the complete duration of the trip. We carefully choose the parameters so that they were as adequate as possible in our case. The WCLC analysis required the specification of four parameters: window size, maximum lag, window increment and lag increment. The first parameter was the window size of the studied segment. The chosen window size was 60 data points (2 seconds). The second parameter was the maximum time lag; this was also 60 data points (2 seconds). The window increment between the two windows was set to 6 data points (200 milliseconds) and the lag increment was set to 2 data points (67 milliseconds). For calculating the WCLC, only positive correlations were included in the analysis. Anti-synchrony, negative correlation values, were disregarded since we were interested in whether the drivers and passengers moved their heads into the same direction. Next, two different peak-picking algorithms were employed, one focussing on the frequency of synchrony and the other on the strength of synchrony. Figure 5 shows the different structure of the two peak-picking algorithms with the different WCLC matrices, R^2 for Altmann and R for Boker. Figure 6 shows the results of a synchronisation interval for a small time window for the head orientation and movement. In Figure 6, a

positive lag value in the synchrony interval indicates passenger synchrony leads and a negative lag value, indicate that the driver leads the synchrony interval.

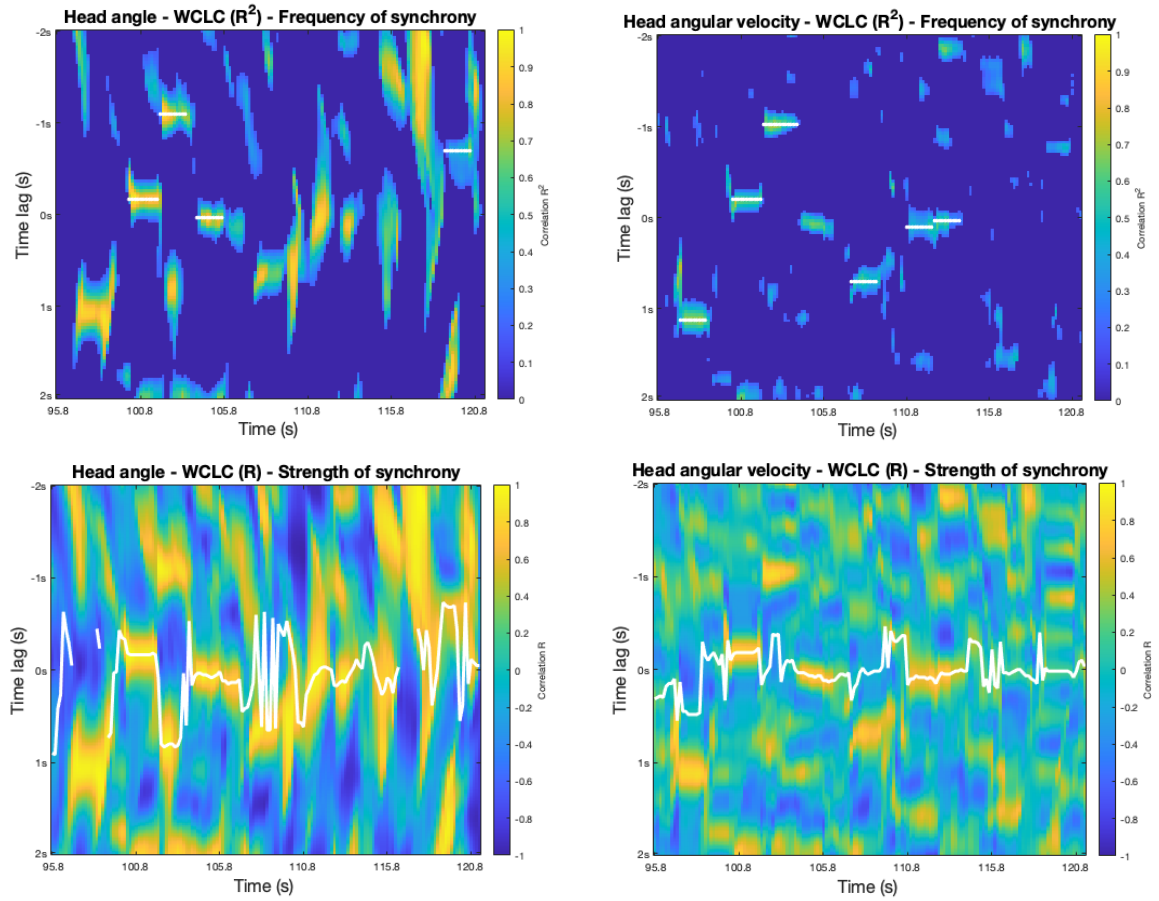

Figure 5. Overview of the results of the windowed cross-lagged correlation (WCLC) and peak-picking algorithms of trip 5 of a time window of 25 seconds for the head angle and angular velocity - yaw. Top left: WCLC + peak-picking Altmann, head angle (white lines: 4 synchrony intervals), Top right: WCLC + peak-picking Altmann , angular velocity (white lines: 6 synchrony intervals). Bottom left: head angle WCLC + peak-picking Boker et al. (white line), Bottom right: head angular velocity WCLC + peak-picking Boker et al. (white line).

VI. Identification frequency of synchrony

The first facet of synchrony analysed, was the frequency of synchrony, also called the occurrence of synchrony. The peak-picking algorithm of Altmann [40], [49] was implemented to identify the frequency of synchrony. First, this algorithm localised all local maxima, peaks, in the R^2 matrix. The squared correlation (R^2) causes that higher correlations weight higher than very low correlations. Next, the neighbouring peaks with an equal time lag were identified. The neighbouring peaks were assembled to peak clusters. A small time lag was tolerated in these peak clusters. Then, all peak clusters smaller than 2 seconds (ten consecutive peaks) were removed, since these short periods are considered too short for meaningful synchrony. Next, the peak clusters containing a lower R^2 average in the presence of overlapping peak clusters were removed. The outcome of this peak-picking algorithm was a sequence of synchrony intervals including frame numbers, their mean peak correlations in R^2 and their corresponding time lags. The last step was calculating the percentage of synchrony intervals over the computed road segments and cornering events. Since the synchrony interval contained the frame numbers of where a synchrony interval was detected, the percentage synchrony over road segments and cornering events could be calculated by the sum of all frames of the synchrony intervals divided by the sum of all frames of the road segment or cornering event under analysis.

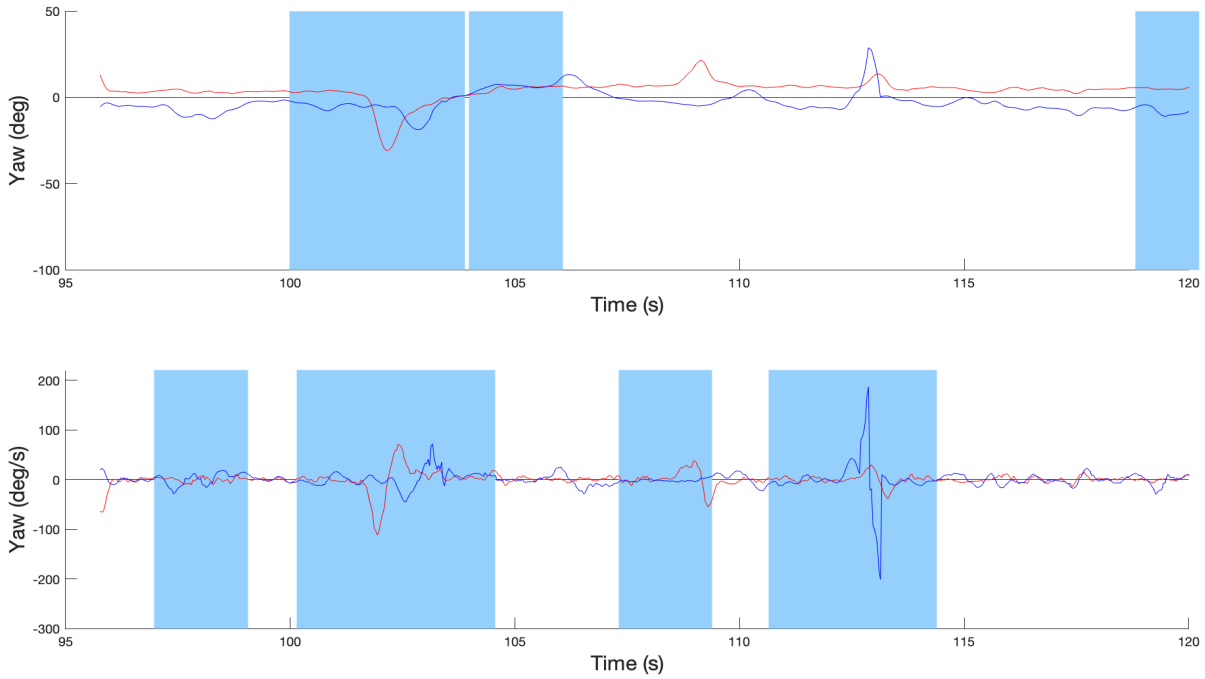

Figure 6: Overview synchrony intervals of trip 5 for a small time window of 25 seconds. Driver (red line), passenger (blue line), synchrony intervals (light blue boxes). Top: Head angle as function of time. Bottom: Head angular velocity as function of time.

VII. Identification strength of synchrony

The second peak-picking algorithm applied, analysed the second facet of synchrony, the strength of synchrony. The peak-picking algorithm developed by Boker et al. focused on finding the maximum cross-correlation, a peak [38]. A value was considered a peak when the values decrease on either side of the peak in a specific local region. In case more than one peak was found, the peak with the lowest time lag was picked. The input of the peak-picking algorithm was a column vector from the cross-correlation including all time-lag options. The cross-correlation data was smoothed with a loess smoothing function. The loess smoother was developed by Cleveland and Devlin [50]. The smoother estimates changes in cross-correlation with regard to lag values using locally weighted regression. The peak-picking algorithm required the definition of two parameters for the loess smoothing, the local search region (L size) and the degree of smoothing (Pspan). The L size signifies the size of the local area that defines the peak. This value should be large enough to reject spurious local noise and small enough to identify meaningful peaks. The Pspan establishes the width of the moving window when smoothing the data. After careful analysis and pilot runs, the selected values for the parameters were for the local search size, L size, 8 data points, and for the degree of smoothing, Pspan, 0.1. The output of the peak-picking algorithm of Boker et al. was a list of local peaks of cross-correlation with their corresponding time lag. To determine the amount of synchrony, the mean of the peak correlation were presented. The mean peak correlation gave insight about the strength of synchrony in the analysed segment.

VIII. Statistical analysis

Concerning the first hypothesis, the ability to distinguish the detected synchrony and pseudosynchrony between drivers and passengers, two analyses were established. The first analysis is on the frequency of synchrony with the peak-picking algorithm of Altmann [40], [49] and the second on the strength of synchrony with the peak-picking algorithm of Boker et al. [38].

For both algorithms the total route, Part 1 – pre-task and Part 2 – post-task were analysed. Also, all road segments were separately analysed. In table 3, an overview of the road types, the associated road segment and cornering events are shown.

Road type	Road Segment	Cornering event
Urban	1, 9	A, B , C, D, N, M , L, K
Outside built-up areas	2, 8	E, J
Entry/Exit from the highway	3, 5, 7	F, I, G, H
Highway	4, 6	

Table 3. Overview of road types with associated road segments and cornering events

The identified synchrony of the real- and surrogate data at different road segments and cornering events were compared. The synchrony intervals and mean peak correlation of all 100 surrogate data streams were derived first. After which, the mean value for those 100 surrogate data streams were obtained for the synchrony percentage and the mean peak correlation for each trip. The derivation of WCLC for 100 surrogate data streams for 24 trips including the two different peak-picking algorithms was computationally expensive. Therefore, the calculations for the surrogate data streams were executed via Amazon Web Services (AWS), an online parallel computing service (Appendix E).

Then, a dependent t-test was employed to compare the percentages of synchrony derived from the synchrony intervals of the real data to the mean value of the one hundred computed surrogate data streams. If the p-value of the dependent t-test was smaller than 0.01, the difference between real– and surrogate data was considered to be significant and therefore, it could be concluded that synchrony was identified. In addition, the effect size estimates (Cohen's d) based on the dependent t-test were reported for the frequency of synchrony. The second analysis focussed on the strength of the synchrony between drivers and passengers for different road segments and cornering events. A dependent t-test compared the mean peak correlation of the real values to the values of the surrogate data for all different road segments. If the p-values of the t-test were smaller than 0.01 a distinction between real- and surrogate data could be made. Also, the effect sizes were calculated.

Only if the detected synchrony was significantly different from pseudosynchrony for the required segments, the analysis to confirm or reject the second hypothesis was executed. The second hypothesis states that in the urban road type more synchrony occurs than outside built-up areas and highway. The statistical method to confirm or reject the second hypothesis was an one-way ANOVA.

Results

In order to create a total overview of the analysed data, Figures 7 to 10 are provided to illustrate a couple of vehicle input parameters for the head angle and angular velocity for the analysed sections. Figure 7 shows the vehicle's speed as a function of the travelled distance for the 24 trips and Figure 8 displays the steering wheel angle as a function of the travelled distance for all the included trips.

Six descriptive graphs on the head orientation and movement of drivers and passengers are presented in Figures 9 and 10. These graphs show the averaged interquartile range of the head angle and angular velocity of drivers and passengers for the studied segments. Since the neutral positions of the head angle differs per position in the vehicle, and per participant, the median value of the participants head angle was subtracted from the head angle before deriving the interquartile range per trip. This leads to a clear overview. Appendix H contains more graphs on the head angle and angular velocity of the driver and passenger for each trip

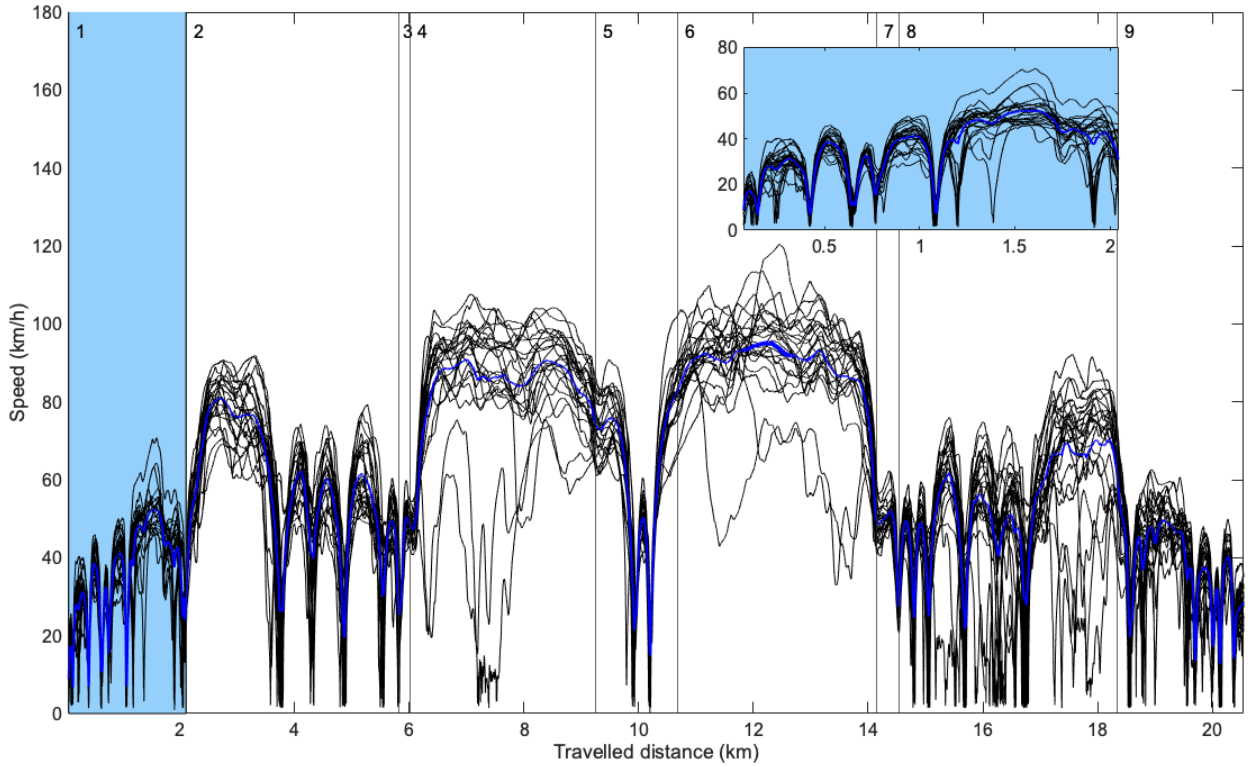

Figure 7. Vehicle speed as a function of travelled distance for 24 trips. The black lines represent the speed of each individual trip, the blue line represents the average speed of the 24 trips. The vertical lines in combination with numbers 1 to 9 indicate the road segments.

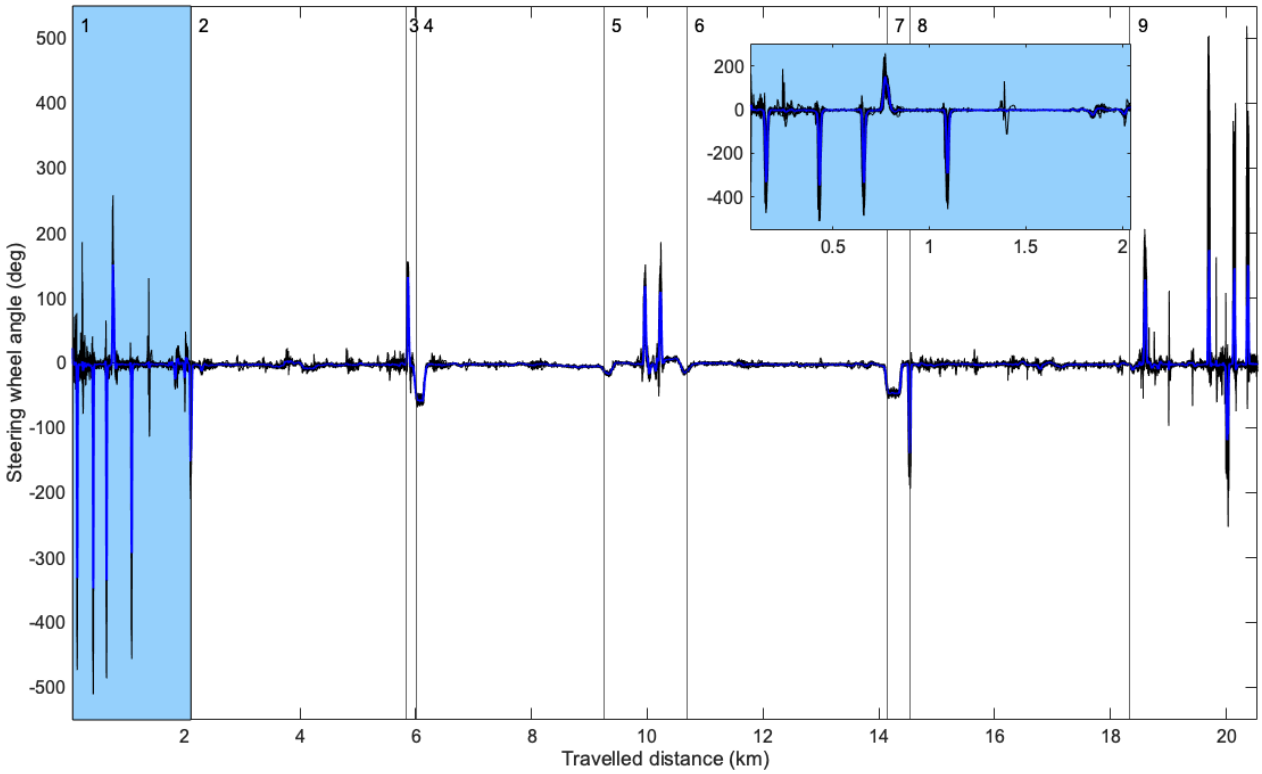

Figure 8. Steering wheel angle as a function of travelled distance for 24 trips. Angle left: positive, angle right: negative. The black lines represent the steering wheel angle of each individual trip, the blue line represents the average steering wheel angle of the 24 trips. The vertical lines in combination with numbers 1 to 9 indicate the road segments.

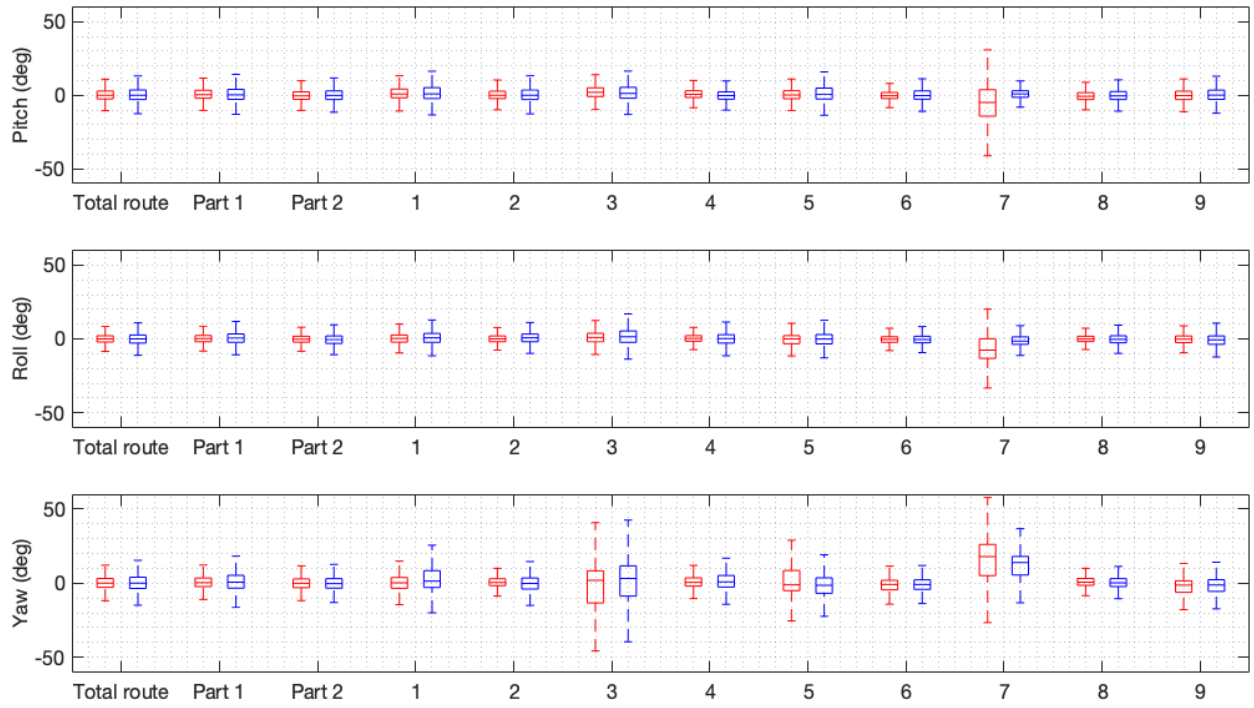

Figure 9. Averaged interquartile range of the head angles, pitch(top), roll(middle) and yaw (bottom) for drivers (red) and passengers (blue) of the 24 included trips. The analysed sections are on the x-axis: Total route, Part 1- pre-task, Part 2- post-task, Segments 1 to 9. (1: Urban, 2: Outside built-up areas, 3: Entry highway, 4: Highway, 5: Exit/ Entry from highway, 6: Highway, 7: Exit highway, 8: Outside built-up areas, 9: Urban). Since the neutral positions of the head angle differs per position in the vehicle, and per participant, the median value of the participants head angle was subtracted from the head angle before deriving the interquartile range per trip.

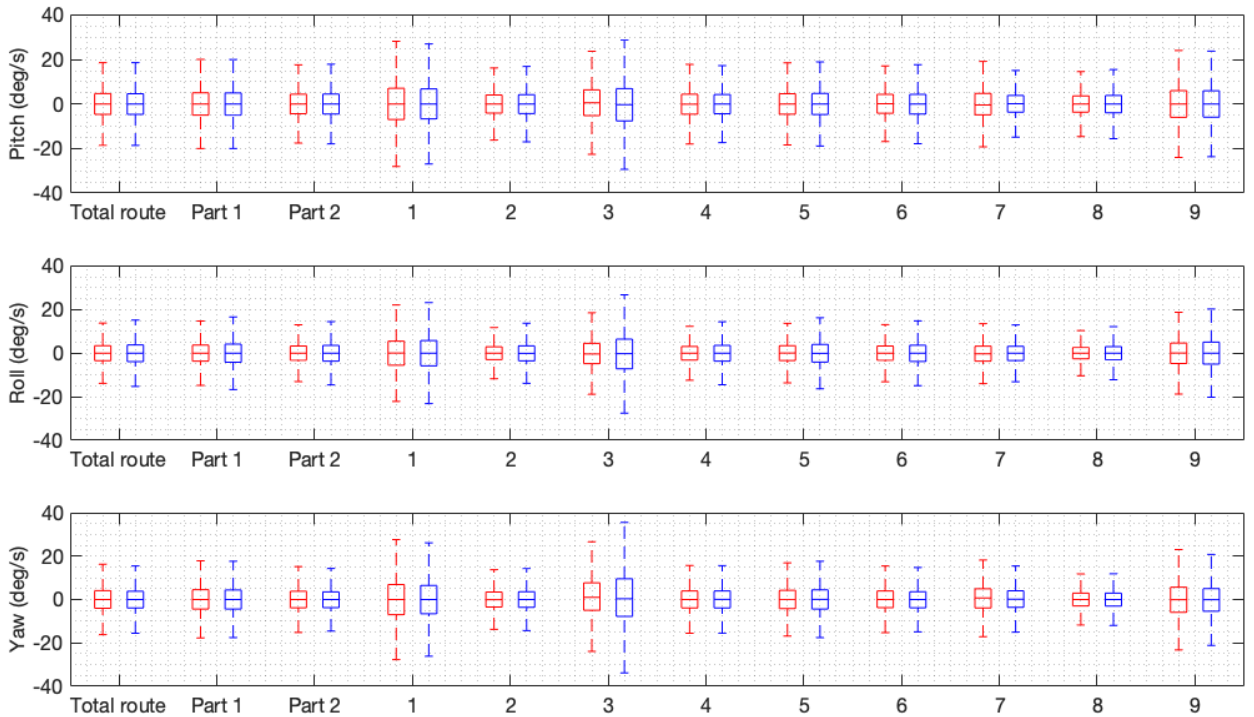

Figure 10. Averaged interquartile range of the head angular velocities, pitch(top), roll(middle) and yaw (bottom) for drivers (red) and passengers (blue) of the 24 included trips. The analysed sections are on the x-axis: Total route, Part 1- pre-task, Part 2- post-task, Segments 1 to 9. (1: Urban, 2: Outside built-up areas, 3: Entry highway, 4: Highway, 5: Exit/ Entry from highway, 6: Highway, 7: Exit highway, 8: Outside built-up areas, 9: Urban).

Frequency of synchrony

First, the results on comparing detected- and pseudosynchrony in head angle and angular velocity between drivers and passengers for the frequency of synchrony are discussed.

	PITCH		ROLL		YAW	
	Angle (%)	Angular velocity (%)	Angle (%)	Angular velocity (%)	Angle (%)	Angular velocity (%)
Total route	**7.4* (0.704)**	**30.5* (1.113)**	**6.4* (1.539)**	**28.5* (1.594)**	4.2 (0.566)	**20.6* (0.665)**
Part 1: Pre-task	**7.5* (0.609)**	**30.8* (0.937)**	**6.5* (0.955)**	**29.4* (1.518)**	4.2 (0.390)	**20.8* (0.816)**
Part 2: Post-task	7.6 (0.552)	**30.5* (0.732)**	**6.5* (0.842)**	**27.8* (0.797)**	4.1 (0.267)	20.2 (0.244)
1: Urban	**8.9* (0.815)**	**32.9* (0.886)**	**8.1* (0.913)**	**33.5* (1.586)**	4.2 (0.284)	**21.5* (0.697)**
2: Outside built-up areas	6.6 (0.266)	29.0 (0.418)	5.8 (0.276)	27.1 (0.522)	3.9 (0.170)	**20.2* (0.620)**
3: Entry highway	9.2 (0.340)	30.1 (0.145)	4.1 (-0.018)	26.3 (-0.006)	5.0 (0.351)	**26.7* (0.915)**
4: Highway	6.9 (0.079)	**31.4* (0.638)**	5.1 (-0.127)	27.1 (0.348)	4.6 (0.372)	20.2 (0.301)
5: Exit and Entry highway	5.6 (-0.543)	29.1 (0.216)	5.6 (0.135)	27.3 (0.550)	4.5 (0.474)	**21.3* (0.593)**
6: Highway	7.4 (-0.088)	30.6 (0.197)	5.5 (-0.283)	26.3 (-0.222)	3.5 (-0.214)	19.3 (0.053)
7: Exit highway	3.5 (-0.684)	28.5 (0.043)	4.8 (-0.016)	26.1 (0.274)	3.3 (-0.042)	18.6 (-0.073)
8: Outside built-up areas	7.3 (0.405)	29.4 (0.341)	5.6 (0.191)	25.2 (0.040)	3.6 (-0.023)	19.3 (0.038)
9: Urban	**8.9* (0.759)**	**32.5* (1.152)**	**8.5* (1.155)**	**32.4* (1.421)**	**5.3* (0.831)**	22.0 (0.414)

*Table 4. Percentage of synchrony intervals of head angles and angular velocity for pitch, roll and yaw for the analysed road parts. In the parenthesis the effect sizes are presented. * $p < 0.01$.*

	PITCH		ROLL		YAW	
	Angle (%)	Angular velocity (%)	Angle (%)	Angular velocity (%)	Angle (%)	Angular velocity (%)
A	11.6 (0.478)	33.4 (0.278)	5.3 (-0.034)	**38.1* (0.832)**	3.3 (-0.129)	22.5 (0.258)
B	10.9 (0.538)	33.2 (0.347)	12.0 (0.453)	**35.4* (0.632)**	2.8 (-0.344)	23.7 (0.240)
C	7.4 (0.073)	28.1 (-0.028)	4.9 (-0.079)	33.7 (0.482)	4.0 (0.030)	23.5 (0.214)
D	9.3 (0.314)	27.7 (0.108)	8.6 (0.220)	30.4 (0.279)	4.7 (0.067)	20.7 (-0.034)
E	5.5 (-0.089)	28.8 (0.027)	5.6 (-0.006)	31.2 (0.286)	4.0 (0.053)	21.6 (-0.031)
F	9.3 (0.269)	24.9 (-0.239)	2.4 (-0.299)	22.8 (-0.257)	3.4 (0.143)	26.2 (0.468)
G	5.9 (-0.100)	27.1 (-0.109)	7.6 (0.272)	31.5 (0.225)	2.6 (-0.112)	20.9 (0.159)
H	3.1 (-1.012)	25.5 (-0.332)	3.2 (-0.733)	26.0 (0.052)	4.7 (0.284)	19.8 (0.369)
I	3.7 (-0.239)	32.2 (0.193)	6.8 ((0.228))	28.6 (0.198)	2.0 (-0.262)	22.1 (0.062)
J	6.0 (0.053)	31.6 (0.397)	4.0 (-0.116)	24.8 (-0.126)	4.6 (0.204)	23.7 (0.267)
K	9.3 (0.183)	31.5 (0.168)	7.6 (0.125)	**37.0* (0.626)**	3.9 (-0.020)	23.9 (0.246)
L	9.6 (0.292)	31.8 (0.205)	9.3 (0.312)	27.6 (0.006)	5.1 (0.180)	20.6 (-0.146)
M	9.0 (0.268)	28.3 (-0.114)	10.2 (0.448)	31.6 (0.249)	6.2 (0.363)	25.8 (0.427)
N	11.6 (0.060)	29.7 (0.159)	**14.6* (0.667)**	37.3 (0.484)	9.8 (0.486)	**28.3* (0.580)**

*Table 5. Percentage of synchrony intervals of head angles and angular velocity for pitch, roll and yaw for all cornering events. In the parenthesis the effect sizes are presented. * $p < 0.01$.*

Head angle

Table 4 shows the results of the analysis of the frequency of synchrony for all head angles for the total route, Part 1 – pre-task, Part 2 – post-task and the different road segments. The percentage of synchrony for the head angle pitch was significantly different between the detected synchrony from the pseudosynchrony for the total trip, Part 1 – pre-task and the road segments 1 and 9 – urban. The head angle roll also showed a significant difference between real- and surrogate data for the total route, Part 1 – pre-task and the road segments 1 – urban. Part 2 – post-task, indicated as well a significant difference for the head angle roll. The head angle yaw showed only one single significant difference between detected- and pseudosynchrony. This was road segment 9 – urban. The only cornering event where a significantly higher percentage of synchrony was detected was cornering event N for the roll angle (Table 5). All other road segments and cornering events did not indicate a significant difference between the detected- and pseudosynchrony.

No differentiation between detected synchrony and pseudosynchrony was found for most of the segments. Therefore, no ANOVA analysis to confirm or reject the second hypothesis was conducted. Since only the urban segments confirmed the frequency of synchrony, the second hypothesis could partly be confirmed. Synchrony was identified in the urban segments, and therefore, more synchrony did occur at this road type than the outside built-up areas and highway segments. However, the frequency

of synchrony for the built-up areas and highway segments could not be confirmed, so it could not be verified that synchrony occurred here at all.

Head angular velocity

Table 4 presents the results of the percentage of synchrony for the angular velocity for all three head angles. The percentage of synchrony for pitch showed a significant difference between detected- and pseudosynchrony for the total route, Part 1 – pre-task, Part 2 – post-task, and road segments 1 and 9 – urban, and segment 4 – highway. The results of the angular velocity in roll directions showed similar results as the head angle roll. Significant differences between detected synchrony of drivers and passengers and pseudosynchrony were indicated for the total route, Part 1- pre-task, Part 2 – post-task, and the road segments 1 and 9 – urban. The results of the percentage of synchrony for yaw showed a significant difference between detected- and pseudosynchrony for the total route, Part 1 – pre-task, and road segment 1 – urban, segment 2 – outside built-up areas, segment 3 – entry highway, and segment 5 – entry and exit from the highway. Significant differences between the real- and surrogate data were found for corners A, B and K for the roll angle (Table 5). The percentage of detected synchrony and pseudosynchrony for cornering event N in angular velocity yaw showed a significant difference. The locations of these corners are in the urban segments. For all other cornering events, no significant difference between real- and surrogate data was identified.

Again, there was no significant differentiation for all urban, outside built-up areas and highway segments between the real- and surrogate data. Therefore, no ANOVA analysis was implemented.

Strength of synchrony

The detected strength of synchrony for a road segment or cornering event between drivers and passengers was compared to pseudosynchrony for all head angles and angular velocities.

Head angle

The mean peak correlation regarding the detected- and pseudosynchrony for the head angles and all road segments are summarised in Table 6. Regarding the head angle pitch, there was a significant difference between real - and surrogate data for the total route, Part 1 – pre-task, Part 2 – post-task, the road segments 1 and 9 – urban, the segment 2 and 8 – outside built-up areas, segment 3 – the entry of highway and segment 4 – highway. The effect sizes of all these findings are large (> 0.700) except segment 4- highway. For corners B, C, F and J, also a significant difference between real- and surrogate data was found for the head angle pitch. The head angle, roll, showed a significant difference for the total route, Part 1-pre task, Part 2 – post-task, road segments 1 and 9 – urban, segment 5 – entry and exit from highway and segment 7 – exit highway. No cornering events showed a significant difference between the detected- and the pseudosynchrony for roll angle (Table 7). Significant differences were found for the yaw angle between detected- and pseudosynchrony for the total route, Part 1 – pre-task and road segment 1 and 9 – urban and segment 3 – entry highway. Cornering events A, C, F, G, I, J, L and N, showed significant differences.

No ANOVA analysis to test the second hypothesis was employed due to the inability to differentiate real- and surrogate data for the required road segment. Again, the urban segments for the pitch, roll and yaw showed a significant difference. Therefore, the strength of synchrony is most likely higher in the urban segments than the other road types.

Head angular velocity

Angular velocity pitch showed a significant difference between detected- and pseudosynchrony for all road segments, except segment 3 – Entry highway. Almost all effect sizes are large (> 0.800). For cornering events, A, C and M, the detected synchrony was differentiated from pseudosynchrony. The angles yaw and roll showed different results. The mean peak correlation in roll direction for the detected synchrony between drivers and passenger versus pseudosynchrony was significantly higher for the total route, Part 1 – pre-task, Part 2 – post-task, road segments 1 and 9 – urban, segment 2 – outside built-up areas, segment 5 – exit and entry highway and segments 4 and 6 – highway (Table 6). The corners A, B, C, K, L and N showed a significantly higher mean peak correlation in the detected synchrony for the real data than the surrogate data. These corners were all located in the urban segments (Table 7). The mean peak correlation between drivers and passengers for the angular velocity in the yaw direction is significantly higher for the total route, Part 1 – pre-task, road segments 1 and 9 – urban, road segment 2 – outside built-up areas and road segment 4 – highway. The cornering events C, E and G showed a significantly higher mean peak correlation for the detected synchrony compared to pseudosynchrony.

The angular velocity in pitch showed a significant difference between real- and surrogate data for all road segments regarding the second hypothesis. Therefore, an analysis to check the second hypothesis was conducted. The one way ANOVA resulted in $F = 2.95$ and $p = 0.055$. Figure 11 shows the results in a boxplot. The p-value > 0.05 indicates no significant difference between the three road types was detected for the strength of synchrony for head angular velocity pitch.

	PITCH		ROLL		YAW	
	Angle	Angular velocity	Angle	Angular velocity	Angle	Angular velocity
Total route	**0.394* (1.631)**	**0.336* (1.401)**	**0.387* (1.079)**	**0.330* (2.617)**	**0.390* (0.956)**	**0.292* (01.106)**
Part 1: Pre-task	**0.397* (0.934)**	**0.338* (1.258)**	**0.392* (0.611)**	**0.334* (1.910)**	**0.394* (0.844)**	**0.297 (0.933)**
Part 2: Post-task	**0.393* (1.143)**	**0.340* (1.470)**	**0.387* (0.888)**	**0.328* (1.452)**	0.385 (0.414)	0.288 (0.199)
1: Urban	**0.398* (0.953)**	**0.346* (1.149)**	**0.400* (0.635)**	**0.352* (1.569)**	**0.402* (0.657)**	**0.304* (0.578)**
2: Outside built-up areas	**0.394* (0.771)**	**0.332* (1.260)**	0.379 (0.077)	**0.322* (1.249)**	0.380 (0.360)	**0.288* (0.580)**
3: Entry highway	**0.451* (0.706)**	0.326 (0.331)	0.402 (0.344)	0.344 (0.424)	**0.486* (1.225)**	0.321 (0.457)
4: Highway	**0.396* (0.569)**	**0.336* (0.888)**	0.384 (0.110)	**0.326* (0.572)**	0.385 (0.211)	**0.303* (0.822)**
5: Exit and Entry highway	0.374 (0.122)	**0.316* (0.724)**	**0.393* (0.633)**	**0.318* (0.640)**	0.391 (0.198)	0.296 (0.346)
6: Highway	0.393 (0.469)	**0.337* (1.016)**	0.377 (0.251)	**0.321* (0.599)**	0.387 (-0.013)	0.284 (-0.215)
7: Exit highway	0.378 (0.310)	**0.323* (0.727)**	**0.404* (0.666)**	0.324 (0.416)	0.414 (0.545)	0.294 (0.242)
8: Outside built-up areas	**0.392* (0.835)**	**0.334* (1.201)**	0.378 (0.334)	0.310 (0.405)	0.375 (0.123)	0.274 (-0.142)
9: Urban	**0.401* (1.194)**	**0.350* (1.436)**	**0.394* (0.763)**	**0.358* (2.082)**	**0.409* (0.813)**	**0.305* (0.606)**

*Table 6. Mean peak correlation of head angles and angular velocity for pitch, roll and yaw for the analysed road parts. In the parenthesis the effect sizes are presented. * $p < 0.01$.*

	PITCH		ROLL		YAW	
	Angle	Angular velocity	Angle	Angular velocity	Angle	Angular velocity
A	0.386 (0.091)	**0.369* (1.046)**	0.399 (0.229)	**0.386* (1.070)**	**0.429* (0.584)**	0.329 (0.387)
B	**0.442* (0.618)**	0.350 (0.565)	0.450 (0.473)	**0.373* (0.857)**	0.421 (0.217)	0.320 (0.213)
C	**0.447* (0.587)**	**0.366* (0.604)**	0.410 (0.167)	**0.378* (0.721)**	0.469 (0.579)	**0.361* (0.674)**
D	0.383 (0.119)	0.314 (0.130)	0.372 (-0.151)	0.331 (0.544)	0.404 (0.184)	0.304 (0.022)
E	0.412 (0.303)	0.332 (0.346)	0.370 (-0.050)	0.331 (0.202)	0.420 (0.270)	**0.357* (0.896)**
F	**0.453* (0.627)**	0.340 (0.348)	0.416 (0.526)	0.355 (0.488)	**0.546* (1.157)**	0.331 (0.451)
G	0.370 (-0.099)	0.305 (0.057)	0.415 (0.276)	0.328 (0.184)	**0.491* (0.808)**	**0.354* (0.697)**
H	0.364 (0.102)	0.313 (0.340)	0.385 (0.282)	0.320 (0.341)	0.390 (0.066)	0.297 (0.079)
I	0.407 (0.278)	0.276 (-0.182)	0.452 (0.445)	0.340 (0.348)	**0.490* (0.584)**	0.337 (0.384)
J	**0.426* (0.591)**	0.315 (0.159)	0.422 (0.448)	0.311 (-0.031)	**0.469* (0.680)**	0.298 (0.014)
K	0.401 (0.208)	0.323 (0.248)	0.395 (0.179)	**0.375* (0.637)**	0.401 (0.205)	0.342 (0.491)
L	0.392 (0.058)	0.324 (0.223)	0.430 (0.414)	**0.368* (0.682)**	**0.487* (0.707)**	0.346 (0.348)
M	0.423 (0.447)	**0.354* (0.787)**	0.393 (0.211)	0.330 (0.180)	0.430 (0.327)	0.320 (0.101)
N	0.371 (0.069)	0.343 (0.509)	0.400 (0.359)	**0.413* (1.190)**	**0.435* (0.780)**	0.328 (0.273)

*Table 7. Mean peak correlation of head angles and angular velocity for pitch, roll and yaw for all cornering events. In the parenthesis the effect sizes are presented. * $p < 0.01$.*

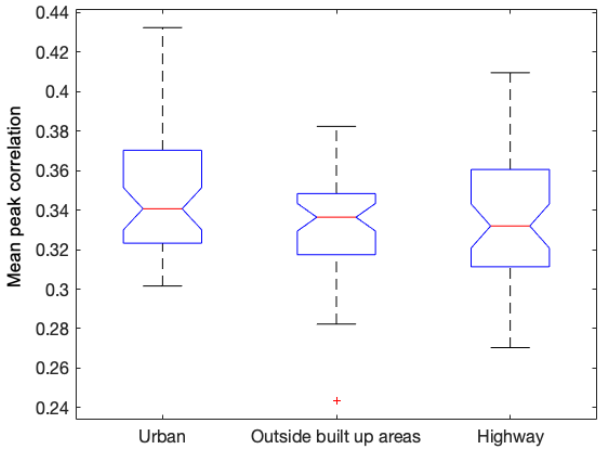

Figure 11. Results of one-way ANOVA for three road types, urban, outside built-up areas and highway versus the mean peak correlation of head angular velocity – pitch.

Overview results

The results of the strength of synchrony showed a significant difference between real- and surrogate data for more road segments than the frequency of synchrony. For the yaw angle, no difference between detected- and pseudosynchrony was found for the frequency of synchrony except the road segment 9 – urban. However, regarding the strength, synchrony was detected for the total route, Part 1 – pre-task, Part 2 – post-task and road segment 1 and 9 – urban and road segment 3 – entry highway. The pitch angle showed the frequency of synchrony for segments 1 and 9 – urban. For comparing real- and surrogate data regarding the strength of synchrony, segments 1 and 9 – urban showed the same results. However, the strength of synchrony showed significant findings for more segments. The last angle, roll, showed synchrony for both frequency and strength of synchrony for the total route, Part 1 – pre-task, Part 2 – post-task and road segments 1 and 9 – urban, segment 5 – exit and entry from the highway and segment 7 – exit highway. However, the effect sizes were medium (< 0.700).

The results of the angular velocity showed a significant difference between the real- and surrogate data for more segments compared to the head angle. The angle pitch showed a significant difference for the mean peak correlation for all road segments except segment 3 – entry highway. The effect sizes of these findings were large. The frequency of synchrony was significantly different for the total route, Part 1 – pre-task, Part 2 – post-task, segments 1 and 9 – urban and segment 4 – highway. The yaw angle showed different findings for the frequency- and strength of synchrony. This amplifies the different nature of both algorithms. The angular velocity in the roll direction showed a significant difference for both algorithms for the total route, Parts 1 – pre-task and Part 2 – post-task again, and road segments 1 and 9 – urban. Also, a higher mean peak correlation was found for segment 2 – outside built-up areas, 5 – entry and exit from highway and 6 – highway.

The results regarding synchrony in the cornering events were mixed. Therefore, no observable patterns were found. The cornering events where the detected synchrony was differentiated from pseudosynchrony did not indicate any correlation between the segment the cornering events was located and the identification of synchrony.

Discussion

The aim of the present study was to identify synchrony of drivers and passengers in head orientation and movement for different road types and cornering events. The data from a real-world driving experiment was used for the analysis. The identification of synchrony was derived by implementing WCLC and two different peak-picking algorithms. The first peak-picking algorithm of Altmann focused on the frequency of synchrony, and the second peak-picking algorithm of Boker et al. determined the strength of synchrony for the total length of the studied interaction. Since behavioural synchrony can appear due to coincidence, the synchrony detected by the algorithm was compared to pseudosynchrony to legitimise the findings.

The results showed that it was impossible to distinguish detected synchrony from pseudosynchrony for each head angle for every road segment and cornering event by the applied methods. The segments where a significant difference between the real- and the surrogate data occurred confirmed that the identification of synchrony between drivers and passengers for that specific road segment or cornering event was possible. The cases where no differentiation was found between detected- and pseudosynchrony could indicate: (1) there is no synchrony between drivers and passengers for that specific head angle or head angular velocity for the analysed road segment or cornering event, or (2) the applied method with the corresponding settings was unable to capture synchrony. In some cases, the two peak-picking algorithms gave different outcomes. Since both algorithms rely on different facets of synchrony, the findings were expected to differ. This highlights the algorithms' differences. Driver-passenger synchrony is a new field of study. Therefore, this was a more exploratory study including two different methods to capture synchrony to better understand this driver-passenger synchrony. Also, identified synchrony for a single head angle did not necessarily indicate synchrony in the other head angles. Consequently, the interpretation of the findings for the different head angles will be discussed separately.

Zikovitz and Harris [13] showed differentiation between active and passive passengers in head tilt (head angle – roll). In the current study, passengers acted like passengers in the first part of the trip. In the second part, the passengers were asked to be attentive. However, the findings did not show results that are in line with the findings of Zikovitz and Harris. The results for Part 2 and the separate segments and corners for the second part of the trip did not show noticeable findings.

Former studies focusing on synchrony in nonverbal behaviour for head movement had considered the head angle pitch [24], [25]. The head angle pitch was studied for DMS [51], [52]. However, the interpretation of the identified synchrony in this study for the pitch angle could reflect various things. First, it could indicate synchrony in head angle and angular velocity. Secondly, the vehicle undergoes vibrations. These vibrations impact the pitch angle of the heads' of drivers and passengers. Therefore, the detected synchrony could not necessarily indicate synchrony in behaviour but could emerge through vibrations of the road. Another element worth noting was the available areas of interest to which the driver and passenger might devote their attention. The driver was able to look into the rear-view mirror and at the dashboard. On the other hand, the passenger was allowed to involve in non-driving-related secondary tasks such as checking messages on their mobile phone. These areas of interest do affect the head pitch angle.

The head angle yaw contributes to attention allocation during driving [51], [52]. The results showed that for both algorithms, detected synchrony could be differentiated from pseudosynchrony for the total route for the head angular velocity of the frequency of synchrony and the head angle and head angular velocity

of the strength of synchrony. This could indicate that passengers and drivers are allocating their attention to the same things regularly.

Validity of algorithms

Figure 6 shows the difficulty of the identification of synchrony sequences by visual inspection. This underlines the need for a visual inspecting algorithm. However, the validity of the algorithms for deriving synchrony between drivers and passengers should be discussed.

In this study, first, the frequency of synchrony was studied. The synchrony calculated for the real data was compared to surrogate data to establish that synchrony was not present by chance. The window size of the WCLC partly determined the possibility to detect synchrony intervals for a segment. A synchrony interval was assigned when at least ten subsequential R^2 values were larger than 0.1. The R^2 values were 200 milliseconds apart, so at least 2 seconds of synchrony was required to be assigned as synchrony intervals. Road segments 3 and 7 were shorter, as well as the cornering events. This made it harder to show a significant difference because there are a smaller number of intervals possible. Therefore, the results of the road segments 3 and 7 and the cornering events are more challenging to interpret.

Secondly, the strength of synchrony over the complete segments was studied by applying the peak-picking algorithm of Boker et al. [38]. This method assumes synchrony was present during the complete duration and calculates the mean peak correlation over the analysed segment. However, during driving, it is not easy to assume synchrony was continuously present.

Limitations and recommendations

A limitation of the OpenFace 2.0 algorithm was its detection rate. For some participants, more than 20% of the data was missing. This occurred primarily in sections where fast and large head movements occurred and the participant's face was difficult to detect due to lighting. However, most of the participants had a good amount of data left (> 90%) for the analysis. Although the OpenFace 2.0 had a high detection rate compared to other face detection algorithms, the algorithm could not detect the drivers' and passengers' heads continuously. Since the algorithm could not detect the drivers' and passengers' heads for every frame, this led to missing values. These missing values were interpolated. The reliability of interpolating the missing values decreased when many missing values occurred in a sequence. In the case of relatively fast and large head movements, the OpenFace 2.0 had more difficulty detecting the head of the drivers and passengers. In future research, studies that incorporate face cameras should look into more improved video-based tracking methods. The pose-estimation OpenFace 2.0 for determining the head orientation of driver and passenger was last updated three years ago. New techniques are continuously developed for head detection. These new techniques will have an improved prediction and accuracy compared to OpenFace 2.0 [52].

The second limitation was the window size. To meet the local stationarity assumption, the window size of the WCLC in this study was 60 frames or 2 seconds. Although literature states that smaller bandwidth (approximately 65 frames) distinguishes well between synchrony and pseudosynchrony [28], improving the sampling frequency during the experiment is recommended. The small window size with a relatively low correlation could lead to less reliable results. For example, the study of Asfenfelter et al. [24] contained a sampling rate of 80 Hz and a window size of 160 observations, e.g. 2 seconds.

Future research for real driving studies could include a screen to separate the front seats, where the participants are seated, from the backseats, where the experimenters are seated. Due to the increased number of visible faces, the OpenFace 2.0 has difficulty recognising the correct head. The detection rate

could be improved by isolating the participants. Additionally, by separating experimenters from the participant, the relationship between driver and passengers could be explored more thoroughly.

Former research revealed that the presence of passengers could have a positive or negative effect on the driver's performance [7], [8]. Since the results indicated that synchronisation might be identified for specific road segments, a future study on the relationship of synchronous behaviour of drivers and passengers and the positive and negative influence the passenger has on driver safety is proposed. Does synchronous behaviour between drivers and passengers indicate that the passengers' presence positively influences driving safety?

The WCLC method was a linear time series method. Continuously, new methods for measuring synchrony are introduced—for example, the Wavelet multiscale synchrony, combining frequency and time series analysis. This new method is still under development. Since this is no linear time series method, the stationarity requirement does not have to be met. For future studies regarding head movement, these methods could be applied to analyse synchrony [53].

Another research opportunity that emerged as a result of this research is examining synchrony in gaze strategy between drivers and passengers. Since both eye- and head movements are used for gaze allocation [51], it is valuable to investigate synchrony incorporating the gaze instead of only eye- or head movement. Numerous variables may influence eye- or head movements for gaze strategy, for instance, the personal preference [51].

This study focussed on the head movements measurable by a camera. Another opportunity that arises from this study is investigating synchrony in attention allocation. Eye-trackers could provide information about where the drivers and passengers are looking during driving.

Conclusion

The current study aimed to identify synchrony in head orientation and movement between drivers and passengers for various road types and cornering events. Drivers and passengers interact and are exposed to the same visual driving scene, which could results in behavioural synchrony. Advanced driving assistance systems can measure synchrony of head angle and head angular velocity, providing insight into the interaction and attention allocation of drivers and passengers. This could be implemented to create a safer driving environment.

Since identifying synchrony between drivers and passengers is a new area of research, this study examined two facets of synchrony: the frequency- and strength of synchrony for various road segments and cornering events. First, a video-based pose estimation method called OpenFace 2.0 was used to determine the drivers'- and passengers' head angles using face cameras mounted in the vehicle.
Next, a windowed cross-lagged correlation method was implemented to determine the correlation between the signals of drivers and passengers with a time lag. Then, two different peak-picking algorithms were employed. The first peak-picking algorithm was based on the frequency of synchrony whereas the second peak-picking algorithm analysed the strength of synchrony. The output of both algorithms was compared to synchrony that may appear by chance, pseudosynchrony. Lastly, the results for the different road types were compared.

The two distinct algorithms for identifying different facets of synchrony resulted in a different outputs. The analysis on the frequency of synchrony showed that only for a couple of road segments the detected synchrony was differentiated from the pseudosynchrony. In the road segments – urban, the detected synchrony was significantly different from pseudosynchrony for almost all conditions. The same results were given for the analysis on the total route and Part 1 – pre-task. Almost no synchrony was identified for the cornering events. The results on the analysis on the strength of synchrony showed that the detected synchrony was significantly different from pseudosynchrony for more road segments compared to the frequency of synchrony. Synchrony was identified for the analysis on the total route and for almost all conditions for Part 1 – pre-task and Part 2 – post-task. Again, the analysis shows that in the road segments – urban synchrony was identified. Some cornering events identified synchrony, however, no observable pattern was found.

The frequency of synchrony showed that synchrony was identified for less road segments than the strength of synchrony showed. However, the results can be summarised which leads to a conclusion regarding the research aim. It was possible for almost all conditions to differentiate between detected synchrony and pseudosynchrony for the total route, Part 1 – pre-task and the road segments – urban. This implies synchrony was present in the urban road types. Also, these results demonstrated that synchrony was detected in segments with a longer duration, the total route and Part 1 – pre-task. The road segments where no synchrony was detected could suggest two things. First, synchrony was not present in the road segment for the analysed condition or second, synchrony could not be measured by the applied method with the applied settings.

Synchrony of head orientation and movement was identified for certain road segments. These findings indicate that this is an area of research with potential for further studies. Since synchrony was detected for some road segments, it is recommended to study what synchrony between drivers and passengers could indicate. Former research showed that interaction between drivers could positively and negatively influence the driver's performance. Thus, a study examining the relationship between synchronisation and the type of influence passengers have on the driver provides an excellent opportunity to learn about driver-passenger interaction in road safety.

References

[1] J. C. Stutts, D. W. Reinfurt, and E. A. Rodgman, 'The role of driver distraction in crashes: an analysis of 1995-1999 Crashworthiness Data System Data', *Annu. Proc. Assoc. Adv. Automot. Med.*, vol. 45, pp. 287–301, 2001.

[2] M. J. M. Sullman, F. Prat, and D. K. Tasci, 'A Roadside Study of Observable Driver Distractions', *Traffic Inj. Prev.*, vol. 16, no. 6, pp. 552–557, Aug. 2015, doi: 10.1080/15389588.2014.989319.

[3] C. Huisingh, R. Griffin, and G. McGwin, 'The prevalence of distraction among passenger vehicle drivers: a roadside observational approach', *Traffic Inj. Prev.*, vol. 16, no. 2, pp. 140–146, 2015, doi: 10.1080/15389588.2014.916797.

[4] K. Prepin and P. Gaussier, 'How an Agent Can Detect and Use Synchrony Parameter of Its Own Interaction with a Human?', in *Development of Multimodal Interfaces: Active Listening and Synchrony: Second COST 2102 International Training School, Dublin, Ireland, March 23-27, 2009, Revised Selected Papers*, A. Esposito, N. Campbell, C. Vogel, A. Hussain, and A. Nijholt, Eds. Berlin, Heidelberg: Springer, 2010, pp. 50–65. Doi: 10.1007/978-3-642-12397-9_4.

[5] O. Mayo and I. Gordon, 'In and out of synchrony—Behavioral and physiological dynamics of

dyadic interpersonal coordination', *Psychophysiology*, vol. 57, no. 6, p. e13574, 2020, doi: https://doi.org/10.1111/psyp.13574.
[6] O. Oullier, G. C. de Guzman, K. J. Jantzen, J. Lagarde, and J. A. Scott Kelso, 'Social coordination dynamics: Measuring human bonding', *Soc. Neurosci.*, vol. 3, no. 2, pp. 178–192, Jun. 2008, doi: 10.1080/17470910701563392.
[7] M. Chan, S. Nyazika, and A. Singhal, 'Effects of a front-seat passenger on driver attention: An electrophysiological approach', *Transp. Res. Part F Traffic Psychol. Behav.*, vol. 43, pp. 67–79, Nov. 2016, doi: 10.1016/j.trf.2016.09.016.
[8] J. P. Allen and B. B. Brown, 'Adolescents, Peers, and Motor Vehicles: The Perfect Storm?', *Am. J. Prev. Med.*, vol. 35, no. 3, Supplement, pp. S289–S293, Sep. 2008, doi: 10.1016/j.amepre.2008.06.017.
[9] B. Aldridge, M. Himmler, L. Aultman-Hall, and N. Stamatiadis, 'Impact of Passengers on Young Driver Safety', *Transp. Res. Rec.*, vol. 1693, no. 1, pp. 25–30, Jan. 1999, doi: 10.3141/1693-05.
[10] C. Orsi, P. Marchetti, C. Montomoli, and A. Morandi, 'Car crashes: The effect of passenger presence and other factors on driver outcome', *Saf. Sci.*, vol. 57, pp. 35–43, Aug. 2013, doi: 10.1016/j.ssci.2013.01.017.
[11] E. K. Chung, B. Choe, J. E. Lee, J. I. Lee, and Y. W. Sohn, 'Effects of an adult passenger on young adult drivers' driving speed: Roles of an adult passenger's presence and driving tips from the passenger', *Accid. Anal. Prev.*, vol. 67, pp. 14–20, Jun. 2014, doi: 10.1016/j.aap.2014.01.024.
[12] L. Chandrasekaran, A. Crookes, and T. C. Lansdown, 'Driver situation awareness – Investigating the effect of passenger experience', *Transp. Res. Part F Traffic Psychol. Behav.*, vol. 61, pp. 152–162, Feb. 2019, doi: https://doi.org/10.1016/j.trf.2017.12.007.
[13] D. C. Zikovitz and L. R. Harris, 'Head tilt during driving', *Ergonomics*, vol. 42, no. 5, pp. 740–746, May 1999, doi: 10.1080/001401399185414.
[14] F. Schewe, H. Cheng, A. Hafner, M. Sester, and M. Vollrath, 'Occupant Monitoring in Automated Vehicles: Classification of Situation Awareness Based on Head Movements While Cornering', *Proc. Hum. Factors Ergon. Soc. Annu. Meet.*, vol. 63, no. 1, pp. 2078–2082, Nov. 2019, doi: 10.1177/1071181319631048.
[15] C. D. D. Cabrall, J. C. F. de Winter, V. Petrovych, and R. Happee, 'Concurrently Recorded Eye Movements of Drivers and Passengers: Towards a Driver Monitoring System [Manuscript in preparation].', 2021.
[16] M. Beggatio, F. Hartwich, K. Schleinitz, J. Krems, I. Othersen, and I. Petermann-Stock, 'What would drivers like to know during automated driving? Information needs at different levels of automation.', p. 6, 2015.
[17] D. Damböck, T. Weißgerber, M. Kienle, and K. Bengler, 'Requirements for cooperative vehicle guidance', in *16th International IEEE Conference on Intelligent Transportation Systems (ITSC 2013)*, Oct. 2013, pp. 1656–1661. Doi: 10.1109/ITSC.2013.6728467.
[18] N. Hatfield *et al.*, 'Analysis of Visual Scanning Patterns Comparing Drivers of Simulated L2 and L0 Systems', *Transp. Res. Rec.*, vol. 2673, no. 10, pp. 755–761, Oct. 2019, doi: 10.1177/0361198119852339.
[19] B. Metz and H.-P. Krueger, 'Measuring visual distraction in driving: the potential of head movement analysis', *IET Intell. Transp. Syst.*, vol. 4, no. 4, pp. 289–297, Dec. 2010, doi: 10.1049/iet-its.2009.0116.
[20] O. Palinko, A. L. Kun, A. Shyrokov, and P. Heeman, 'Estimating cognitive load using remote eye tracking in a driving simulator', in *Proceedings of the 2010 Symposium on Eye-Tracking Research & Applications – ETRA '10*, Austin, Texas, 2010, p. 141. Doi: 10.1145/1743666.1743701.
[21] J. Schmidt, R. Laarousi, W. Stolzmann, and K. Karrer-Gauß, 'Eye blink detection for different driver states in conditionally automated driving and manual driving using EOG and a driver camera',

Behav. Res. Methods, vol. 50, no. 3, pp. 1088–1101, Jun. 2018, doi: 10.3758/s13428-017-0928-0.
[22] G. Marquart, C. Cabrall, and J. de Winter, 'Review of Eye-related Measures of Drivers' Mental Workload', *Procedia Manuf.*, vol. 3, pp. 2854–2861, Jan. 2015, doi: 10.1016/j.promfg.2015.07.783.
[23] A. C. Hayley, B. Shiferaw, B. Aitken, F. Vinckenbosch, T. L. Brown, and L. A. Downey, 'Driver monitoring systems (DMS): The future of impaired driving management?', *Traffic Inj. Prev.*, vol. 22, no. 4, pp. 313–317, May 2021, doi: 10.1080/15389588.2021.1899164.
[24] K. Ashenfelter, S. Boker, J. Waddell, and N. Vitanov, 'Spatiotemporal Symmetry and Multifractal Structure of Head Movements During Dyadic Conversation', *J. Exp. Psychol. Hum. Percept. Perform.*, vol. 35, pp. 1072–91, Aug. 2009, doi: 10.1037/a0015017.
[25] S. Bhatia, R. Goecke, Z. Hammal, and J. F. Cohn, 'Automated Measurement of Head Movement Synchrony during Dyadic Depression Severity Interviews', in *2019 14th IEEE International Conference on Automatic Face Gesture Recognition (FG 2019)*, May 2019, pp. 1–8. Doi: 10.1109/FG.2019.8756509.
[26] A. Paxton and R. Dale, 'Interpersonal Movement Synchrony Responds to High- and Low-Level Conversational Constraints', *Front. Psychol.*, vol. 8, 2017, doi: 10.3389/fpsyg.2017.01135.
[27] D. Schoenherr *et al.*, 'Identification of movement synchrony: Validation of windowed cross-lagged correlation and -regression with peak-picking algorithm', *PloS ONE*, vol. 14, no. 2, Feb. 2019, doi: 10.1371/journal.pone.0211494.
[28] R. G. Moulder, S. M. Boker, F. Ramseyer, and W. Tschacher, 'Determining synchrony between behavioral time series: An application of surrogate data generation for establishing falsifiable null-hypotheses', *Psychol. Methods*, vol. 23, no. 4, pp. 757–773, 2018, doi: 10.1037/met0000172.
[29] F. Ramseyer and W. Tschacher, 'Nonverbal Synchrony in Psychotherapy: Coordinated Body Movement Reflects Relationship Quality and Outcome', *J. Consult. Clin. Psychol.*, vol. 79, pp. 284–95, Jun. 2011, doi: 10.1037/a0023419.
[30] R. Feniger-Schaal, D. Schönherr, U. Altmann, and B. Strauss, 'Movement Synchrony in the Mirror Game', *J. Nonverbal Behav.*, vol. 45, no. 1, pp. 107–126, Mar. 2021, doi: 10.1007/s10919-020-00341-3.
[31] J. Paulick *et al.*, 'Nonverbal Synchrony: A New Approach to Better Understand Psychotherapeutic Processes and Drop-Out', *J. Psychother. Integr.*, vol. 28, Dec. 2017, doi: 10.1037/int0000099.
[32] F. Ramseyer and W. Tschacher, 'Nonverbal Synchrony or Random Coincidence? How to Tell the Difference', in *Development of Multimodal Interfaces: Active Listening and Synchrony*, vol. 5967, A. Esposito, N. Campbell, C. Vogel, A. Hussain, and A. Nijholt, Eds. Berlin, Heidelberg: Springer Berlin Heidelberg, 2010, pp. 182–196. Doi: 10.1007/978-3-642-12397-9_15.
[33] K. Fujiwara and K. Yokomitsu, 'Video-based tracking approach for nonverbal synchrony: A comparison of Motion Energy Analysis and OpenPose', *Behav. Res. Methods*, May 2021, doi: 10.3758/s13428-021-01612-7.
[34] L. A. Renier, M. Schmid Mast, N. Dael, and E. P. Kleinlogel, 'Nonverbal Social Sensing: What Social Sensing Can and Cannot Do for the Study of Nonverbal Behavior From Video', *Front. Psychol.*, vol. 12, p. 606548, Jul. 2021, doi: 10.3389/fpsyg.2021.606548.
[35] T. Baltrusaitis, A. Zadeh, Y. C. Lim, and L. Morency, 'OpenFace 2.0: Facial Behavior Analysis Toolkit', in *2018 13th IEEE International Conference on Automatic Face Gesture Recognition (FG 2018)*, May 2018, pp. 59–66. Doi: 10.1109/FG.2018.00019.
[36] D. Schoenherr *et al.*, 'Quantification of nonverbal synchrony using linear time series analysis methods: Lack of convergent validity and evidence for facets of synchrony', *Behav. Res. Methods*, vol. 51, no. 1, pp. 361–383, Feb. 2019, doi: 10.3758/s13428-018-1139-z.
[37] E. Delaherche, M. Chetouani, A. Mahdhaoui, C. Saint-Georges, S. Viaux, and D. Cohen, 'Interpersonal Synchrony: A Survey of Evaluation Methods across Disciplines', *IEEE Trans. Affect.*

Comput., vol. 3, no. 3, pp. 349–365, Jul. 2012, doi: 10.1109/T-AFFC.2012.12.
[38] S. M. Boker, M. Xu, J. L. Rotondo, and K. King, 'Windowed cross-correlation and peak picking for the analysis of variability in the association between behavioral time series', *Psychol. Methods*, pp. 338–355.
[39] F. D. Schönbrodt and M. Perugini, 'At what sample size do correlations stabilize?', *J. Res. Personal.*, vol. 47, no. 5, pp. 609–612, Oct. 2013, doi: 10.1016/j.jrp.2013.05.009.
[40] U. Altmann, 'Investigation of Movement Synchrony Using Windowed Cross-Lagged Regression', in *Analysis of Verbal and Nonverbal Communication and Enactment. The Processing Issues*, vol. 6800, A. Esposito, A. Vinciarelli, K. Vicsi, C. Pelachaud, and A. Nijholt, Eds. Berlin, Heidelberg: Springer Berlin Heidelberg, 2011, pp. 335–345. Doi: 10.1007/978-3-642-25775-9_31.
[41] E. Delaherche and M. Chetouani, 'Multimodal coordination: exploring relevant features and measures', in *Proceedings of the 2nd international workshop on Social signal processing – SSPW '10*, Firenze, Italy, 2010, p. 47. Doi: 10.1145/1878116.1878131.
[42] E. Murphy-Chutorian and M. M. Trivedi, 'Head Pose Estimation in Computer Vision: A Survey', *IEEE Trans. Pattern Anal. Mach. Intell.*, vol. 31, no. 4, pp. 607–626, Apr. 2009, doi: 10.1109/TPAMI.2008.106.
[43] E. Murphy-Chutorian and M. M. Trivedi, 'Head Pose Estimation and Augmented Reality Tracking: An Integrated System and Evaluation for Monitoring Driver Awareness', *IEEE Trans. Intell. Transp. Syst.*, vol. 11, no. 2, pp. 300–311, Jun. 2010, doi: 10.1109/TITS.2010.2044241.
[44] C. D. D. Cabrall, V. Petrovych, and R. Happee, 'Looking at Drivers and Passengers to Inform Automated Driver State Monitoring of In and Out of the Loop', in *Advances in Human Aspects of Transportation*, Cham, 2018, pp. 695–707. Doi: 10.1007/978-3-319-60441-1_67.
[45] Y. Zhu and K. Fujimura, 'Head pose estimation for driver monitoring', in *IEEE Intelligent Vehicles Symposium, 2004*, Jun. 2004, pp. 501–506. Doi: 10.1109/IVS.2004.1336434.
[46] M. Riehle, J. Kempkensteffen, and T. M. Lincoln, 'Quantifying Facial Expression Synchrony in Face-To-Face Dyadic Interactions: Temporal Dynamics of Simultaneously Recorded Facial EMG Signals', *J. Nonverbal Behav.*, vol. 41, no. 2, pp. 85–102, Jun. 2017, doi: 10.1007/s10919-016-0246-8.
[47] N. Lozza *et al.*, 'Nonverbal Synchrony and Complementarity in Unacquainted Same-Sex Dyads: A Comparison in a Competitive Context', *J. Nonverbal Behav.*, vol. 42, no. 2, pp. 179–197, Jun. 2018, doi: 10.1007/s10919-018-0273-8.
[48] L. Fridman, D. E. Brown, W. Angell, I. Abdić, B. Reimer, and H. Y. Noh, 'Automated synchronization of driving data using vibration and steering events', *Pattern Recognit. Lett.*, vol. 75, pp. 9–15, May 2016, doi: 10.1016/j.patrec.2016.02.011.
[49] U. Altmann, 'Synchronisation des nonverbalen Verhaltens', in *Synchronisation nonverbalen Verhaltens: Weiterentwicklung und Anwendung zeitreihenanalytischer Identifikationsverfahren*, U. Altmann, Ed. Wiesbaden: Springer Fachmedien, 2013, pp. 7–17. Doi: 10.1007/978-3-531-19815-6_2.
[50] W. S. Cleveland and S. J. Devlin, 'Locally Weighted Regression: An Approach to Regression Analysis by Local Fitting', *J. Am. Stat. Assoc.*, vol. 83, no. 403, pp. 596–610, Sep. 1988, doi: 10.1080/01621459.1988.10478639.
[51] L. Fridman, J. Lee, B. Reimer, and T. Victor, '"Owl" and "Lizard": patterns of head pose and eye pose in driver gaze classification', *IET Comput. Vis.*, vol. 10, no. 4, pp. 308–313, 2016, doi: 10.1049/iet-cvi.2015.0296.
[52] E. Murphy-Chutorian, A. Doshi, and M. M. Trivedi, 'Head Pose Estimation for Driver Assistance Systems: A Robust Algorithm and Experimental Evaluation', in *2007 IEEE Intelligent Transportation Systems Conference*, Sep. 2007, pp. 709–714. Doi: 10.1109/ITSC.2007.4357803.
[53] A. D. Likens and T. J. Wiltshire, 'Windowed multiscale synchrony: modeling time-varying and scale-localized interpersonal coordination dynamics', *Soc. Cogn. Affect. Neurosci.*, vol. 16, no. 1–2, pp. 232–245, Jan. 2021, doi: 10.1093/scan/nsaa130.

Appendix

Appendix A. Pre-processing the data

The face cameras employed in the real-world driving experiment captured the faces of the drivers and passengers. The videos are processed by the Facial behavioural toolbox, also called OpenFace 2.0, to extract valuable data from these facecam videos [35]. The OpenFace 2.0 toolkit recognises faces sufficiently although wearing eye-tracker glasses, can analyse video files and contains a high detection rate. The output of the OpenFace 2.0 includes facial landmarks, gaze and head orientation and facial action units. The head orientation is applicable for this study.

The OpenFace 2.0 could run the algorithm for two main settings: detecting one single face, or detecting multiple faces. The current application required the setting of multiple faces. Although the analysis takes more computer power and time, it is necessary since the participants in the front and the experiments in the back are visible on the facecams. The next step is to differentiate between the multiple faces detected by the OpenFace 2.0 declared in Figure A1by 'Filter 1'. The most reliable measure to distinguish the persons, drivers and passengers in the front from the experimenters in the back is the p-scale. The p-scale parameter, one of the outputs by the toolbox, signifies the distance to the camera. A larger p-scale indicates closer to the camera. So, if a frame_id occurs more than once in the data, OpenFace 2.0 has detected multiple faces. Then the data row containing the highest p-scale value is kept (the 'Filtered 1 data' in Figure A1).

The 'Filtered 1 data' regularly contains a significantly lower or higher p-scale value than the mean p-scale value. This can indicate two things: one, the algorithm has only detected one or two experimenters in the back or second, the algorithm cannot correctly detect the face and scaled the face smaller or larger. A second filtering method is required to remove the distinctly incorrect data samples, 'Filter 2' (Figure A1). Different approaches were implemented to differentiate between the correct and incorrect data samples. The most suitable method found for 'Filter 2' is a Gaussian Mixture Model(GMM) for first clustering the different detected faces by the p-scale values and next keeping the data within the mean +/- 3 standard deviation of the largest cluster found by the GMM (Figure A2). This method is shown to be robust and keeps 99,7% of the data of the largest detected cluster.

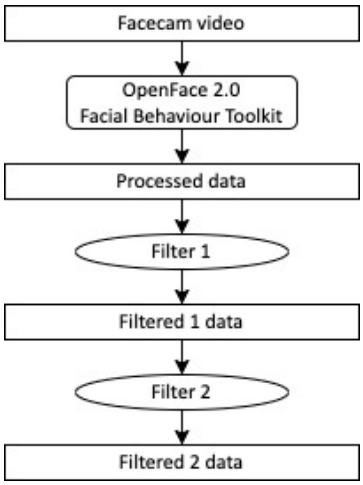

Figure A1. Overview steps pre-processing the data

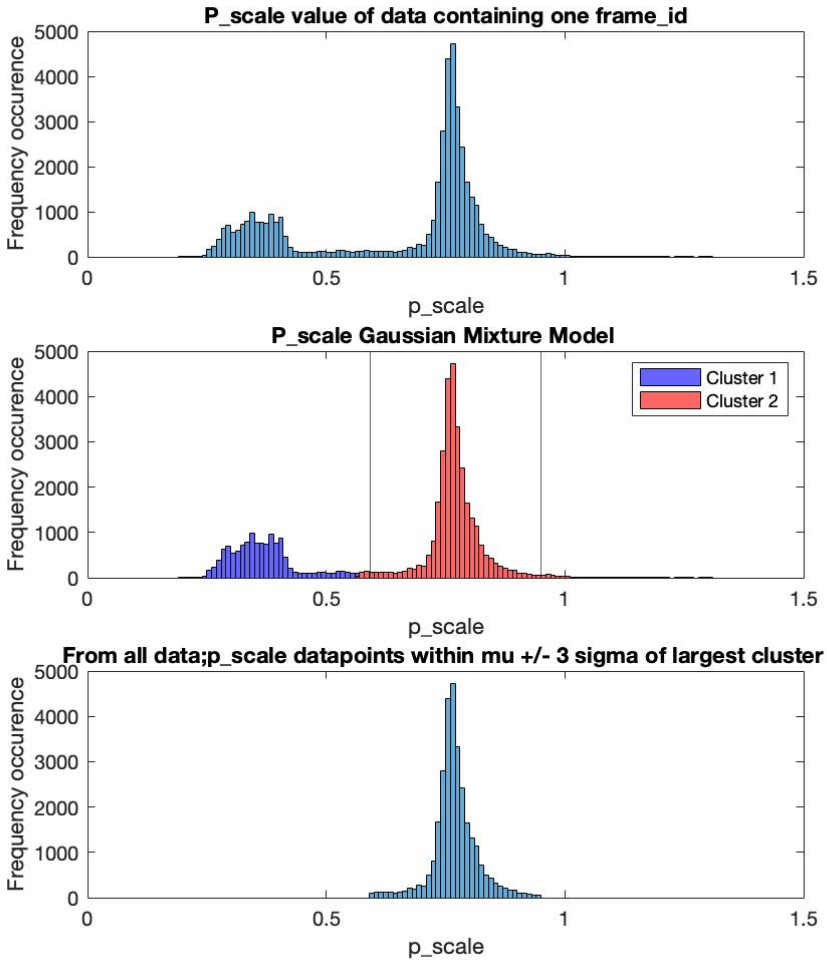

Figure A2. Driver data (trip 1) and filter method Filter 2

Appendix B. Missing values analysis

The OpenFace 2.0 detection algorithm could not detect the participants face continuously due to the limitations and challenges of the video tracking algorithm. Therefore, there are some instances in the data, the OpenFace 2.0 did not detect the head of the driver and/or passenger leading to data gaps. The data must be analysed to create insight into the frequency and positions of the missing data before synchrony calculations. The percentage of missing data for the total route, part 1 and part 2, all segments and the areas around the corner are analysed during the inspection of data presented by the OpenFace 2.0 algorithm. Since synchrony is calculated for dyads, both the driver and the passenger data of one trip should not contain too many missing values. Figures B1 and B2 shows the frequency and position of the missing values of trip 5, with only a small amount of missing values and of trip 12, which contains a lot of missing values.

Since the missing values are more occurring in the cornering areas and some trips have a high percentage of missing values for the total trip, a couple were excluded from the analysis. These trips are 11, 12, 13, 22 and 27. The missing values are for the total trip more than 20% for the driver and/or passenger role. In Table B1 an overview of percentage detected values for all trips for driver and passenger are displayed.

To conclude, the data analysis on missing values shows that a relatively higher percentage of data gaps occurred in corner regions compared to other segments. Therefore, it can be concluded that cornering head detection was more difficult for the video-tracking algorithm leading to less reliable results about synchrony in cornering areas. The second remark about the missing data analysis is about the missing values in corners for different road segments. The corners in the urban region show more missing values than those of the other areas. This can be due to the corner angle or due to other road parameters and distractions. A more complex traffic scene is more occurring in an urban region than the highway.

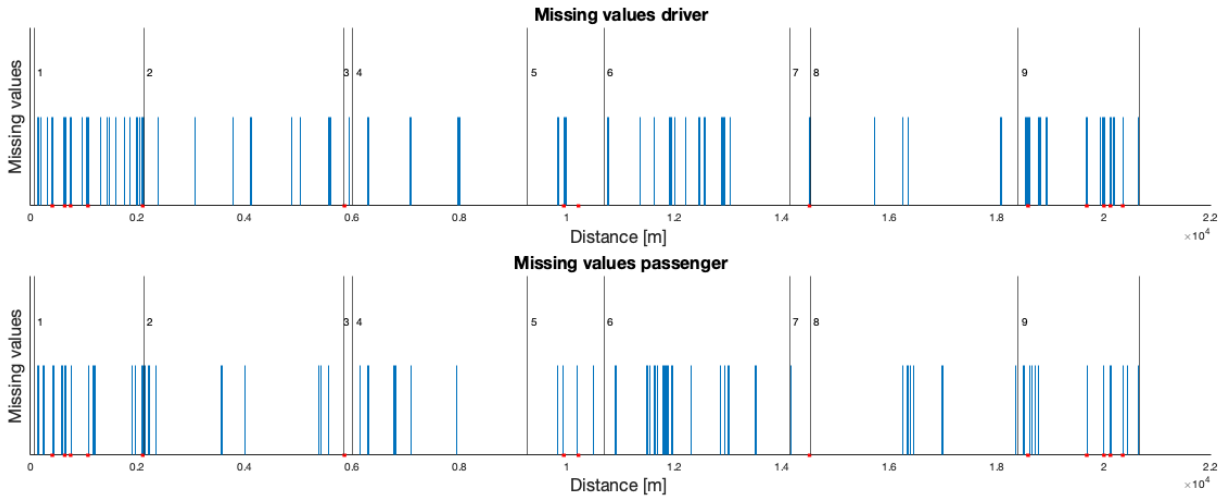

Figure B1. Overview missing values trip 5 versus the travelled distance. Blue: missing values, red: cornering events areas, the vertical black lines with the corresponding numbers indicate road segments.

Figure B2. Overview missing values trip 12 versus the travelled distance. Blue: missing values, red: cornering events areas, the vertical black lines with the corresponding numbers indicate road segments.

Trip number	Percentage detected head driver [%]	Percentage detected head passenger [%]
1	95.58	95.02
2	94.46	98.20
3	96.75	98.27
4	86.20	96.43
5	97.31	97.90
6	96.10	92.93
7	-	-
8	97.33	97.12
9	-	-
10	91.74	95.97
11	86.67	78.00
12	69.73	83.91
13	77.66	95.27
14	93.68	84.54
15	94.15	95.92
16	94.61	91.79
17	87.18	95.46
18	96.44	97.30
19	94.81	96.23
20	90.60	95.93
21	96.03	92.41
22	53.01	92.27
23	94.91	97.15
24	92.97	89.96
25	95.79	94.82
26	97,25	94.67
27	77.23	84.28
28	96.68	95.44
29	92.63	96.62
30	97.20	94.69
31	92.55	96.04
32	-	-

Table B1. Overview percentage detected values. Highlighted values: Detection rate < 80%.

Appendix C. Results processing detected signal

This section includes graphs that show information about the interpolation and smoothing of the detected head position by the OpenFace 2.0 algorithm. All plots included are of trip number 5. The raw data is first interpolated (spline) and subsequential smoothed by a moving average of 8 frames (0.267 s)
Black line: raw data, dotted line: interpolated data, red line: smoothed data and the blue line: derivative of the smoothed data (red line).

Role: Driver
Segment: Urban

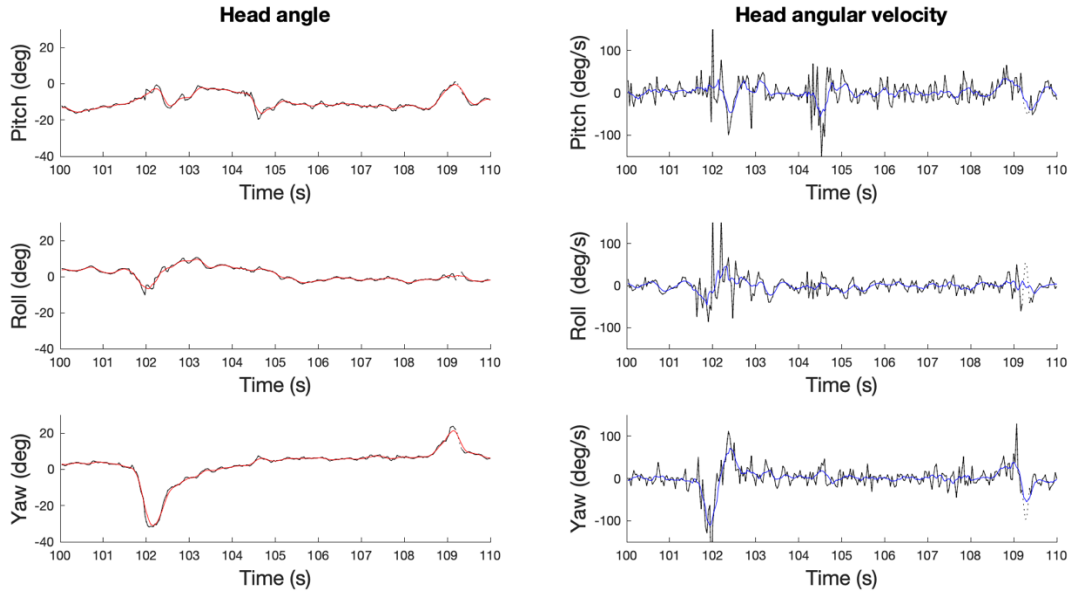

Role: Passenger
Segment: 1: Urban

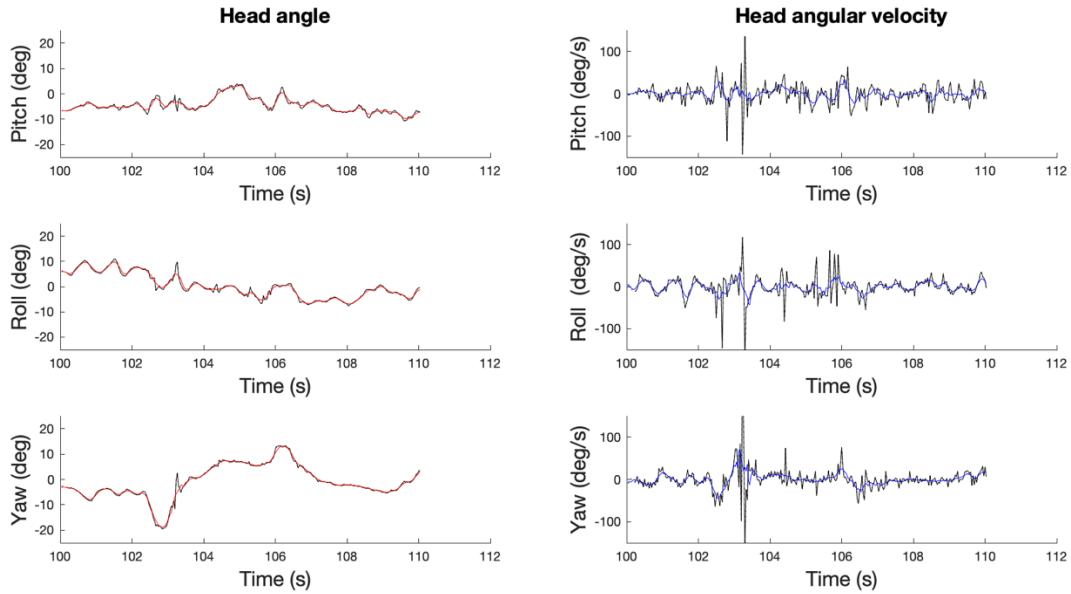

Role: Driver
Segment: 2: Outside built-up areas

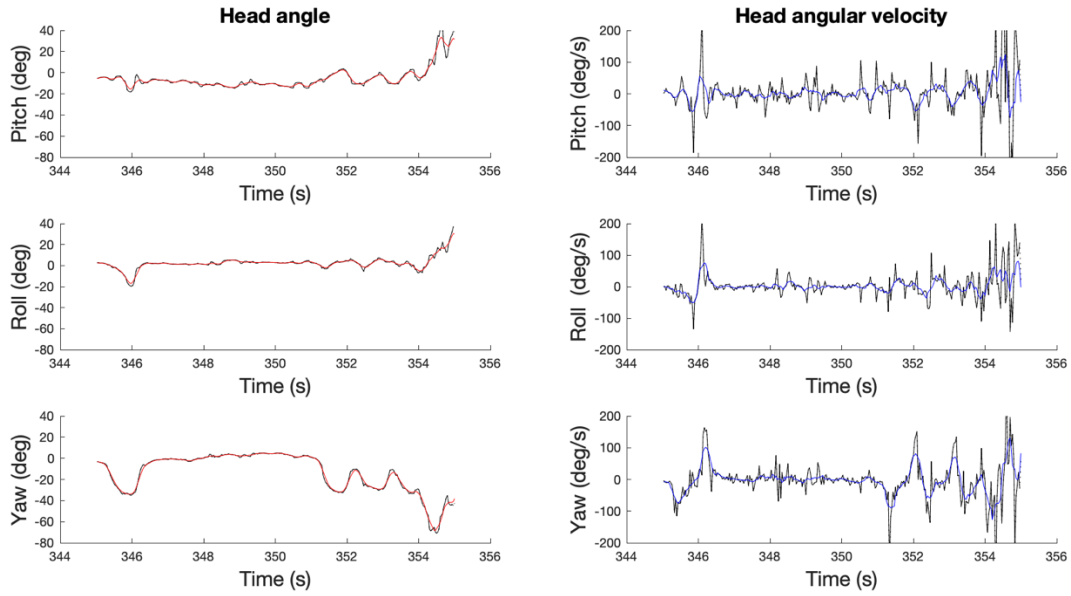

Role: Passenger
Segment: 2: Outside built-up areas

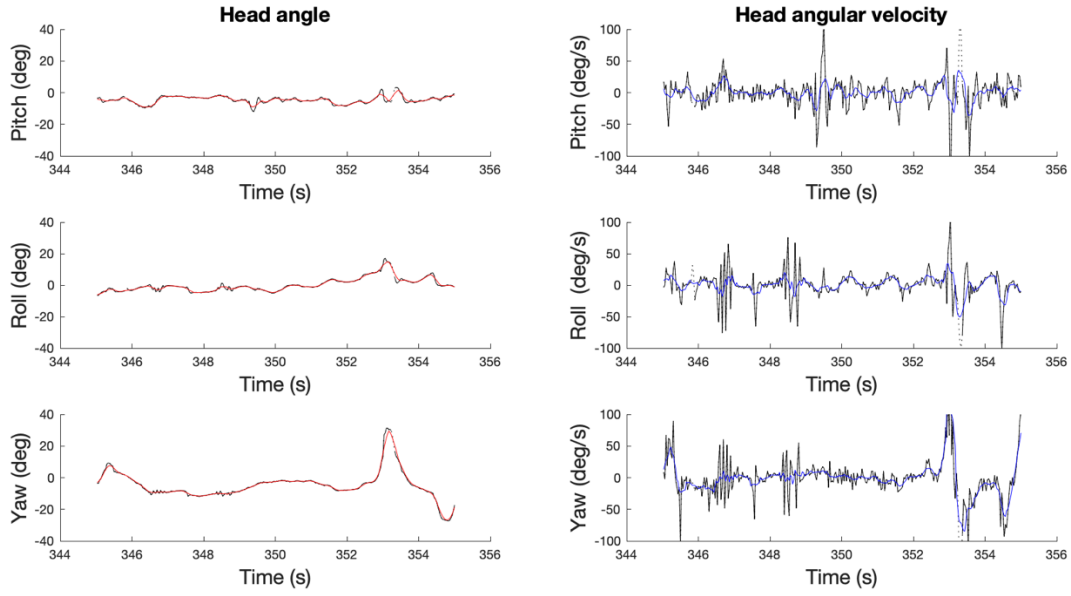

Role: Driver
Segment: 4: Highway

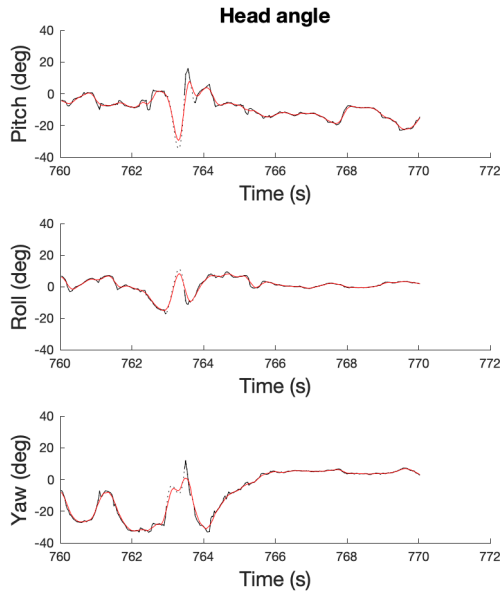

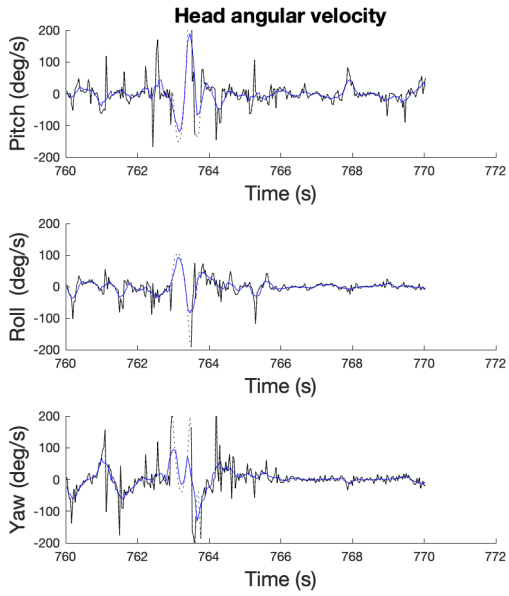

Role: Passenger
Segment: 4: Highway

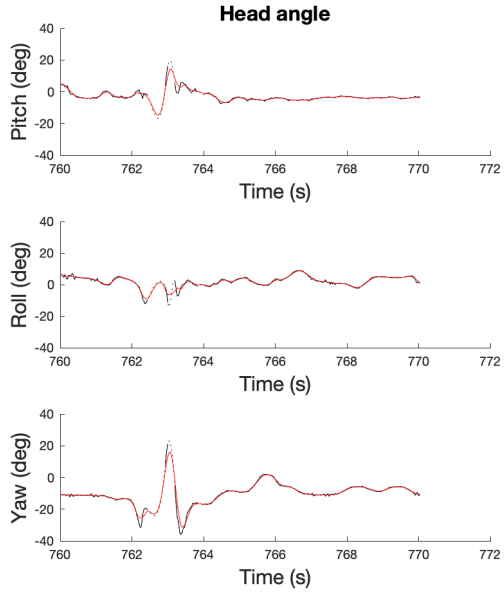

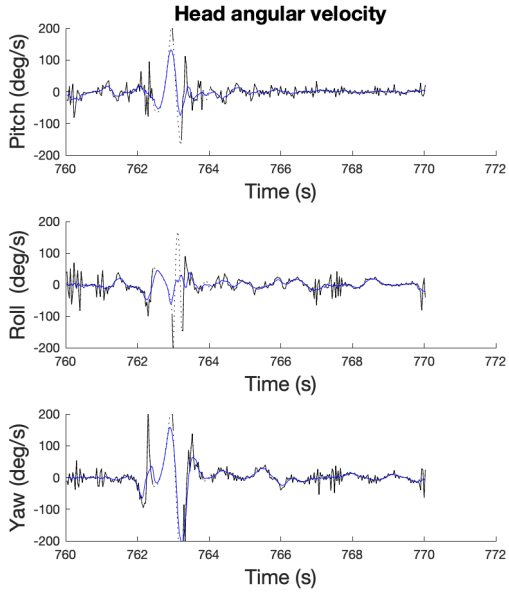

Appendix D. Syncing the data

Since syncing car data and facecam data was not possible by using the epoch timestamps in the INS data files, another method was applied. Fridman et al. proposed a method for syncing driver data using vibrations [48]. This method has an accuracy of 14.2 milliseconds for syncing acceleration in the Z-axis of the vehicle with the optical flow of the facecam frames in the y-axis. The accuracy of 14.2 milliseconds holds for trips longer or equal to 37 minutes in total. Since the trips of the driving experiments in this research had a shorter duration, about 30 minutes, the accuracy of syncing the data streams will decrease. From the paper, a synchronisation error around 20 milliseconds is stated for trips longer than 23 minutes. Another important aspect, is the resolution of the signals. The facecam data has a resolution of 30 fps and the car data of 25 Hz. The car data is interpolated to a resolution of 30 Hz to compare the signals. The 30 fps results in a resolution of 1/30 second, which is approximately 33 milliseconds.

The paper of Fridman et al. contains also the open-source computer vision code for deriving the optical flow from facecam videos. Since the facecam video of the driver included the steering wheel, the facecam video of the passenger was preferred for the identification of the optical flow in the y-axis. The drivers' and passengers' facecam videos are already synced. After collecting the dense optical flow for the passengers from all trips, the cross-correlation between the flow of the passenger and the acceleration of the vehicle is derived.

Figure D1 displays the signal of the body acceleration in Z-direction and the signal of the optical flow of the facecam video in the y-axis of trip 11. After calculating the maximum correlation between the optical flow and the body acceleration, the two signals are aligned.

In conclusion, for syncing the car data to the facecam data, the method proposed by Fridman is used. For this application, the generated result for syncing is satisfactory. To have more accurate results, longer recordings would be necessary and to generate more precise measurements, a higher resolution is recommended.

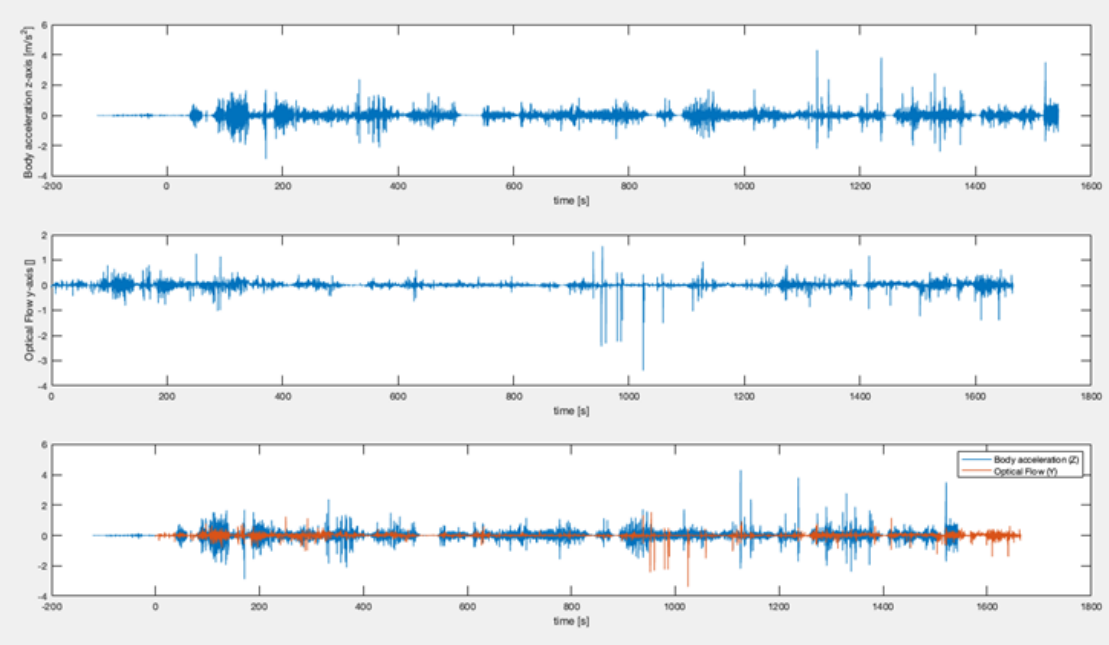

Figure D1. Trip 11. Top: Body acceleration vehicle Z-axis as function of time. Middle: Optical flow y-axis of passengers' facecam video as function of time. Bottom: Body acceleration vehicle synced with the optical flow passenger y-axis as function of time.

Appendix E. Amazon Web Services

To correctly apply the pseudosynchrony, it is necessary to calculate a large number of surrogate data streams. The data streams were created in several steps, as explained in the methods. The creation of surrogate data is not computational expensive. The challenge lies in calculating the WCLC and applying the two peak-picking algorithms for one hundred surrogate data streams for each trip. This process should be repeated for the head angle and angular velocity for pitch, roll and yaw. Although calculating the WCLC and performing peak-picking Altmann and Boker et al., for one head angle – yaw, only takes approximately 10 minutes, the total duration increases fast. The following formulae was applied to approximate the total computation duration.

$$
\begin{aligned}
&2400\ hours\ (Total\ computation\ duration)\\
&\quad = 10\ minutes\ (duration\ WCLC + peak - picking)\\
&\quad * 2\ (head\ angle\ \&\ angular\ velocity) * 3\ (roll, pitch\ and\ yaw)\\
&\quad * 24\ (number\ of\ trips) * 100\ (number\ of\ surrogate\ datastreams)
\end{aligned}
$$

The Amazon Web Services (AWS) service was used to calculate the surrogate data streams in an acceptable time frame. AWS was used for parallel computing of the WCLC and peak-picking algorithms for the different trips for the current application.

Amazon Web Services grants virtual servers in the cloud. In other words, it provides access to lots of computer power. The results calculated via the virtual servers are stored in Amazon Simple Storage Service (S3). Computing the amount of data required is not free. Depending on the selected type and number of virtual servers you require, Amazon derives the costs.

Before you can use the virtual servers of AWS, several steps must be completed first. For example, you have to create an account with AWS and connect it to a cloud location. These can be locations in Europe, America, actually all over the world. The account I made is under the designation of scientific purposes, student. This affects the type and amount of virtual servers made available to you.

Next, I linked my Matlab account via the cloud to my AWS account. Since AWS takes time to start, it is advised to adjust your code and run it locally from your computer via parallel computing. For example, you can convert all your for loops to parfor loops and try whether it works. If you got it running, you can select the type and the numbers of machines you would like to access and start AWS. The maximum number of workers I was allowed to use is 24.

The results obtained from the virtual machines are then stored in the S3. The last step is getting your results from the cloud. This is done via a short script since the manually downloading takes much time for many files.

Appendix F. Results statistical analysis

* $p < 0.01$: detected synchrony > pseudosynchrony, ** $p < 0.01$: pseudosynchrony > detected synchrony

PITCH

Frequency of synchrony – head angle

	Percentage synchrony intervals				t	p-value	Cohen's d
	Mean Detected synchrony (%)	Mean Pseudo-synchrony (%)	SD- Detected synchrony (%)	SD- Pseudo-synchrony (%)			
Total route	**7.4***	6.6	1.4	0.5	3.447	0.002	0.704
Part 1: Pre-task	**7.5***	6.4	2.0	0.5	2.983	0.007	0.609
Part 2: Post-task	7.6	6.7	1.7	0.5	2.706	0.013	0.552
S1: Urban	**8.9***	6.7	3.1	0.7	3.995	0.001	0.815
S2: Outside built-up areas	6.6	6.1	1.9	0.5	1.303	0.205	0.266
S3: Entry highway	9.2	5.5	11.5	1.1	1.665	0.110	0.34
S4: Highway	6.9	6.6	3.6	1	0.388	0.702	0.079
S5: Exit and Entry highway	5.6	6.7	2.0	0.6	-2.662	0.014	-0.543
S6: Highway	7.4	7.7	3.2	0.9	-0.43	0.671	-0.088
S7: Exit highway	3.5**	6.3	3.4	1.4	-3.349	0.003	-0.684
S8: Outside built-up areas	7.3	6.5	2.1	0.6	1.984	0.059	0.405
S9: Urban	**8.9***	6.7	3.1	0.7	3.72	0.001	0.759

	Percentage synchrony intervals				t	p-value	Cohen's d
	Mean Detected synchrony (%)	Mean Pseudo-synchrony (%)	SD- Detected synchrony (%)	SD- Pseudo-synchrony (%)			
A	11.6	7.0	10.7	2.3	2.344	0.028	0.478
B	10.9	6.7	8	1.4	2.635	0.015	0.538
C	7.4	6.6	12	1.7	0.357	0.725	0.073
D	9.3	6.2	9.9	0.9	1.54	0.137	0.314
E	5.5	6.2	8.4	1.3	-0.437	0.666	-0.089
F	9.3	5.6	13.8	1.2	1.319	0.200	0.269
G	5.9	6.9	9.3	1.9	-0.49	0.629	-0.1
H	**3.1****	6.8	3.5	1.3	-4.957	< 0.001	-1.012
I	3.7	5.7	8.8	1.2	-1.169	0.254	-0.239
J	6.0	5.7	7.0	0.6	0.259	0.798	0.053
K	9.3	7.3	11.4	1.2	0.897	0.379	0.183
L	9.6	5.8	13.4	1.3	1.431	0.166	0.292
M	9.0	7.3	6.5	1.0.0	1.314	0.202	0.268
N	7.1	6.6	7.6	2.2	0.295	0.771	0.06

Frequency of synchrony – head angular velocity

	Percentage synchrony intervals				t	p-value	Cohen's d
	Mean Detected synchrony (%)	Mean Pseudo-synchrony (%)	SD- Detected synchrony (%)	SD- Pseudo-synchrony (%)			
Total route	**30.5***	28.2	2.8	1.6	5.452	< 0.001	1.113
Part 1: Pre-task	**30.8***	28.1	3.5	1.5	4.592	< 0.001	0.937
Part 2: Post-task	**30.5***	28.3	3.2	2.0	3.588	0.002	0.732
S1: Urban	**32.9***	28.9	5.0	1.6	4.342	< 0.001	0.886
S2: Outside built-up areas	29.0	27.4	4.5	1.8	2.045	0.052	0.418
S3: Entry highway	30.1	27.8	15.9	2.5	0.71	0.485	0.145
S4: Highway	**31.4***	28.4	5.3	1.5	3.128	0.005	0.638
S5: Exit and Entry highway	29.1	27.9	6.1	2.1	1.058	0.301	0.216
S6: Highway	30.6	29.8	4.6	1.8	0.965	0.345	0.197
S7: Exit highway	28.5	28.0	10.7	2.3	0.21	0.835	0.043
S8: Outside built-up areas	29.4	27.9	4.3	2.1	1.672	0.108	0.341
S9: Urban	**32.5***	28.3	4.2	2.6	5.641	< 0.001	1.152

	Percentage synchrony intervals				t	p-value	Cohen's d
	Mean Detected synchrony (%)	Mean Pseudo-synchrony (%)	SD- Detected synchrony (%)	SD- Pseudo-synchrony (%)			
A	33.4	28.9	17.3	4.8	1.363	0.186	0.278
B	33.2	29.2	12.1	2.2	1.701	0.102	0.347
C	28.1	28.5	16.0	3.7	-0.136	0.893	-0.028
D	27.7	26.5	10.7	3.6	0.528	0.602	0.108
E	28.8	28.4	16.1	4.0	0.132	0.896	0.027
F	24.9	28.6	15.3	3.1	-1.169	0.254	-0.239
G	27.1	29.0	17.9	3.4	-0.536	0.597	-0.109
H	25.5	28.2	8.1	3.3	-1.625	0.118	-0.332
I	32.2	28.1	20.7	4.6	0.943	0.355	0.193
J	31.6	26.6	13.0	2.9	1.943	0.064	0.397
K	31.5	29.6	11.4	3.1	0.821	0.420	0.168
L	31.8	28.2	16.8	3.2	1.006	0.325	0.205
M	28.3	29.5	11.7	3.8	-0.557	0.583	-0.114
N	29.7	27.9	13.4	5.3	0.779	0.444	0.159

Strength of synchrony – head angle

	Mean peak correlation				t	p-value	Cohen's d
	Mean Detected synchrony (%)	Mean Pseudo-synchrony (%)	SD- Detected synchrony (%)	SD- Pseudo-synchrony (%)			
Total route	**0.394***	0.371	0.437	0.441	7.989	< 0.001	1.631
Part 1: Pre-task	**0.397***	0.373	0.435	0.442	4.577	< 0.001	0.934
Part 2: Post-task	**0.393***	0.370	0.436	0.439	5.601	< 0.001	1.143
S1: Urban	**0.398***	0.373	0.427	0.431	4.668	< 0.001	0.953
S2: Outside built-up areas	**0.394***	0.372	0.440	0.446	3.779	0.001	0.771
S3: Entry highway	**0.451***	0.373	0.411	0.448	3.457	0.002	0.706
S4: Highway	**0.396***	0.375	0.435	0.443	2.789	0.010	0.569
S5: Exit and Entry highway	0.374	0.368	0.454	0.444	0.599	0.555	0.122
S6: Highway	0.393	0.377	0.421	0.425	2.298	0.031	0.469
S7: Exit highway	0.378	0.356	0.445	0.444	1.518	0.143	0.31
S8: Outside built-up areas	**0.392***	0.369	0.447	0.442	4.089	< 0.001	0.835
S9: Urban	**0.401***	0.368	0.420	0.437	5.851	< 0.001	1.194

	Mean peak correlation				t	p-value	Cohen's d
	Mean Detected synchrony (%)	Mean Pseudo-synchrony (%)	SD- Detected synchrony (%)	SD- Pseudo-synchrony (%)			
A	0.386	0.376	0.407	0.416	0.445	0.661	0.091
B	**0.442***	0.379	0.418	0.420	3.029	0.006	0.618
C	**0.447***	0.381	0.399	0.406	2.875	0.009	0.587
D	0.383	0.371	0.400	0.410	0.585	0.564	0.119
E	0.412	0.373	0.404	0.423	1.486	0.151	0.303
F	**0.453***	0.375	0.398	0.431	3.071	0.005	0.627
G	0.370	0.382	0.448	0.419	-0.487	0.631	-0.099
H	0.364	0.356	0.459	0.445	0.502	0.620	0.102
I	0.407	0.368	0.451	0.426	1.362	0.186	0.278
J	**0.426***	0.377	0.402	0.422	2.897	0.008	0.591
K	0.401	0.376	0.395	0.419	1.021	0.318	0.208
L	0.392	0.381	0.411	0.420	0.417	0.680	0.085
M	0.423	0.378	0.400	0.422	2.191	0.039	0.447
N	0.371	0.363	0.404	0.418	0.34	0.737	0.069

Strength of synchrony – head angular velocity

	Mean peak correlation				t	p-value	Cohen's d
	Mean Detected synchrony (%)	Mean Pseudo-synchrony (%)	SD- Detected synchrony (%)	SD- Pseudo-synchrony (%)			
Total route	**0.336***	0.292	0.252	0.262	6.861	< 0.001	1.401
Part 1: Pre-task	**0.338***	0.291	0.251	0.260	6.163	< 0.001	1.258
Part 2: Post-task	**0.340***	0.293	0.251	0.261	7.203	< 0.001	1.47
S1: Urban	**0.346***	0.298	0.246	0.261	5.631	< 0.001	1.149
S2: Outside built-up areas	**0.332***	0.287	0.253	0.258	6.175	< 0.001	1.26
S3: Entry highway	0.326	0.298	0.252	0.253	1.623	0.118	0.331
S4: Highway	**0.336***	0.288	0.249	0.255	4.349	< 0.001	0.888
S5: Exit and Entry highway	**0.316***	0.291	0.256	0.266	3.545	0.002	0.724
S6: Highway	**0.337***	0.300	0.247	0.263	4.977	< 0.001	1.016
S7: Exit highway	**0.323***	0.292	0.255	0.258	3.562	0.002	0.727
S8: Outside built-up areas	**0.334***	0.288	0.253	0.259	5.885	< 0.001	1.201
S9: Urban	**0.350***	0.297	0.246	0.260	7.033	< 0.001	1.436

	Mean peak correlation				t	p-value	Cohen's d
	Mean Detected synchrony (%)	Mean Pseudo-synchrony (%)	SD- Detected synchrony (%)	SD- Pseudo-synchrony (%)			
A	**0.369***	0.313	0.228	0.254	5.126	< 0.001	1.046
B	0.350	0.307	0.263	0.262	2.767	0.011	0.565
C	**0.366***	0.317	0.244	0.253	2.96	0.007	0.604
D	0.314	0.306	0.245	0.257	0.637	0.530	0.13
E	0.332	0.299	0.244	0.254	1.695	0.104	0.346
F	0.340	0.299	0.230	0.249	1.704	0.102	0.348
G	0.305	0.301	0.261	0.261	0.28	0.782	0.057
H	0.313	0.297	0.248	0.266	1.666	0.109	0.34
I	0.276	0.294	0.241	0.248	-0.892	0.382	-0.182
J	0.315	0.303	0.228	0.259	0.78	0.443	0.159
K	0.323	0.302	0.233	0.252	1.217	0.236	0.248
L	0.324	0.304	0.238	0.254	1.091	0.287	0.223
M	**0.354***	0.310	0.241	0.258	3.856	0.001	0.787
N	0.343	0.306	0.225	0.245	2.492	0.021	0.509

ROLL

Frequency of synchrony – head angle

	Percentage synchrony intervals				t	p-value	Cohen's d
	Mean Detected synchrony (%)	Mean Pseudo-synchrony (%)	SD- Detected synchrony (%)	SD- Pseudo-synchrony (%)			
Total route	**6.4***	5.5	0.7	0.5	7.541	< 0.001	1.539
Part 1: Pre-task	**6.5***	5.4	1.0	0.6	4.677	< 0.001	0.955
Part 2: Post-task	**6.5***	5.5	1.3	0.5	4.125	< 0.001	0.842
S1: Urban	**8.1***	5.8	2.7	0.8	4.474	< 0.001	0.913
S2: Outside built-up areas	5.8	5.2	2.1	0.7	1.352	0.190	0.276
S3: Entry highway	4.1	4.2	5.4	0.9	-0.091	0.929	-0.018
S4: Highway	5.1	5.4	2.8	0.6	-0.624	0.539	-0.127
S5: Exit and Entry highway	5.6	5.3	2.2	0.7	0.662	0.515	0.135
S6: Highway	5.5	6.3	2.8	0.8	-1.386	0.179	-0.283
S7: Exit highway	4.8	4.9	5.2	1.3	-0.077	0.939	-0.016
S8: Outside built-up areas	5.6	5.3	1.6	0.7	0.937	0.358	0.191
S9: Urban	**8.5***	5.6	2.8	0.5	5.658	< 0.001	1.155

	Percentage synchrony intervals				t	p-value	Cohen's d
	Mean Detected synchrony (%)	Mean Pseudo-synchrony (%)	SD- Detected synchrony (%)	SD- Pseudo-synchrony (%)			
A	5.3	5.5	6.4	1.0	-0.167	0.869	-0.034
B	12.0	6.4	12.2	0.8	2.22	0.037	0.453
C	4.9	5.5	8.2	1.1	-0.389	0.701	-0.079
D	8.6	6.4	10.0	1.3	1.077	0.293	0.22
E	5.6	5.7	10.5	1.4	-0.031	0.975	-0.006
F	2.4	4.5	7.1	1.4	-1.463	0.157	-0.299
G	7.6	5.4	8.6	1.4	1.332	0.196	0.272
H	**3.2****	5.4	3.3	1.5	-3.592	0.002	-0.733
I	6.8	4.3	11	2.1	1.118	0.275	0.228
J	4.0	4.9	7.3	0.8	-0.566	0.577	-0.116
K	7.6	6.7	8.0	1.0	0.612	0.546	0.125
L	9.3	6.0	10.4	1.3	1.53	0.140	0.312
M	10.2	6.0	9.4	1.4	2.194	0.039	0.448
N	**14.6***	6.1	12.8	1.5	3.266	0.003	0.667

Frequency of synchrony – head angular velocity

	Percentage synchrony intervals				t	p-value	Cohen's d
	Mean Detected synchrony (%)	Mean Pseudo-synchrony (%)	SD- Detected synchrony (%)	SD- Pseudo-synchrony (%)			
Total route	**28.5***	25.7	2.4	2.2	7.808	< 0.001	1.594
Part 1: Pre-task	**29.4***	25.8	2.3	2.2	7.437	< 0.001	1.518
Part 2: Post-task	**27.8***	25.9	3.3	2.5	3.904	0.001	0.797
S1: Urban	**33.5***	26.9	4.5	2.4	7.769	< 0.001	1.586
S2: Outside built-up areas	27.1	25.0	3.9	2.6	2.558	0.018	0.522
S3: Entry highway	26.3	26.4	13.5	2.4	-0.03	0.976	-0.006
S4: Highway	27.1	25.4	5.4	2.0	1.703	0.102	0.348
S5: Exit and Entry highway	27.3	24.8	5.1	2.8	2.694	0.013	0.55
S6: Highway	26.3	27.4	5.4	3.3	-1.087	0.288	-0.222
S7: Exit highway	26.1	23.9	8.8	5.4	1.344	0.192	0.274
S8: Outside built-up areas	25.2	25	4.4	3.0	0.195	0.847	0.04
S9: Urban	**32.4***	26.6	5.0	2.2	6.963	< 0.001	1.421

	Percentage synchrony intervals				t	p-value	Cohen's d
	Mean Detected synchrony (%)	Mean Pseudo-synchrony (%)	SD- Detected synchrony (%)	SD- Pseudo-synchrony (%)			
A	**38.1***	27.5	12.2	2.2	4.074	< 0.001	0.832
B	**35.4***	28.1	12.2	2.5	3.095	0.005	0.632
C	33.7	27.0	14.6	3.5	2.361	0.027	0.482
D	30.4	27.1	11.6	3.6	1.368	0.184	0.279
E	31.2	26.9	14.5	3.7	1.401	0.175	0.286
F	22.8	27.4	17.2	4.7	-1.258	0.221	-0.257
G	31.5	27.3	19.3	4.2	1.103	0.282	0.225
H	26.0	25.5	9.8	5.0	0.253	0.803	0.052
I	28.6	24.8	19.4	3.3	0.971	0.342	0.198
J	24.8	26.5	13.6	2.2	-0.619	0.542	-0.126
K	**37.0***	28.9	13.1	3.6	3.068	0.005	0.626
L	27.6	27.5	18.2	3.8	0.03	0.977	0.006
M	31.6	27.7	16.2	3.0	1.22	0.235	0.249
N	37.3	28.6	19.4	4.8	2.372	0.026	0.484

Strength of synchrony – head angle

	Mean peak correlation				t	p-value	Cohen's d
	Mean Detected synchrony	Mean Pseudo-synchrony	SD- Detected synchrony	SD- Pseudo-synchrony			
Total route	**0.387***	0.372	0.455	0.456	5.284	< 0.001	1.079
Part 1: Pre-task	**0.392***	0.376	0.448	0.455	2.992	0.007	0.611
Part 2: Post-task	**0.387***	0.370	0.454	0.455	4.349	< 0.001	0.888
S1: Urban	**0.400***	0.376	0.438	0.448	3.111	0.005	0.635
S2: Outside built-up areas	0.379	0.377	0.458	0.457	0.376	0.710	0.077
S3: Entry highway	0.402	0.355	0.460	0.467	1.687	0.105	0.344
S4: Highway	0.384	0.378	0.456	0.456	0.538	0.596	0.11
S5: Exit and Entry highway	**0.393***	0.369	0.470	0.463	3.099	0.005	0.633
S6: Highway	0.377	0.368	0.451	0.444	1.231	0.231	0.251
S7: Exit highway	**0.404***	0.358	0.473	0.460	3.264	0.003	0.666
S8: Outside built-up areas	0.378	0.369	0.464	0.458	1.635	0.116	0.334
S9: Urban	**0.394***	0.370	0.437	0.451	3.739	0.001	0.763

	Mean peak correlation				t	p-value	Cohen's d
	Mean Detected synchrony	Mean Pseudo-synchrony	SD- Detected synchrony	SD- Pseudo-synchrony			
A	0.399	0.376	0.406	0.427	1.121	0.274	0.229
B	0.450	0.396	0.411	0.428	2.315	0.030	0.473
C	0.410	0.389	0.414	0.425	0.816	0.423	0.167
D	0.372	0.387	0.428	0.429	-0.738	0.468	-0.151
E	0.370	0.377	0.442	0.437	-0.246	0.808	-0.050
F	0.416	0.350	0.442	0.448	2.577	0.017	0.526
G	0.415	0.375	0.448	0.437	1.351	0.190	0.276
H	0.385	0.357	0.469	0.462	1.38	0.181	0.282
I	0.452	0.361	0.437	0.443	2.181	0.040	0.445
J	0.422	0.368	0.449	0.448	2.195	0.039	0.448
K	0.395	0.371	0.397	0.421	0.878	0.389	0.179
L	0.430	0.387	0.401	0.430	2.028	0.054	0.414
M	0.393	0.377	0.399	0.421	1.033	0.313	0.211
N	0.400	0.366	0.415	0.415	1.758	0.093	0.359

Strength of synchrony – head angular velocity

	Mean peak correlation				t	p-value	Cohen's d
	Mean Detected synchrony	Mean Pseudo-synchrony	SD- Detected synchrony	SD- Pseudo-synchrony			
Total route	**0.330***	0.304	0.261	0.253	12.823	< 0.001	2.617
Part 1: Pre-task	**0.334***	0.304	0.262	0.254	9.356	< 0.001	1.910
Part 2: Post-task	**0.328***	0.305	0.261	0.252	7.112	< 0.001	1.452
S1: Urban	**0.352***	0.308	0.260	0.253	7.687	< 0.001	1.569
S2: Outside built-up areas	**0.322***	0.301	0.257	0.253	6.117	< 0.001	1.249
S3: Entry highway	0.344	0.313	0.247	0.247	2.075	0.049	0.424
S4: Highway	**0.326***	0.303	0.260	0.253	2.802	0.010	0.572
S5: Exit and Entry highway	**0.318***	0.301	0.266	0.256	3.134	0.005	0.640
S6: Highway	**0.321***	0.309	0.253	0.246	2.936	0.007	0.599
S7: Exit highway	0.324	0.301	0.268	0.252	2.04	0.053	0.416
S8: Outside built-up areas	0.310	0.302	0.257	0.252	1.982	0.060	0.405
S9: Urban	**0.358***	0.307	0.260	0.251	10.199	< 0.001	2.082

	Mean peak correlation				t	p-value	Cohen's d
	Mean Detected synchrony	Mean Pseudo-synchrony	SD- Detected synchrony	SD- Pseudo-synchrony			
A	**0.386***	0.313	0.250	0.245	5.244	< 0.001	1.070
B	**0.373***	0.312	0.261	0.252	4.198	< 0.001	0.857
C	**0.378***	0.313	0.244	0.247	3.535	0.002	0.721
D	0.331	0.310	0.258	0.249	2.667	0.014	0.544
E	0.331	0.312	0.264	0.243	0.992	0.332	0.202
F	0.355	0.312	0.243	0.237	2.393	0.025	0.488
G	0.328	0.312	0.272	0.244	0.902	0.376	0.184
H	0.320	0.299	0.265	0.250	1.67	0.109	0.341
I	0.340	0.307	0.275	0.242	1.703	0.102	0.348
J	0.311	0.313	0.252	0.244	-0.15	0.882	-0.031
K	**0.375***	0.315	0.231	0.240	3.119	0.005	0.637
L	**0.368***	0.313	0.245	0.244	3.342	0.003	0.682
M	0.330	0.316	0.247	0.247	0.881	0.387	0.180
N	**0.413***	0.311	0.252	0.232	5.829	< 0.001	1.190

YAW

Frequency of synchrony – head angle

	Percentage synchrony intervals						
	Mean Detected synchrony (%)	Mean Pseudo-synchrony (%)	SD- Detected synchrony (%)	SD- Pseudo-synchrony (%)	t	p-value	Cohen's d
Total route	4.2	3.7	0.8	0.3	2.771	0.011	0.566
Part 1: Pre-task	4.2	3.7	1.1	0.2	1.912	0.068	0.39
Part 2: Post-task	4.1	3.7	1.5	0.4	1.308	0.204	0.267
S1: Urban	4.2	3.8	1.4	0.3	1.39	0.178	0.284
S2: Outside built-up areas	3.9	3.7	1.2	0.4	0.832	0.414	0.17
S3: Entry highway	5.0	2.7	6.9	0.8	1.721	0.099	0.351
S4: Highway	4.6	3.8	2.1	0.4	1.82	0.082	0.372
S5: Exit and Entry highway	4.5	3.5	2.2	0.5	2.322	0.029	0.474
S6: Highway	3.5	4.1	2.6	0.8	-1.05	0.304	-0.214
S7: Exit highway	3.3	3.5	5.2	0.9	-0.204	0.840	-0.042
S8: Outside built-up areas	3.6	3.7	1.9	0.5	-0.114	0.910	-0.023
S9: Urban	**5.3***	3.7	1.9	0.4	4.07	< 0.001	0.831

	Percentage synchrony intervals						
	Mean Detected synchrony (%)	Mean Pseudo-synchrony (%)	SD- Detected synchrony (%)	SD- Pseudo-synchrony (%)	t	p-value	Cohen's d
A	3.3	4.0	5.8	0.6	-0.63	0.535	-0.129
B	2.8	4.3	4.7	1.1	-1.686	0.105	-0.344
C	4.0	3.8	7.4	0.9	0.148	0.883	0.03
D	4.7	4.2	8.2	0.6	0.327	0.747	0.067
E	4.0	3.6	7.5	0.6	0.258	0.798	0.053
F	3.4	2.3	7.5	0.5	0.7	0.491	0.143
G	2.6	3.1	5.2	0.9	-0.549	0.588	-0.112
H	4.7	3.2	5.0	1.7	1.392	0.177	0.284
I	2.0	3.8	6.6	1.2	-1.285	0.212	-0.262
J	4.6	2.7	9.2	0.9	1	0.328	0.204
K	3.9	4.0	6.5	0.8	-0.098	0.923	-0.02
L	5.1	3.7	8.0	0.7	0.882	0.387	0.18
M	6.2	3.9	6.3	0.5	1.78	0.088	0.363
N	9.8	3.7	12.7	0.8	2.383	0.026	0.486

Frequency of synchrony – head angular velocity

	Percentage synchrony intervals						
	Mean Detected synchrony (%)	Mean Pseudo-synchrony (%)	SD- Detected synchrony (%)	SD- Pseudo-synchrony (%)	t	p-value	Cohen's d
Total route	**20.6***	19.0	2.9	1.2	3.257	0.003	0.665
Part 1: Pre-task	**20.8***	18.5	3.4	1.4	3.999	0.001	0.816
Part 2: Post-task	20.2	19.5	3.2	1.3	1.195	0.244	0.244
S1: Urban	**21.5***	19.7	3.1	1.4	3.417	0.002	0.697
S2: Outside built-up areas	**20.2***	17.6	4.7	1.6	3.037	0.006	0.62
S3: Entry highway	**26.7***	18.2	9.3	2.4	4.483	< 0.001	0.915
S4: Highway	20.2	18.4	6.0	1.9	1.474	0.154	0.301
S5: Exit and Entry highway	**21.3***	18.2	5.9	2.2	2.907	0.008	0.593
S6: Highway	19.3	19.0	5.1	1.9	0.26	0.797	0.053
S7: Exit highway	18.6	19.3	8.7	3.9	-0.358	0.724	-0.073
S8: Outside built-up areas	19.3	19.1	4.9	1.6	0.184	0.855	0.038
S9: Urban	22.0	20.3	4.4	1.3	2.027	0.054	0.414

	Percentage synchrony intervals						
	Mean Detected synchrony (%)	Mean Pseudo-synchrony (%)	SD- Detected synchrony (%)	SD- Pseudo-synchrony (%)	t	p-value	Cohen's d
A	22.5	19.8	10.8	2.2	1.264	0.219	0.258
B	23.7	21.3	10.5	1.8	1.176	0.252	0.24
C	23.5	20.5	13.8	2.6	1.049	0.305	0.214
D	20.7	21.1	11.2	2.9	-0.169	0.867	-0.034
E	21.6	22.1	16.1	3.3	-0.153	0.880	-0.031
F	26.2	19.2	15.1	2.4	2.294	0.031	0.468
G	20.9	18.5	15.6	2.3	0.777	0.445	0.159
H	19.8	16.8	8.3	3.6	1.807	0.084	0.369
I	22.1	20.8	20.0	4.5	0.303	0.765	0.062
J	23.7	20.2	12.6	2.4	1.309	0.203	0.267
K	23.9	20.5	13.7	1.6	1.203	0.241	0.246
L	20.6	22.8	15.0	2.6	-0.717	0.481	-0.146
M	25.8	20.7	12.2	1.7	2.093	0.048	0.427
N	**28.3***	20.1	14.9	2.6	2.84	0.009	0.58

Strength of synchrony – head angle

	Mean peak correlation				t	p-value	Cohen's d
	Mean Detected synchrony	Mean Pseudo-synchrony	SD- Detected synchrony	SD- Pseudo-synchrony			
Total route	**0.390***	0.374	0.486	0.49	4.683	< 0.001	0.956
Part 1: Pre-task	**0.394***	0.372	0.484	0.485	4.136	< 0.001	0.844
Part 2: Post-task	0.385	0.374	0.487	0.492	2.03	0.054	0.414
S1: Urban	**0.402***	0.376	0.480	0.479	3.217	0.004	0.657
S2: Outside built-up areas	0.380	0.369	0.487	0.489	1.766	0.091	0.36
S3: Entry highway	**0.486***	0.350	0.471	0.501	6	< 0.001	1.225
S4: Highway	0.385	0.376	0.482	0.479	1.032	0.313	0.211
S5: Exit and Entry highway	0.391	0.382	0.496	0.496	0.968	0.343	0.198
S6: Highway	0.387	0.387	0.493	0.484	-0.064	0.950	-0.013
S7: Exit highway	0.414	0.359	0.482	0.490	2.669	0.014	0.545
S8: Outside built-up areas	0.375	0.371	0.486	0.493	0.604	0.551	0.123
S9: Urban	**0.409***	0.372	0.471	0.490	3.985	0.001	0.813

	Mean peak correlation				t	p-value	Cohen's d
	Mean Detected synchrony	Mean Pseudo-synchrony	SD- Detected synchrony	SD- Pseudo-synchrony			
A	**0.429***	0.381	0.449	0.455	2.862	0.009	0.584
B	0.421	0.394	0.484	0.465	1.064	0.298	0.217
C	**0.469***	0.367	0.460	0.484	2.838	0.009	0.579
D	0.404	0.385	0.463	0.46	0.901	0.377	0.184
E	0.420	0.375	0.454	0.463	1.323	0.199	0.27
F	**0.546***	0.341	0.426	0.506	5.667	< 0.001	1.157
G	**0.491***	0.373	0.456	0.495	3.957	0.001	0.808
H	0.390	0.383	0.483	0.487	0.322	0.75	0.066
I	**0.490***	0.348	0.439	0.472	2.862	0.009	0.584
J	**0.469***	0.358	0.463	0.505	3.332	0.003	0.68
K	0.401	0.378	0.459	0.469	1.002	0.327	0.205
L	**0.487***	0.372	0.458	0.480	3.465	0.002	0.707
M	0.430	0.389	0.421	0.458	1.603	0.123	0.327
N	**0.435***	0.361	0.439	0.459	3.821	0.001	0.78

Strength of synchrony – head angular velocity

	Mean peak correlation				t	p-value	Cohen's d
	Mean Detected synchrony	Mean Pseudo-synchrony	SD- Detected synchrony	SD- Pseudo-synchrony			
Total route	**0.292***	0.283	0.276	0.273	5.418	< 0.001	1.106
Part 1: Pre-task	**0.297***	0.28	0.275	0.271	4.571	< 0.001	0.933
Part 2: Post-task	0.288	0.285	0.276	0.273	0.973	0.341	0.199
S1: Urban	**0.304***	0.29	0.28	0.271	2.83	0.009	0.578
S2: Outside built-up areas	**0.288***	0.274	0.27	0.268	2.844	0.009	0.580
S3: Entry highway	0.321	0.289	0.29	0.265	2.237	0.035	0.457
S4: Highway	**0.303***	0.279	0.27	0.266	4.026	0.001	0.822
S5: Exit and Entry highway	0.296	0.284	0.285	0.281	1.697	0.103	0.346
S6: Highway	0.284	0.291	0.28	0.278	-1.055	0.302	-0.215
S7: Exit highway	0.294	0.284	0.29	0.269	1.185	0.248	0.242
S8: Outside built-up areas	0.274	0.278	0.263	0.269	-0.697	0.493	-0.142
S9: Urban	**0.305***	0.289	0.278	0.272	2.967	0.007	0.606

	Mean peak correlation				t	p-value	Cohen's d
	Mean Detected synchrony	Mean Pseudo-synchrony	SD- Detected synchrony	SD- Pseudo-synchrony			
A	0.329	0.306	0.275	0.263	1.895	0.071	0.387
B	0.320	0.307	0.303	0.272	1.042	0.308	0.213
C	**0.361***	0.317	0.282	0.267	3.304	0.003	0.674
D	0.304	0.303	0.286	0.266	0.109	0.914	0.022
E	**0.357***	0.29	0.264	0.261	4.39	< 0.001	0.896
F	0.331	0.292	0.288	0.265	2.209	0.037	0.451
G	**0.354***	0.300	0.292	0.275	3.414	0.002	0.697
H	0.297	0.292	0.286	0.280	0.387	0.702	0.079
I	0.337	0.292	0.276	0.258	1.88	0.073	0.384
J	0.298	0.297	0.302	0.272	0.069	0.946	0.014
K	0.342	0.298	0.278	0.265	2.406	0.025	0.491
L	0.346	0.305	0.257	0.264	1.704	0.102	0.348
M	0.320	0.311	0.279	0.269	0.493	0.627	0.101
N	0.328	0.298	0.259	0.253	1.336	0.195	0.273

Appendix G. The dataset

The data analysed to study driver-passenger synchrony originated from real-world driving research conducted at Delft University of Technology. This dataset has already been the subject of one publication [45]. A second paper is also being considered [15]. The three main components of this real-world driving study's dataset were eye-trackers, video data, and vehicle data. The current research concentrated on video data, specifically facecam video and vehicle data.

Since both eye- and head movement are associated with gaze, the initial intention was to incorporate the eye-tracker data in this study. Therefore, the data from the eye-trackers and the facecam videos had to be synchronised. Since half of the eye-tracker recordings were missing and an incorrect epoch timestamp was indicated in the eye-tracker data, synchronising eye- and head data proved impossible in the order of the resolution. Data loss for some trips was another concern with the eye-tracker data. The trips data loss that occurred in the eye-trackers were not similar trips of the facecam videos. Table G1 shows an overview of the missing data of the facecam videos and eye-tracker data and videos.

A proposed strategy for syncing data streams for future studies that integrate facecam videos and eye-tracker videos when incorrect timestamps are given is calculating the correlation between the sound waves of the facecam videos and forward videos from the eye-tracker. This requires that all videos should include sound. The used dataset missed sound for one day of the driving experiment. However, future researchers should know a syncing method for the different data streams before executing the experiment.

	Facecam videos		Eye-tracker data				
Trip	Driver	Passenger	Driver data	Driver video	Passenger data	Passenger video	Notes
1						Data loss	Driver was experimenter
2				Data loss	Data loss	Data loss	Passenger was experimenter
3				Data loss		Data loss	
4				Data loss		Data loss	
5			Data loss	Data loss		Data loss	
6				Data loss	Data loss	Data loss	
7	Data loss	Data loss				Data loss	Took detour of 7 km
8				Data loss	Cut-off end		
9						Data loss	Passenger was experimenter
10				Data loss			Driver was experimenter
11				Data loss			
12						Data loss	
13			Cut-off end	Data loss			
14					Issue starting	Data loss	
15				Data loss			
16						Data loss	
17	Missing sound	Missing sound		Data loss			Passenger was experimenter
18	Missing sound	Missing sound				Data loss	Driver was experimenter
19	Missing sound	Missing sound				Data loss	
20	Missing sound	Missing sound		Data loss			
21	Missing sound	Missing sound		Data loss			
22	Missing sound	Missing sound				Data loss	
23	Missing sound	Missing sound		Data loss			
24	Missing sound	Missing sound				Data loss	
25						Data loss	
26				Data loss			
27			Data loss			Data loss	Passenger was experimenter
28				Data loss	Issue starting		Driver was experimenter
29						Data loss	
30				Data loss			
31						Data loss	
32	Data loss	Data loss		Data loss			

Table G1. Overview dataset facecam videos and eye-tracker data

Appendix H. Head angles

This section contains graphs of all head angles of drivers and passengers for the 24 included trips from the analysis. For all twenty-four trips the same five graphs are showed. Therefore, the description of the five different graphs will be explained in the next paragraph.

Graphs D-E

Graph D	Histogram head angles for driver and passenger	
Graph E	Histogram head angular velocity for driver and passenger	
Legend:	Red:	Driver
	Blue:	Passenger

Trip 1

D

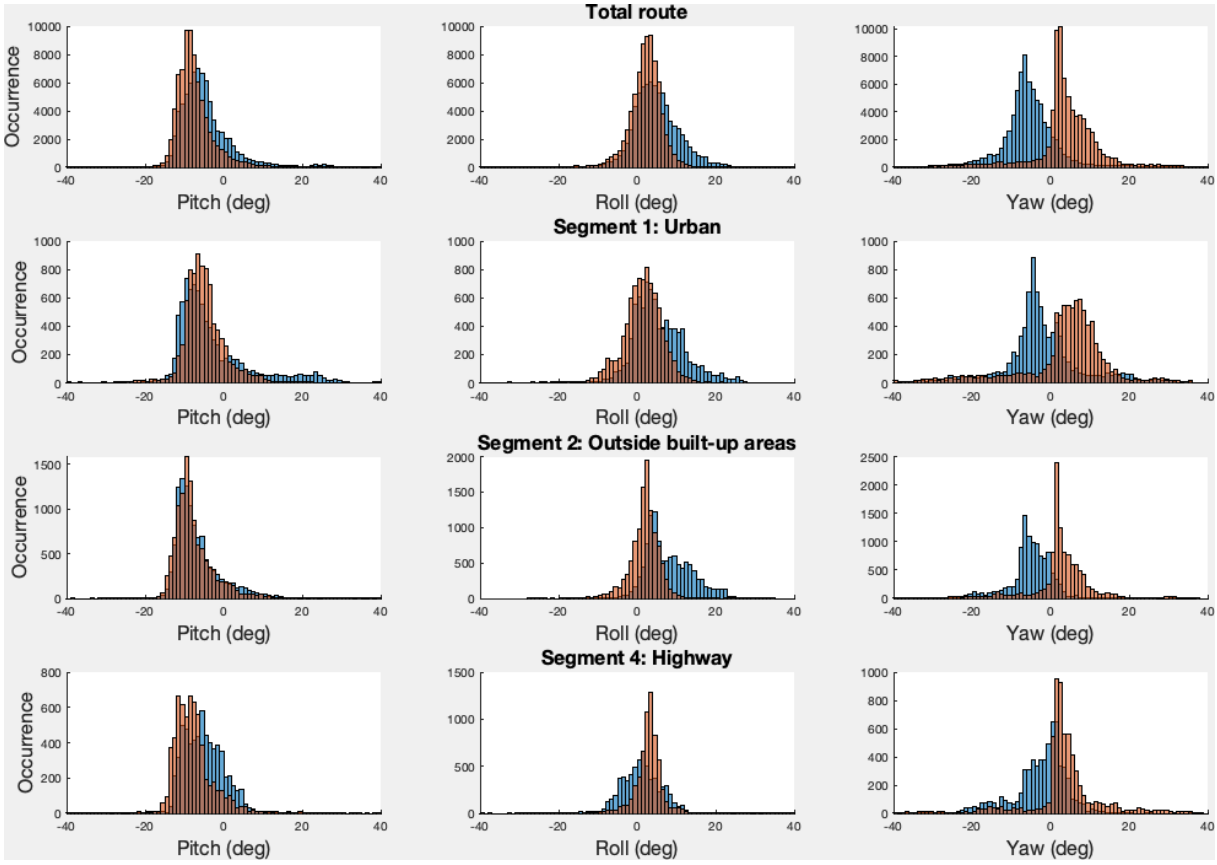
Total route
Occurrence
Pitch (deg)
Roll (deg)
Yaw (deg)
Segment 1: Urban
Segment 2: Outside built-up areas
Segment 4: Highway

E

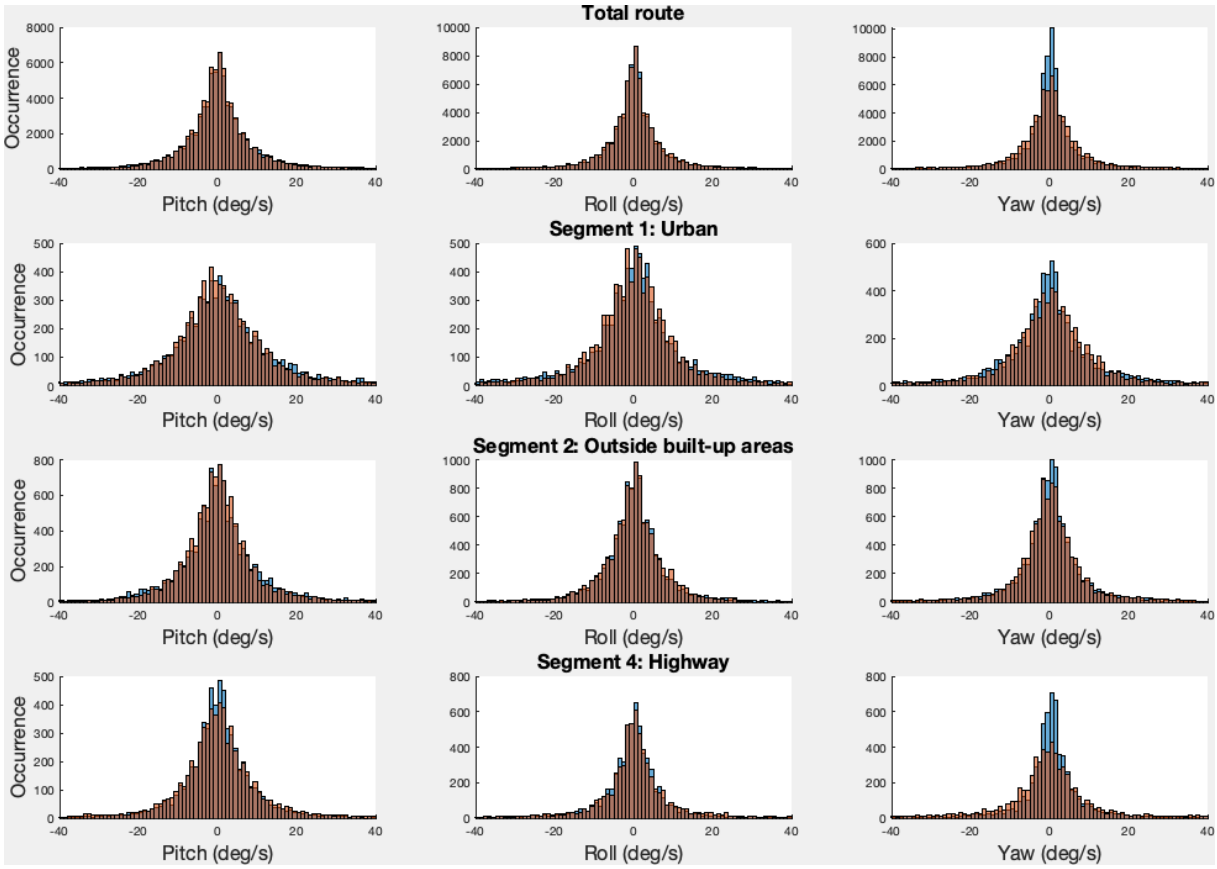
Total route
Occurrence
Pitch (deg/s)
Roll (deg/s)
Yaw (deg/s)
Segment 1: Urban
Segment 2: Outside built-up areas
Segment 4: Highway

Trip 2

D

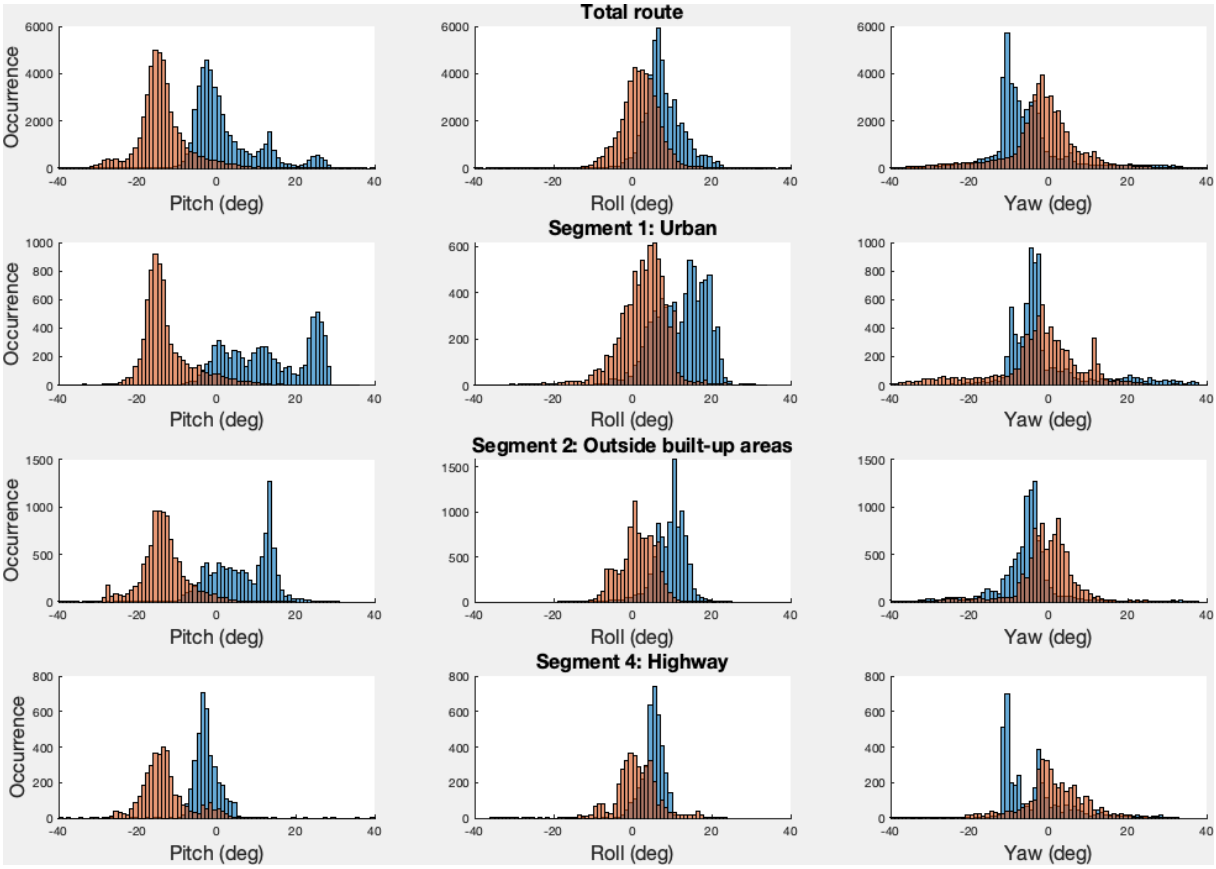
Total route
Occurrence
Pitch (deg)
Roll (deg)
Yaw (deg)
Segment 1: Urban
Segment 2: Outside built-up areas
Segment 4: Highway

E

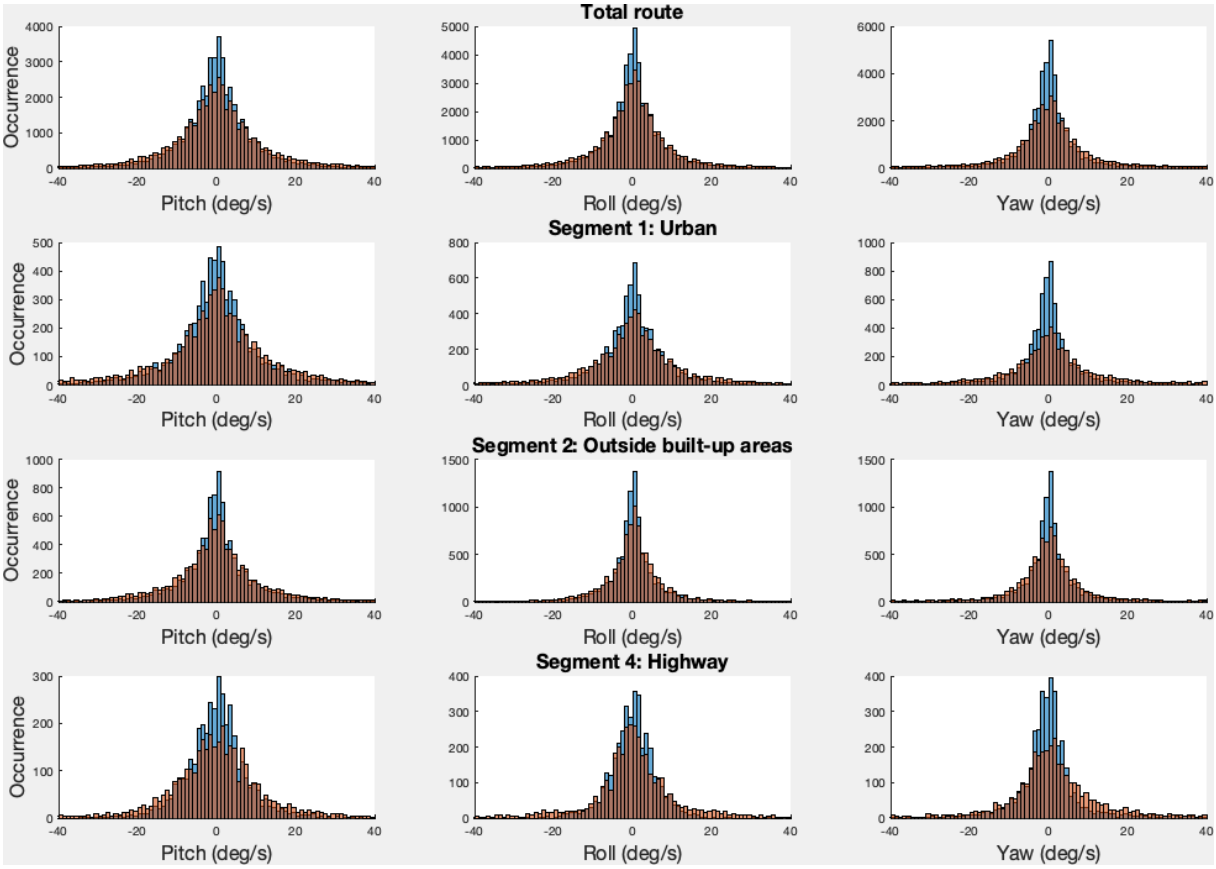
Total route
Occurrence
Pitch (deg/s)
Roll (deg/s)
Yaw (deg/s)
Segment 1: Urban
Segment 2: Outside built-up areas
Segment 4: Highway

Trip 3

D

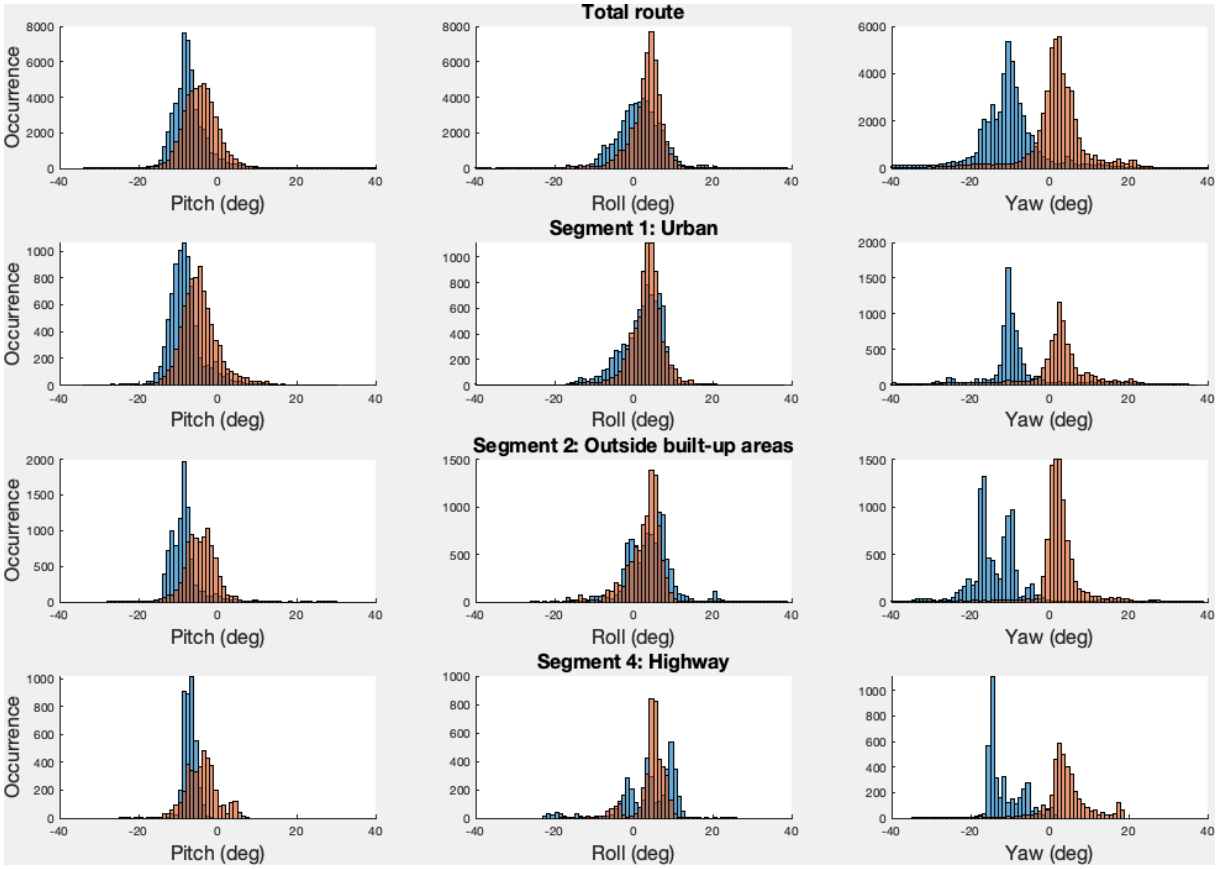
Total route
Occurrence
Pitch (deg)
Roll (deg)
Yaw (deg)
Segment 1: Urban
Segment 2: Outside built-up areas
Segment 4: Highway

E

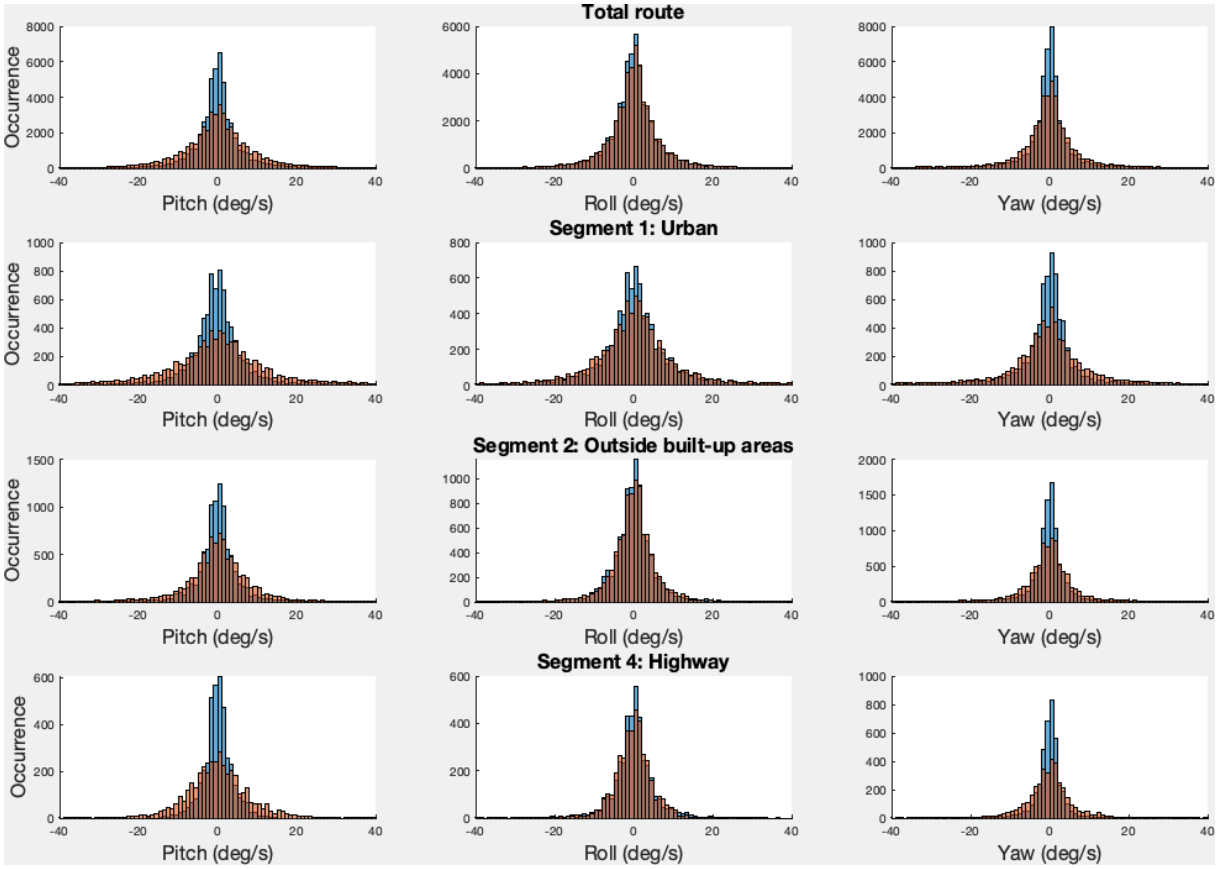
Total route
Occurrence
Pitch (deg/s)
Roll (deg/s)
Yaw (deg/s)
Segment 1: Urban
Segment 2: Outside built-up areas
Segment 4: Highway

Trip 4

D

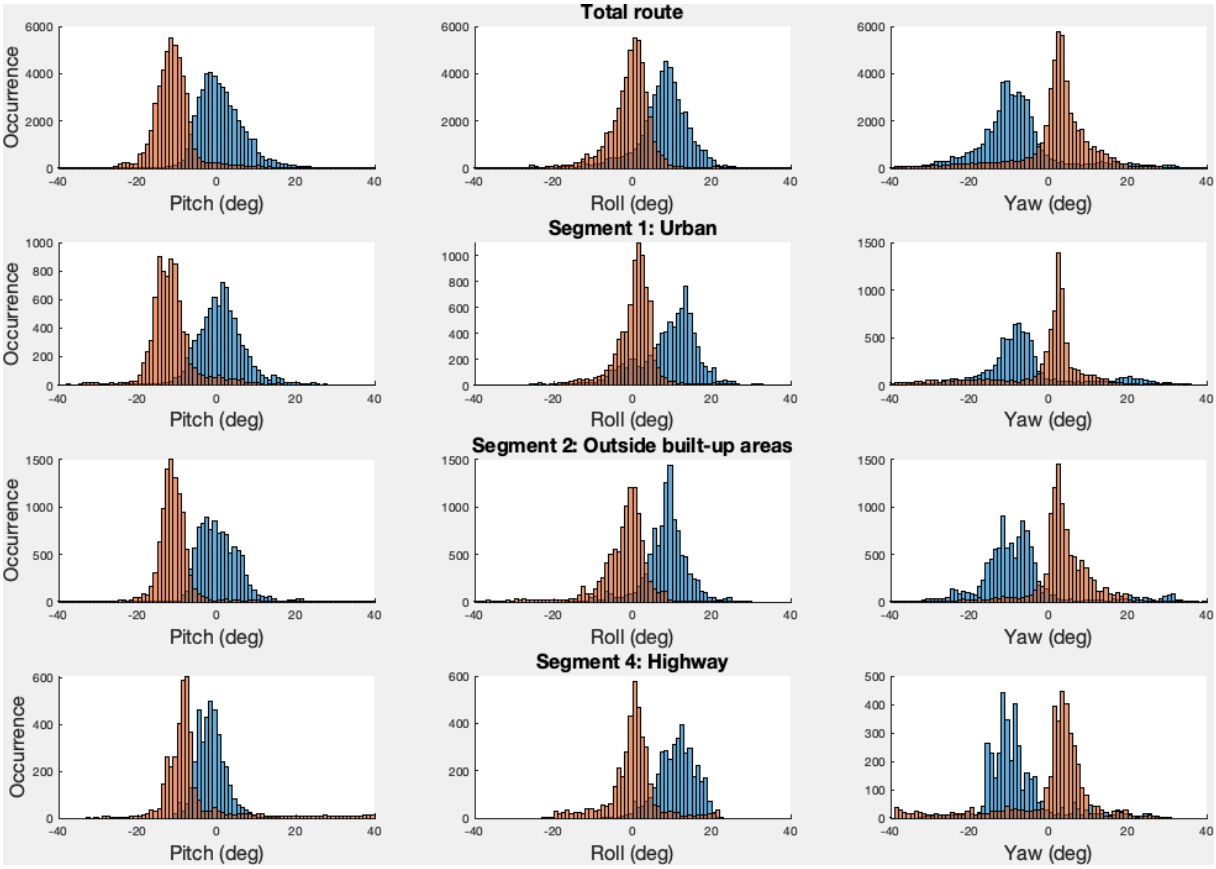
Total route
Segment 1: Urban
Segment 2: Outside built-up areas
Segment 4: Highway
Occurrence
Pitch (deg)
Roll (deg)
Yaw (deg)

E

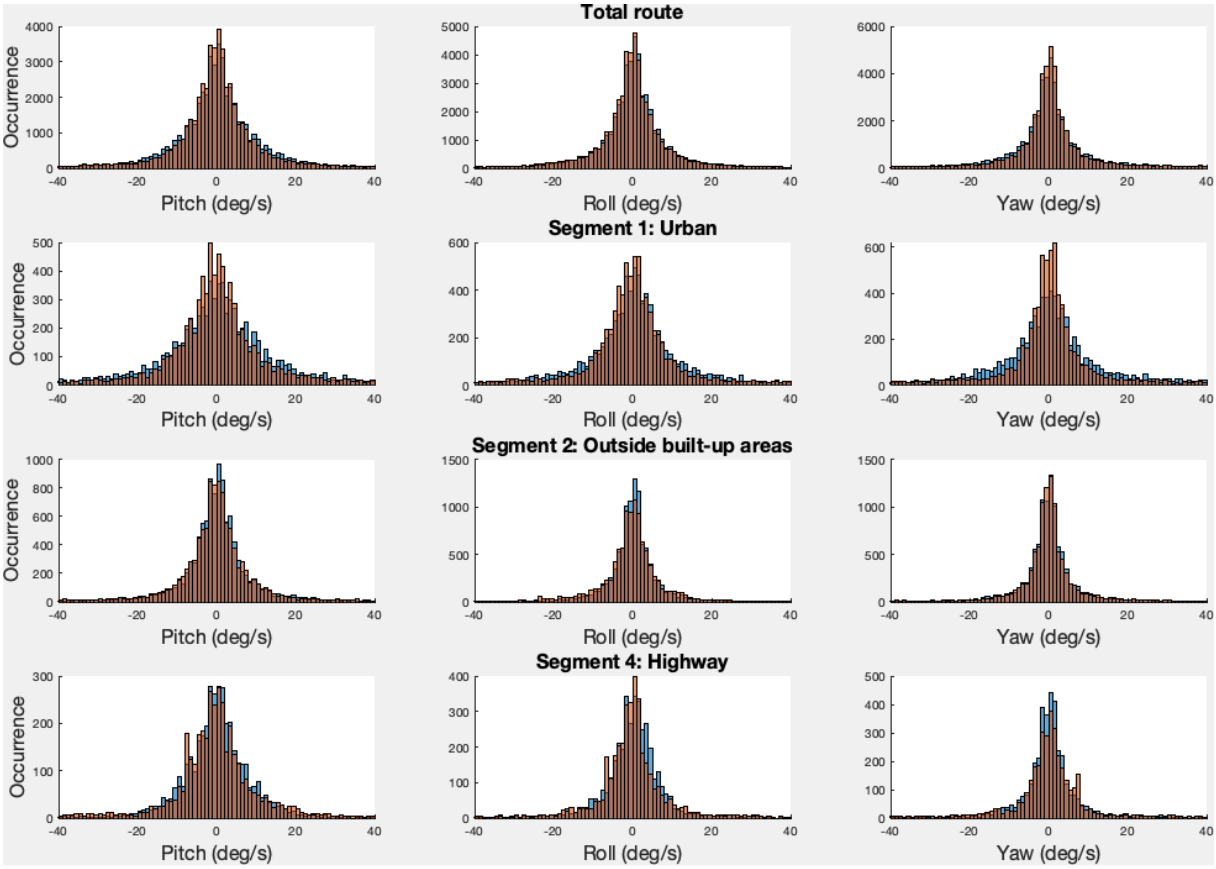
Total route
Segment 1: Urban
Segment 2: Outside built-up areas
Segment 4: Highway
Occurrence
Pitch (deg/s)
Roll (deg/s)
Yaw (deg/s)

Trip 5

D

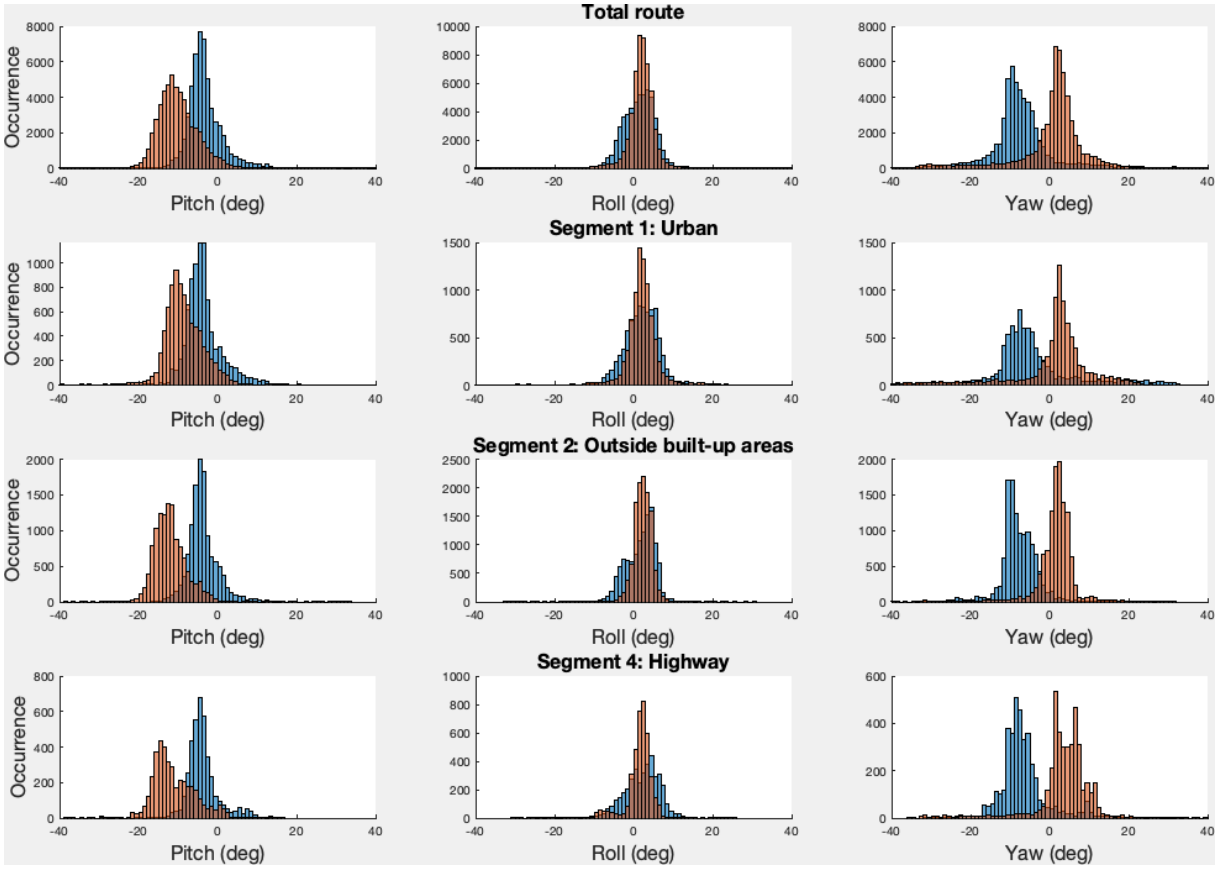
Total route
Segment 1: Urban
Segment 2: Outside built-up areas
Segment 4: Highway
Occurrence
Pitch (deg)
Roll (deg)
Yaw (deg)

E

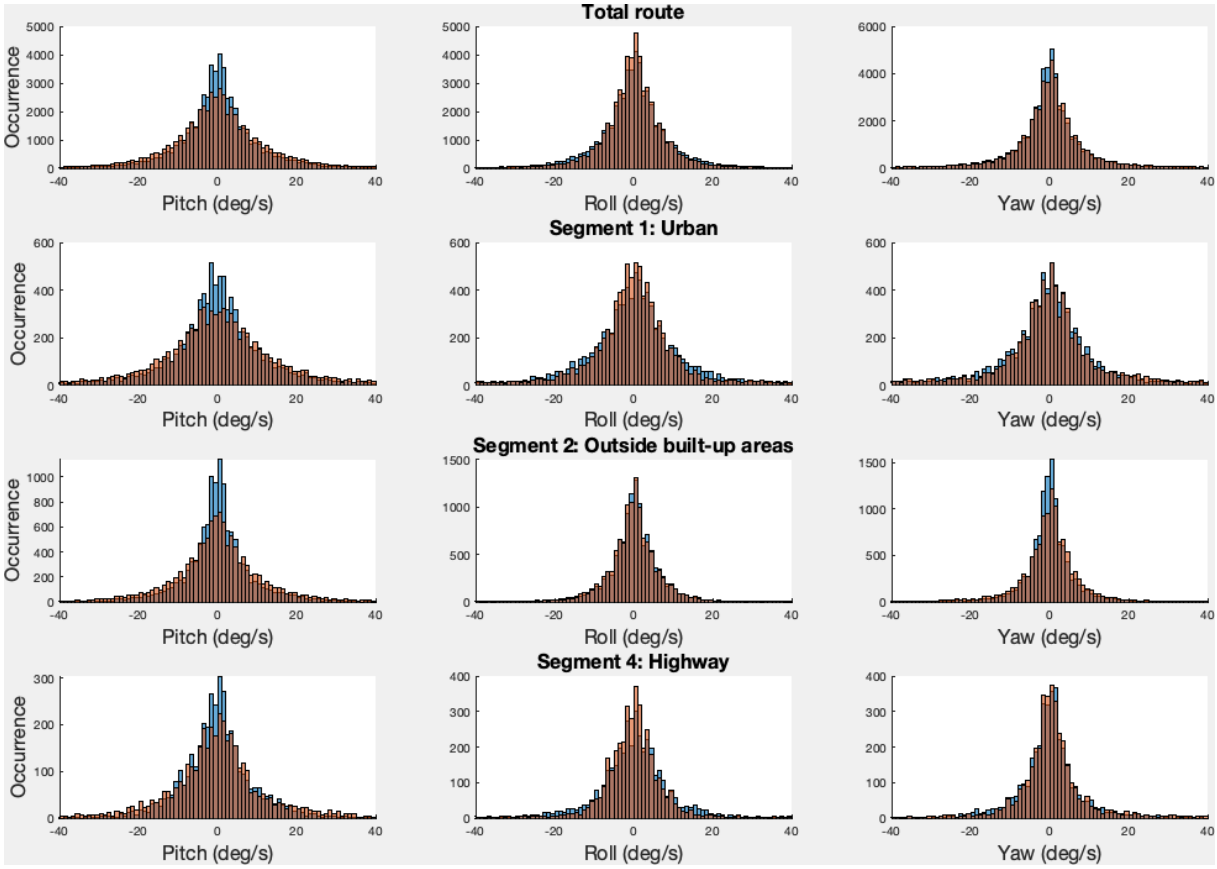
Total route
Segment 1: Urban
Segment 2: Outside built-up areas
Segment 4: Highway
Occurrence
Pitch (deg/s)
Roll (deg/s)
Yaw (deg/s)

Trip 6

D

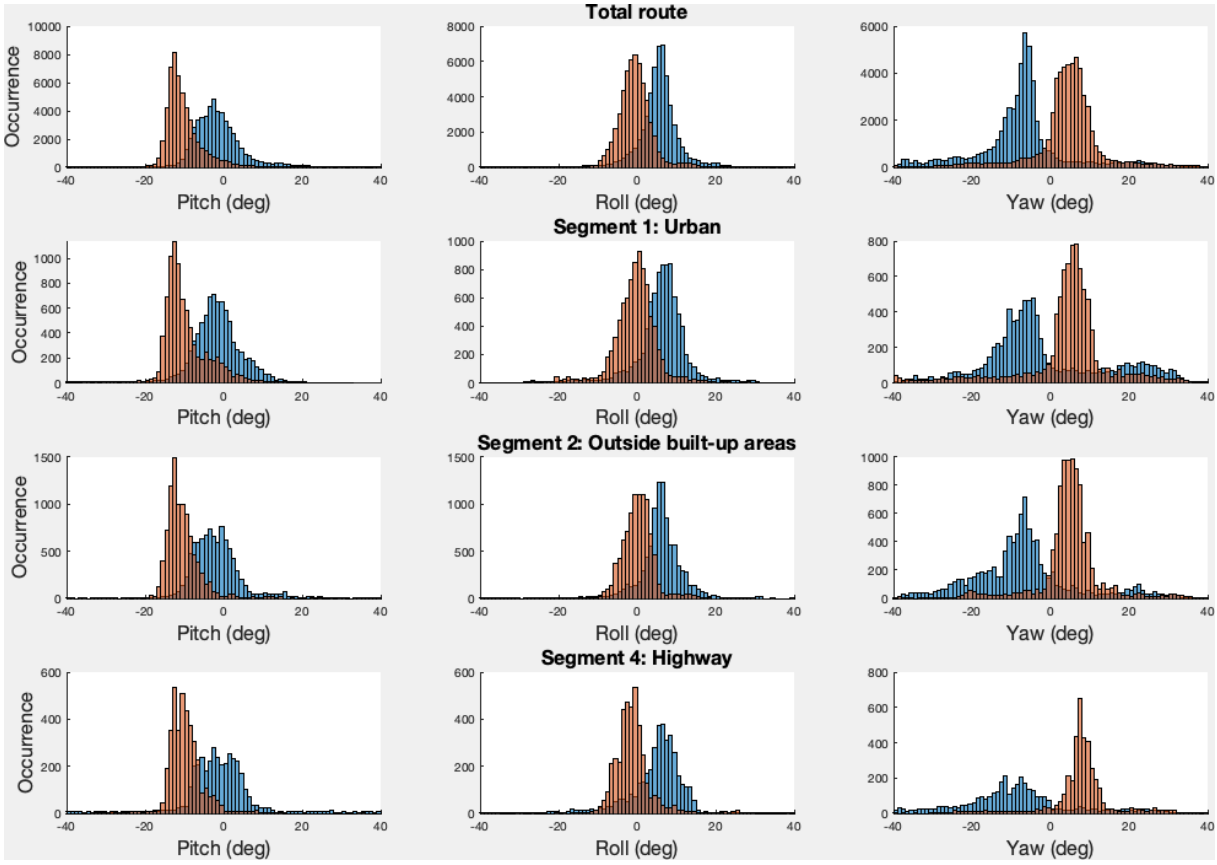
Total route
Segment 1: Urban
Segment 2: Outside built-up areas
Segment 4: Highway
Occurrence
Pitch (deg)
Roll (deg)
Yaw (deg)

E

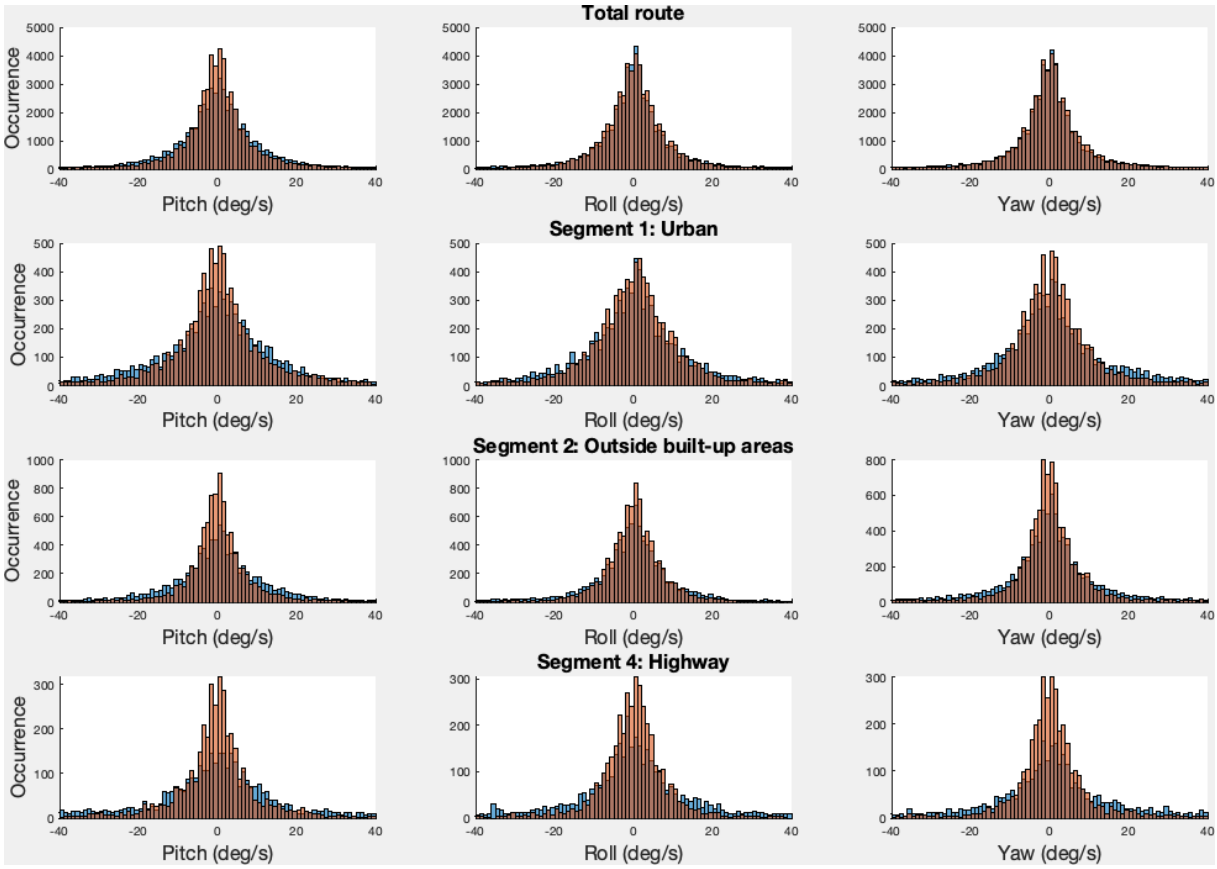
Total route
Segment 1: Urban
Segment 2: Outside built-up areas
Segment 4: Highway
Occurrence
Pitch (deg/s)
Roll (deg/s)
Yaw (deg/s)

Trip 8

D

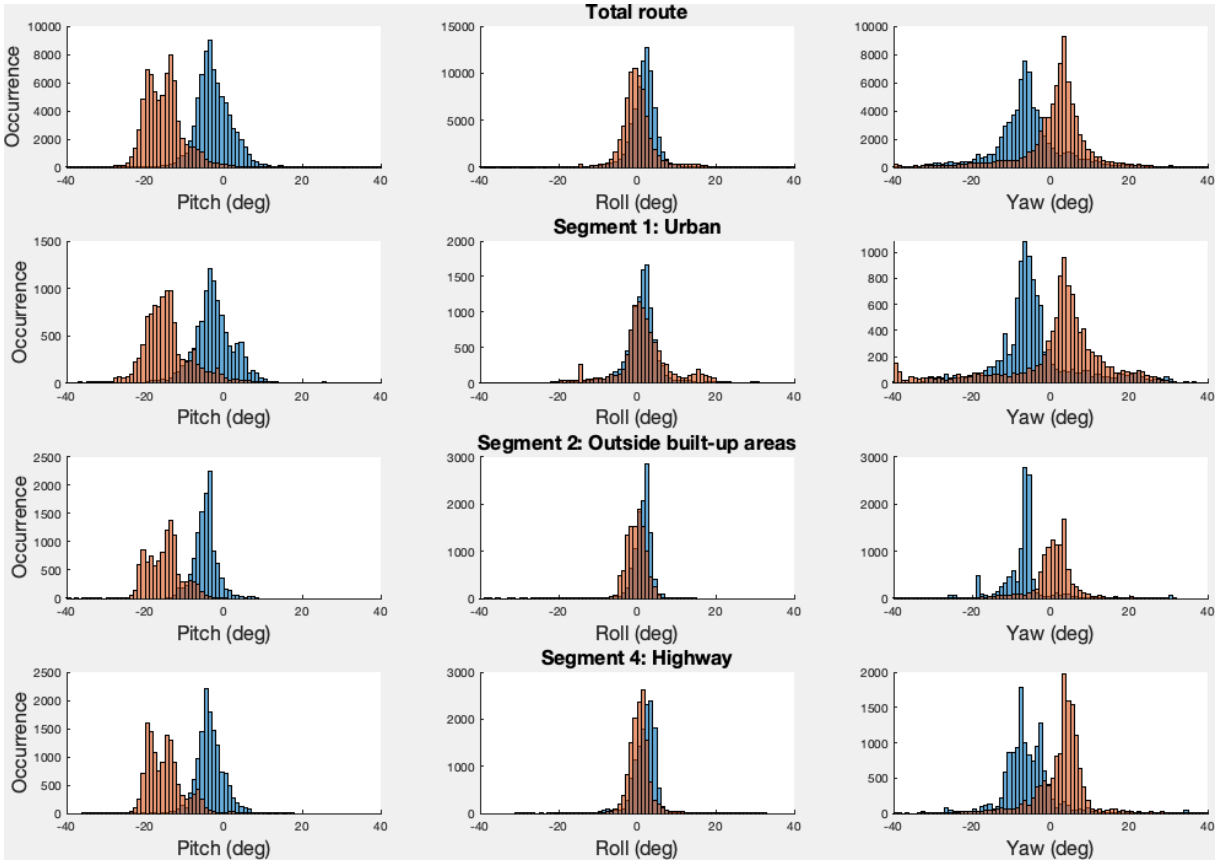
Total route
Segment 1: Urban
Segment 2: Outside built-up areas
Segment 4: Highway
Occurrence
Pitch (deg)
Roll (deg)
Yaw (deg)

E

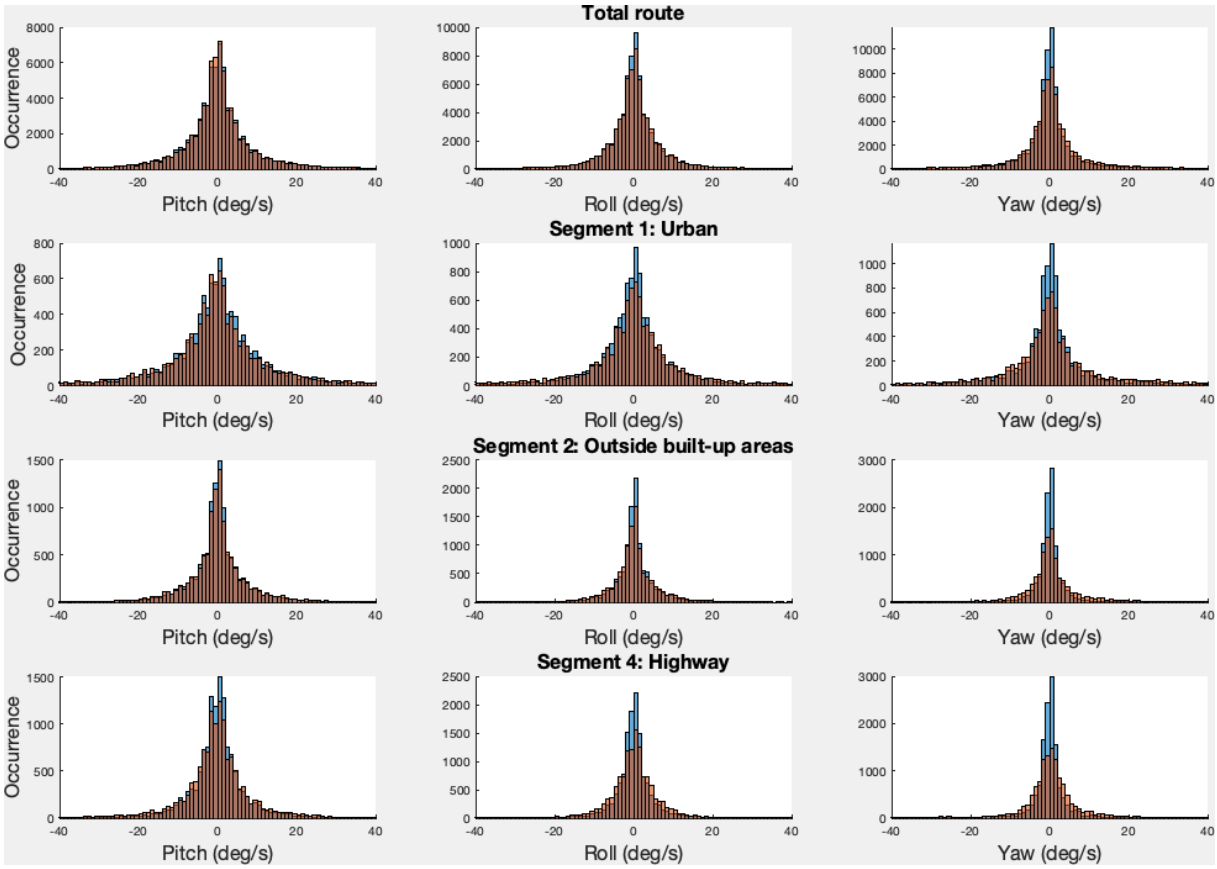
Total route
Segment 1: Urban
Segment 2: Outside built-up areas
Segment 4: Highway
Occurrence
Pitch (deg/s)
Roll (deg/s)
Yaw (deg/s)

Trip 10

D

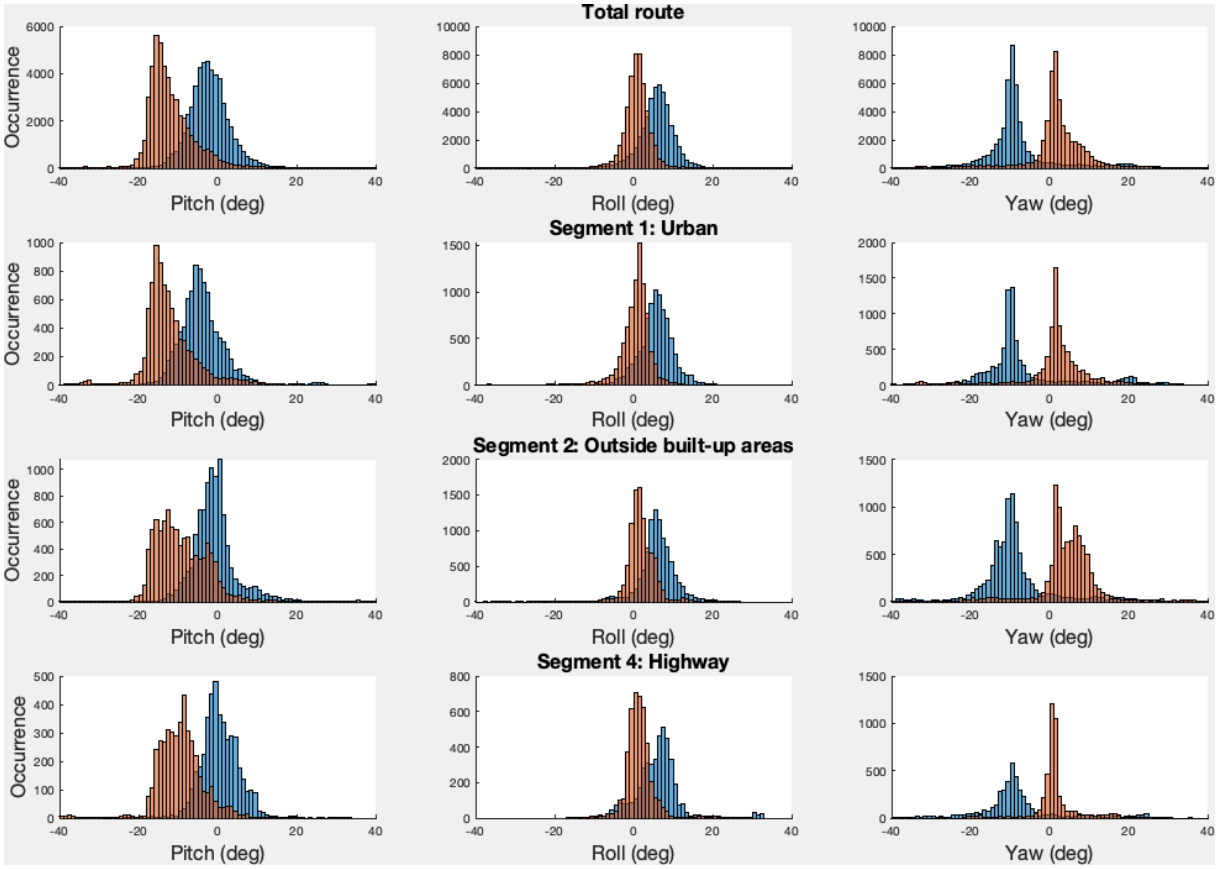
Total route
Segment 1: Urban
Segment 2: Outside built-up areas
Segment 4: Highway
Occurrence
Pitch (deg)
Roll (deg)
Yaw (deg)

E

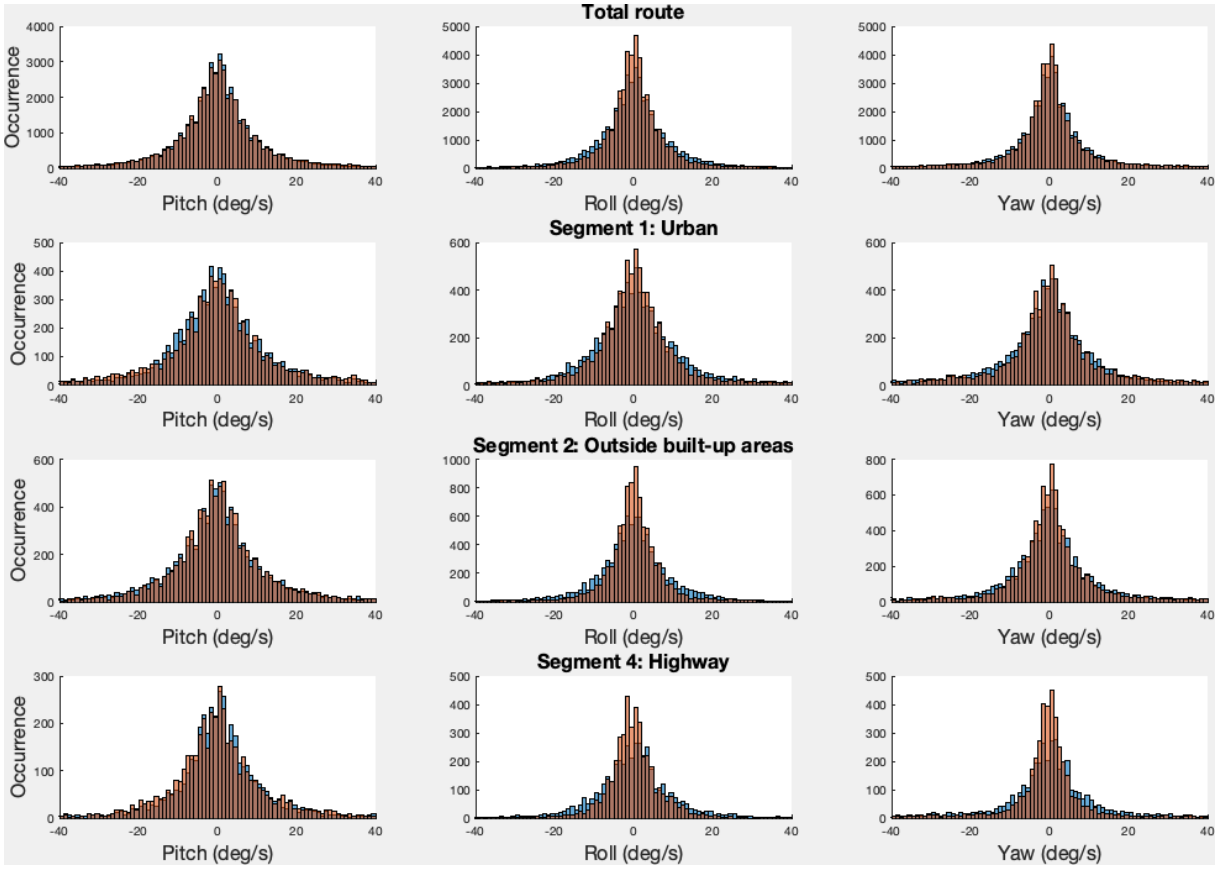
Total route
Segment 1: Urban
Segment 2: Outside built-up areas
Segment 4: Highway
Occurrence
Pitch (deg/s)
Roll (deg/s)
Yaw (deg/s)

Trip 14

D

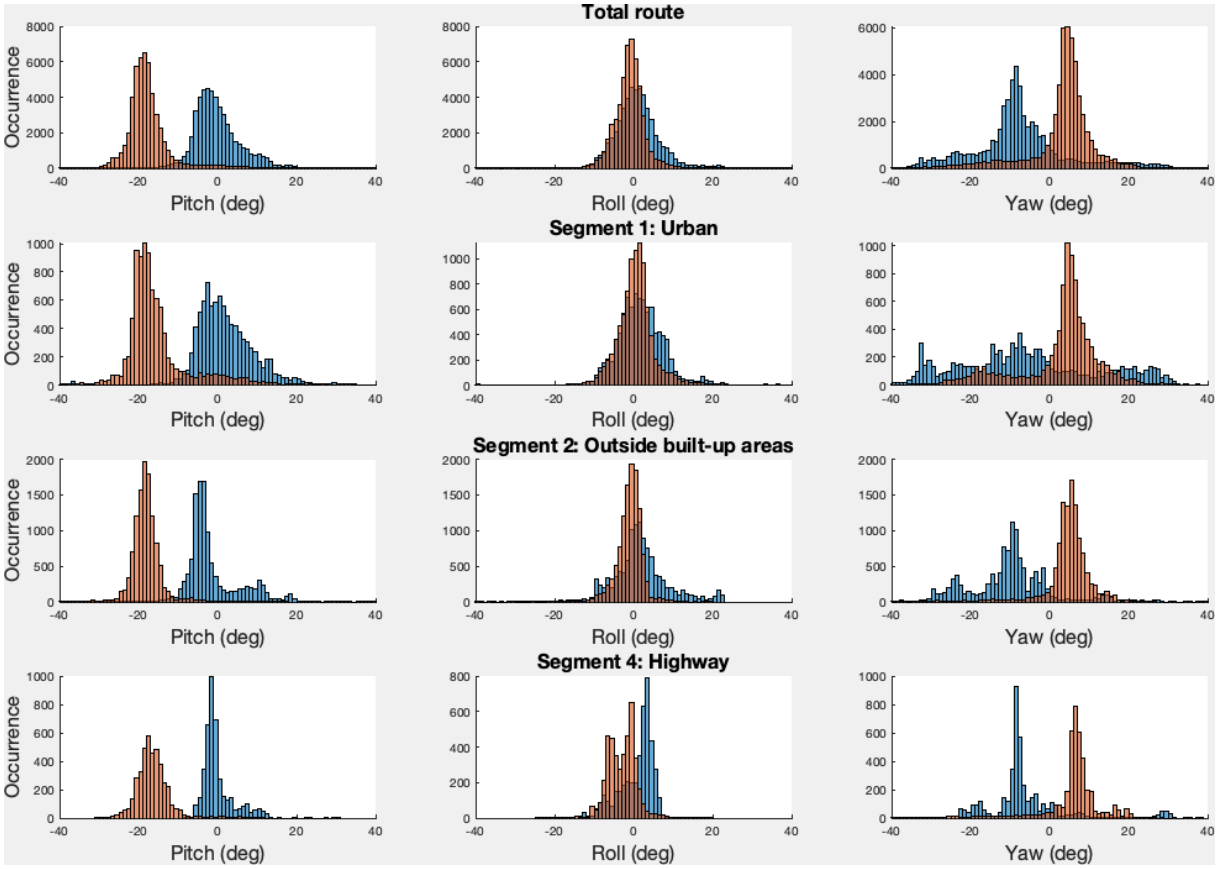
Total route
Occurrence
Pitch (deg)
Roll (deg)
Yaw (deg)
Segment 1: Urban
Segment 2: Outside built-up areas
Segment 4: Highway

E

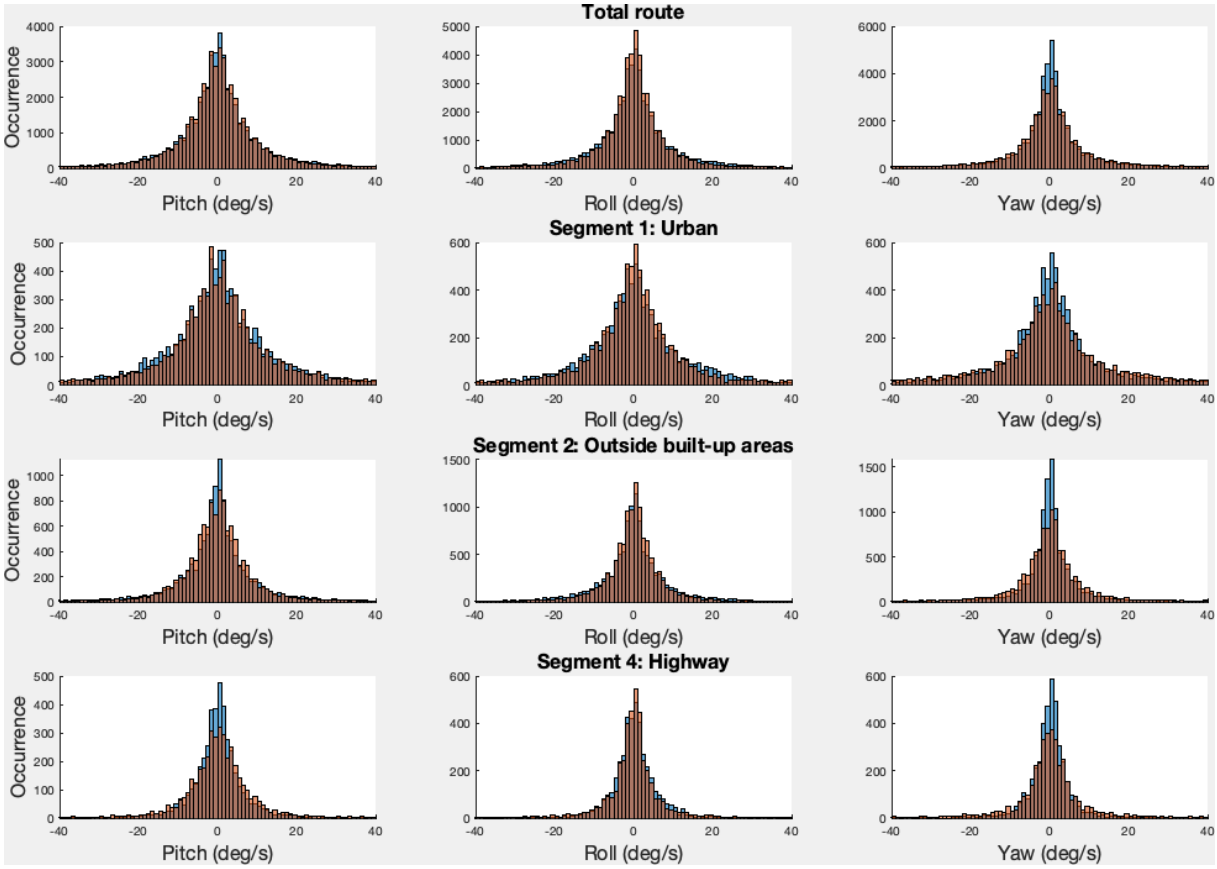
Total route
Occurrence
Pitch (deg/s)
Roll (deg/s)
Yaw (deg/s)
Segment 1: Urban
Segment 2: Outside built-up areas
Segment 4: Highway

Trip 15

D

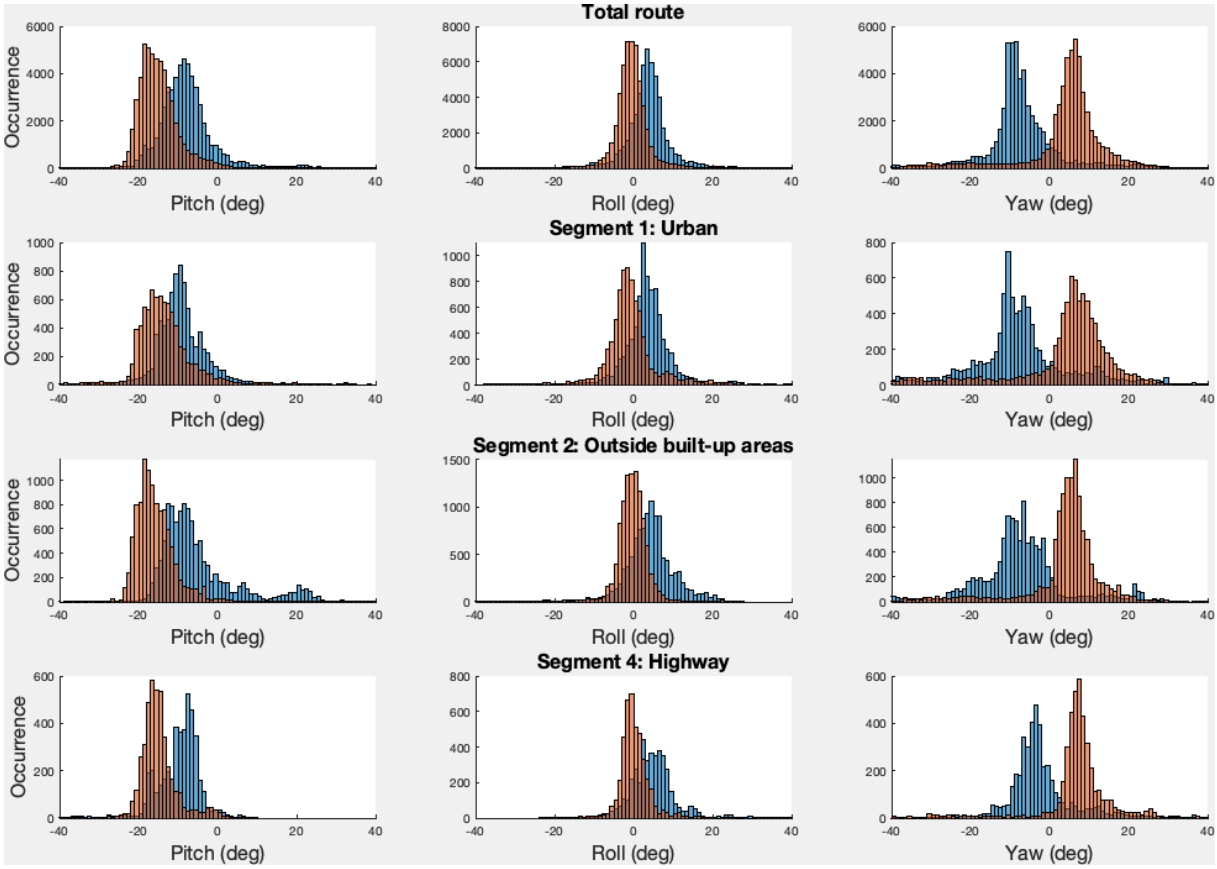
Total route
Occurrence
Pitch (deg)
Roll (deg)
Yaw (deg)
Segment 1: Urban
Segment 2: Outside built-up areas
Segment 4: Highway

E

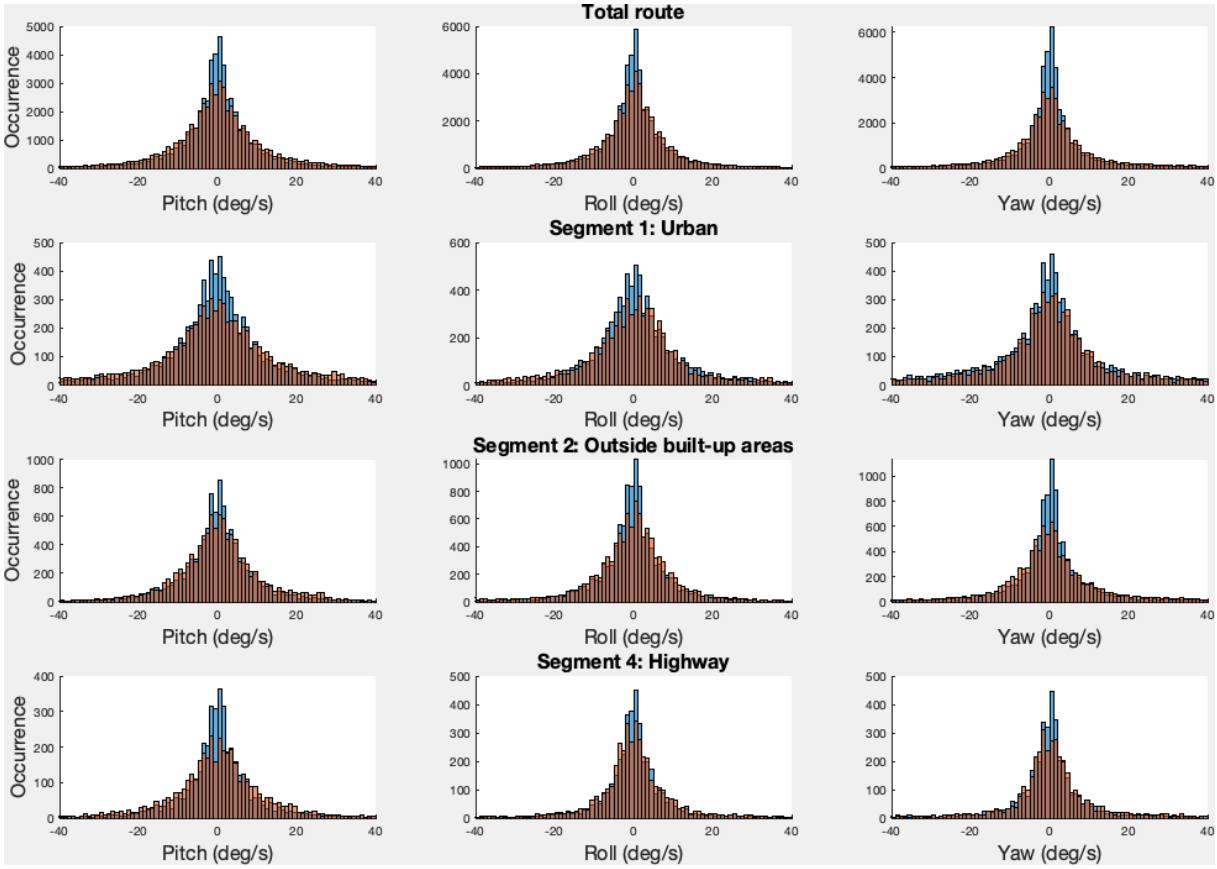
Total route
Occurrence
Pitch (deg/s)
Roll (deg/s)
Yaw (deg/s)
Segment 1: Urban
Segment 2: Outside built-up areas
Segment 4: Highway

Trip 16

D

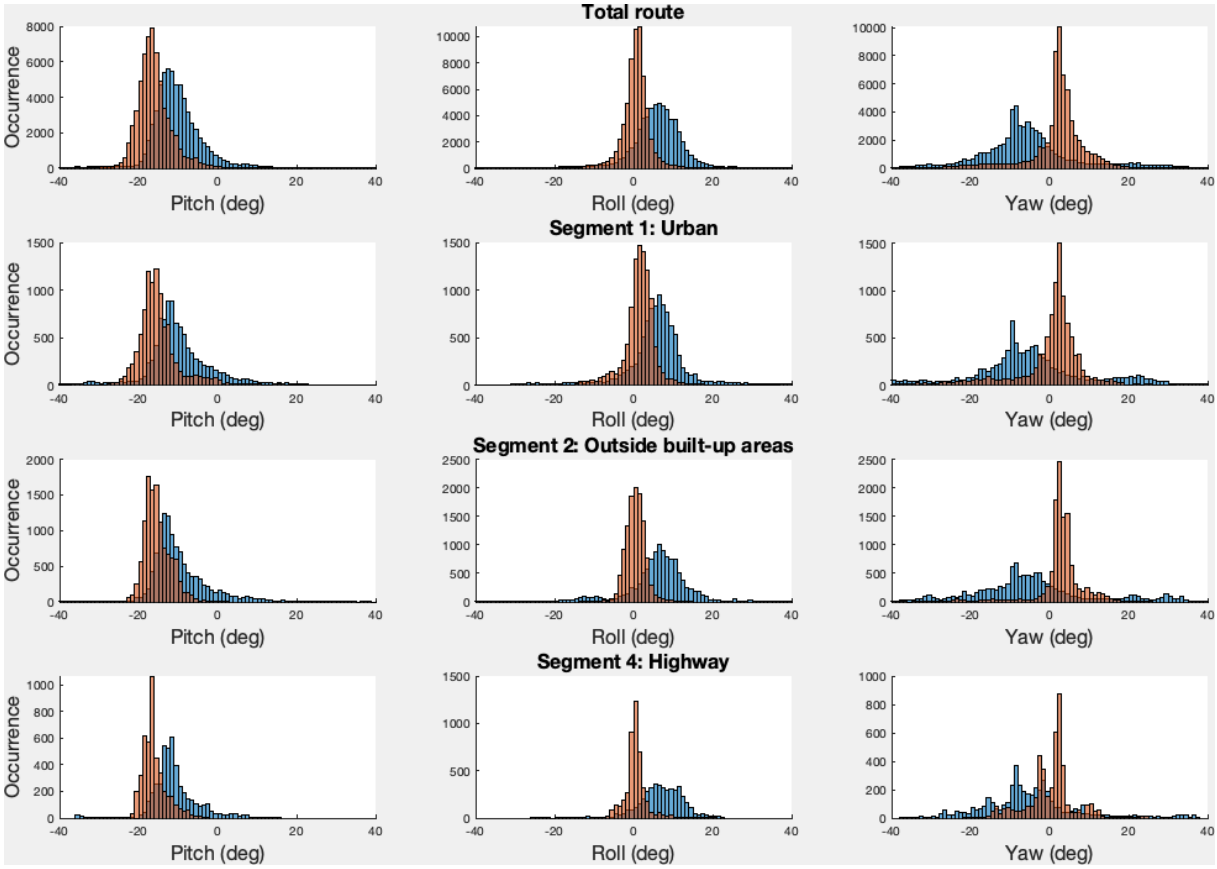
Total route
Occurrence
Pitch (deg)
Roll (deg)
Yaw (deg)
Segment 1: Urban
Segment 2: Outside built-up areas
Segment 4: Highway

E

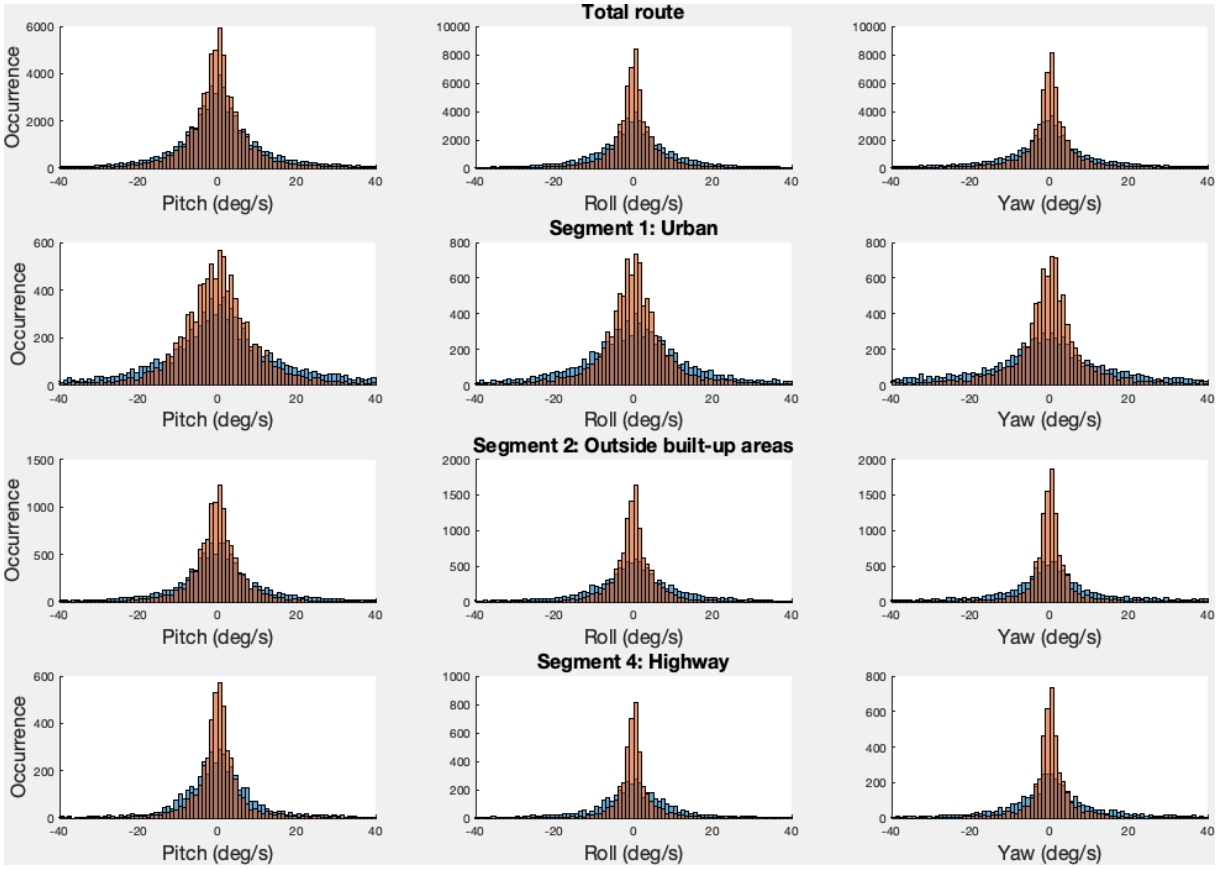
Total route
Occurrence
Pitch (deg/s)
Roll (deg/s)
Yaw (deg/s)
Segment 1: Urban
Segment 2: Outside built-up areas
Segment 4: Highway

Trip 17

D

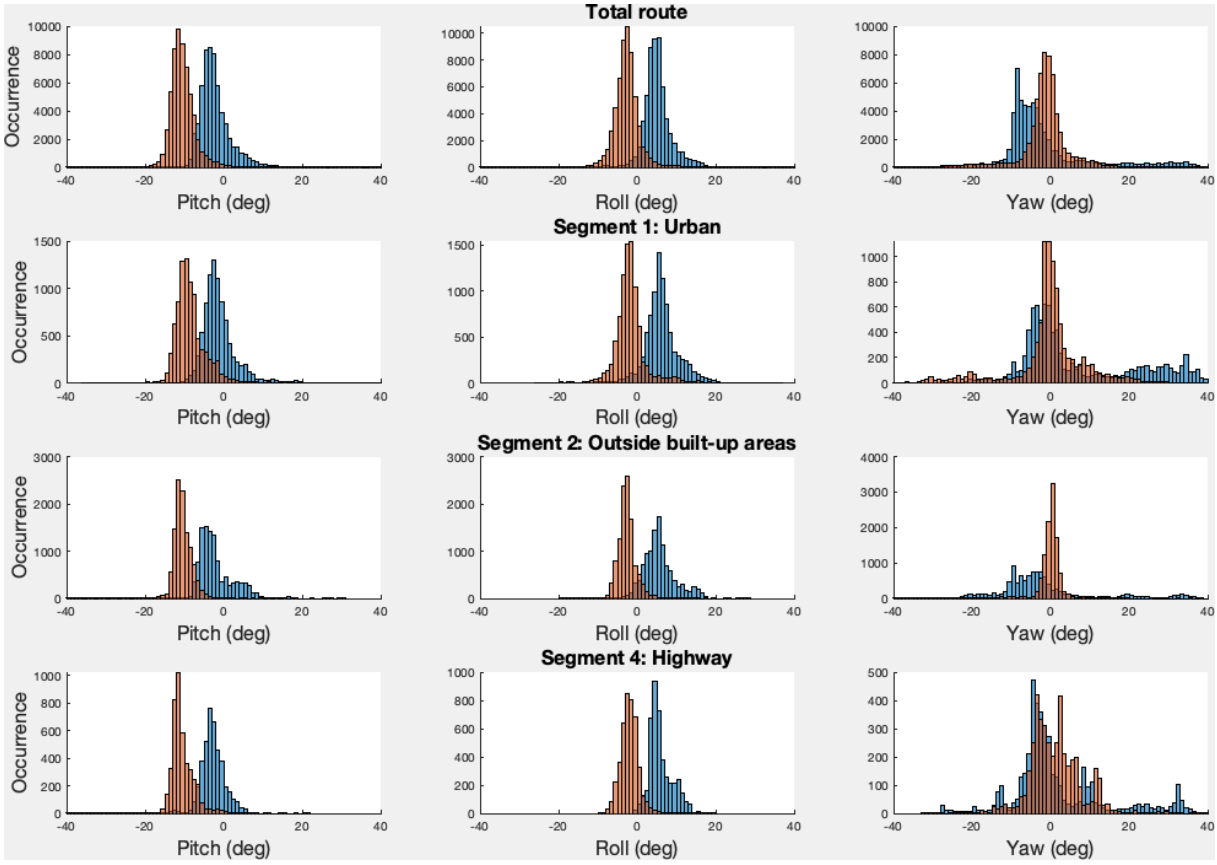
Total route
Occurrence
Pitch (deg)
Roll (deg)
Yaw (deg)
Segment 1: Urban
Segment 2: Outside built-up areas
Segment 4: Highway

E

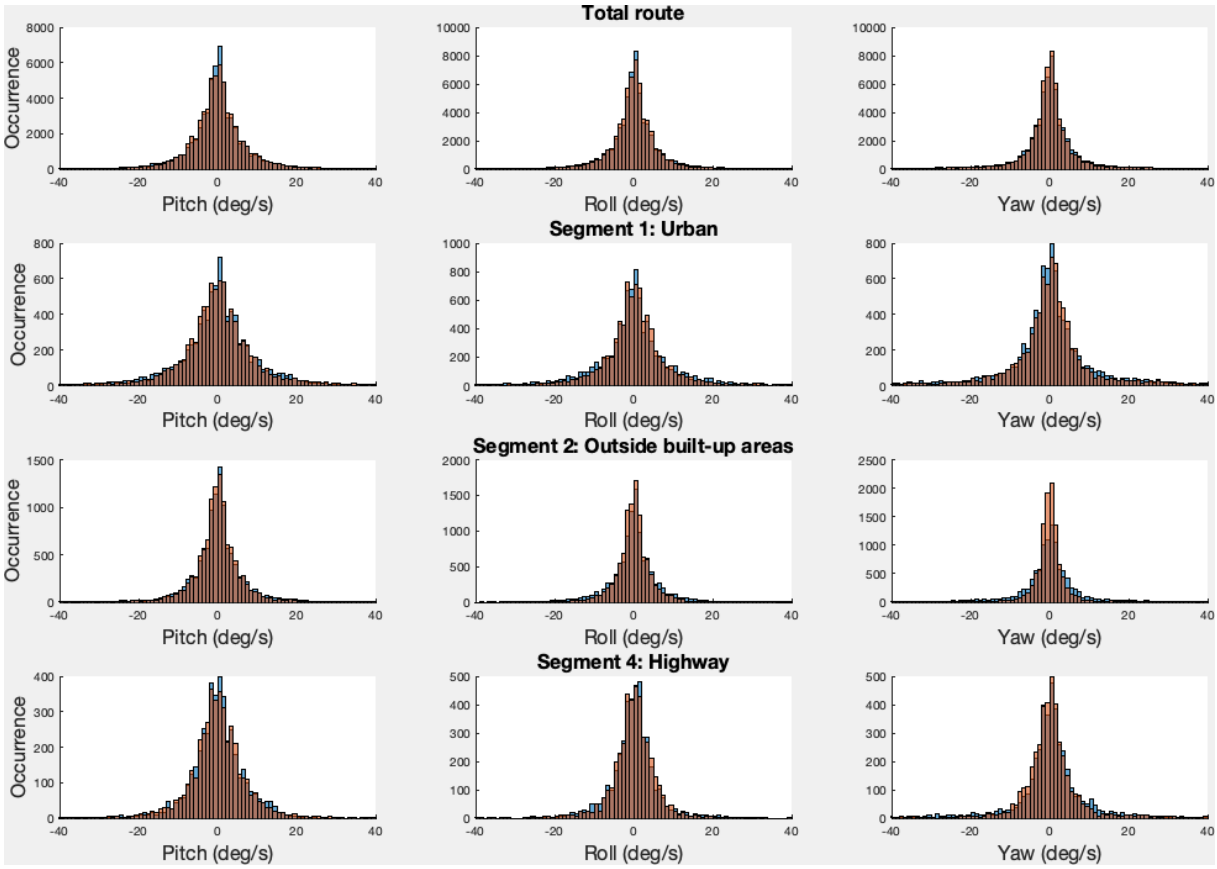
Total route
Occurrence
Pitch (deg/s)
Roll (deg/s)
Yaw (deg/s)
Segment 1: Urban
Segment 2: Outside built-up areas
Segment 4: Highway

Trip 18

D

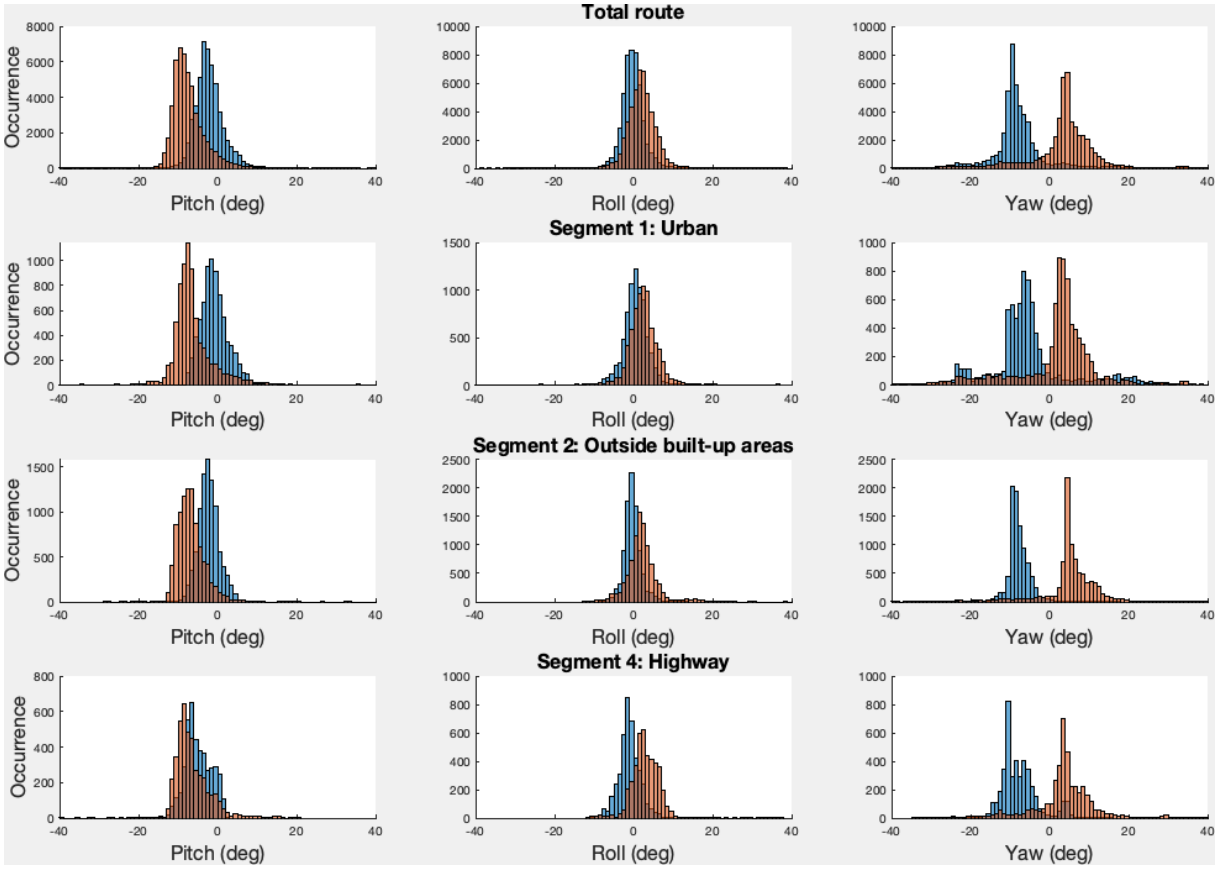
Total route
Segment 1: Urban
Segment 2: Outside built-up areas
Segment 4: Highway
Occurrence
Pitch (deg)
Roll (deg)
Yaw (deg)

E

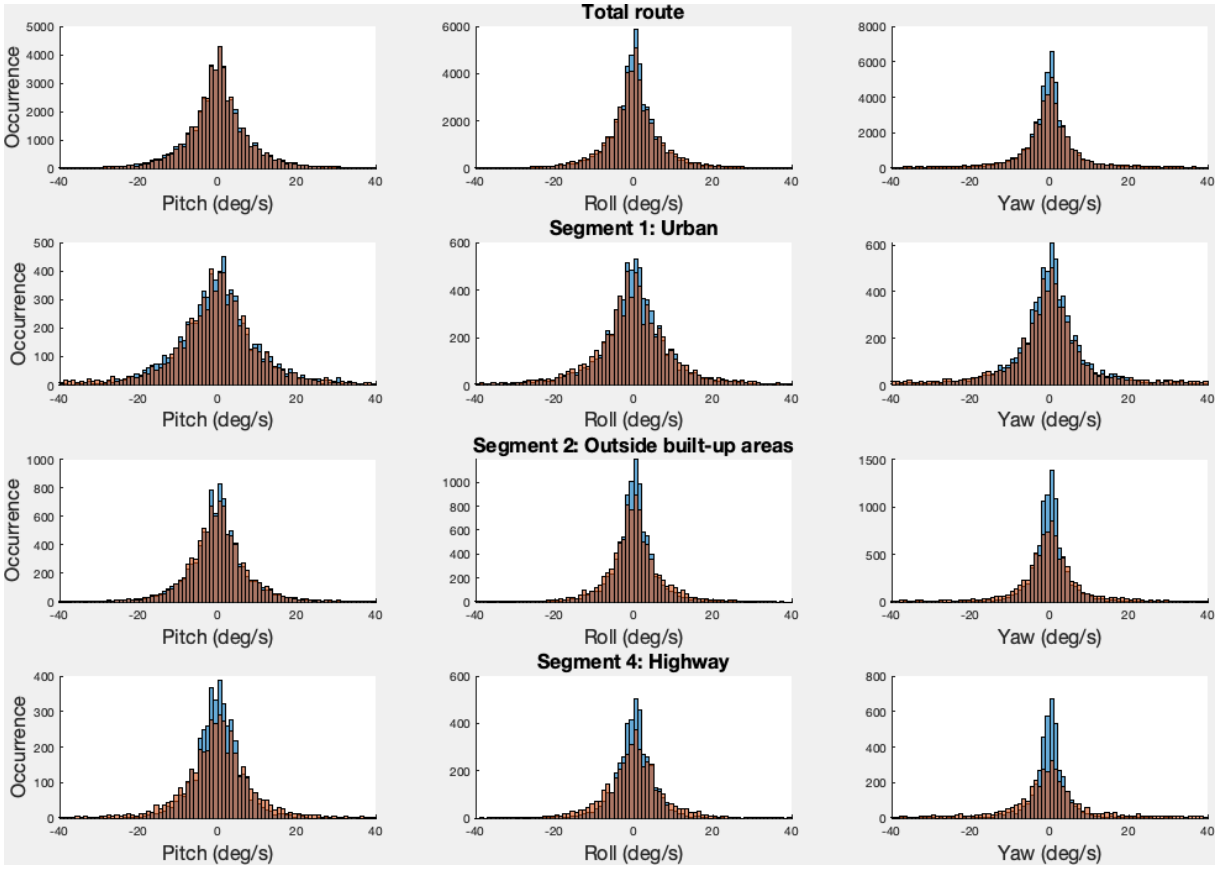
Total route
Segment 1: Urban
Segment 2: Outside built-up areas
Segment 4: Highway
Occurrence
Pitch (deg/s)
Roll (deg/s)
Yaw (deg/s)

Trip 19

D

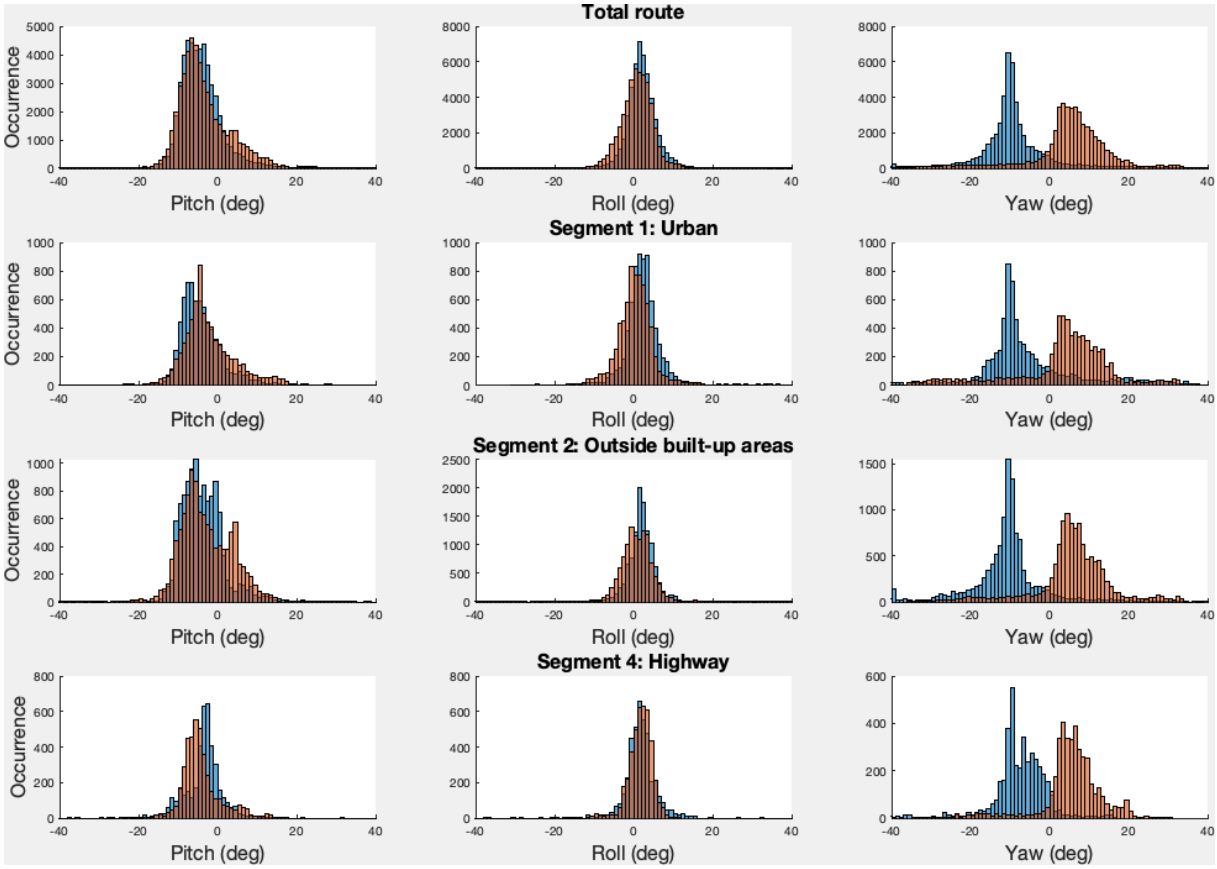
Total route
Segment 1: Urban
Segment 2: Outside built-up areas
Segment 4: Highway
Occurrence
Pitch (deg)
Roll (deg)
Yaw (deg)

E

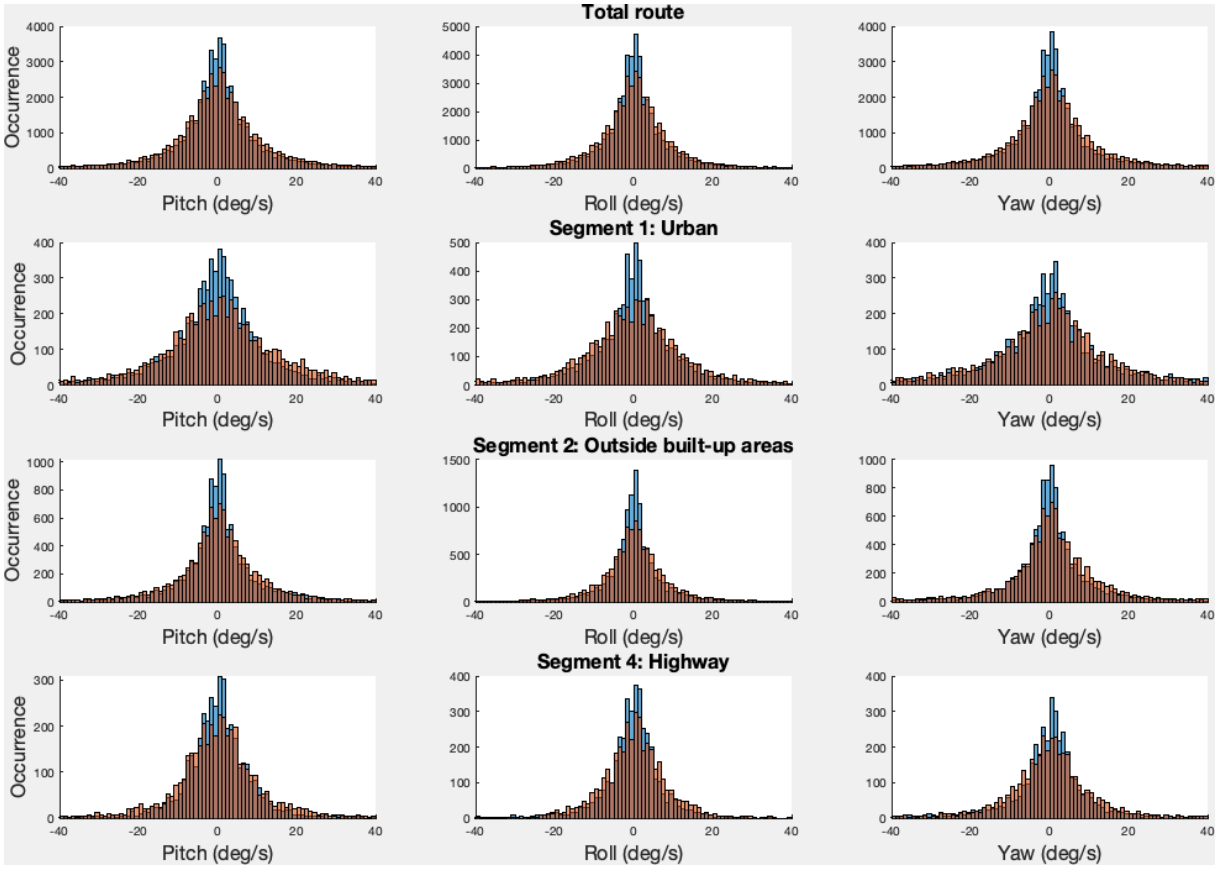
Total route
Segment 1: Urban
Segment 2: Outside built-up areas
Segment 4: Highway
Occurrence
Pitch (deg/s)
Roll (deg/s)
Yaw (deg/s)

Trip 20

D

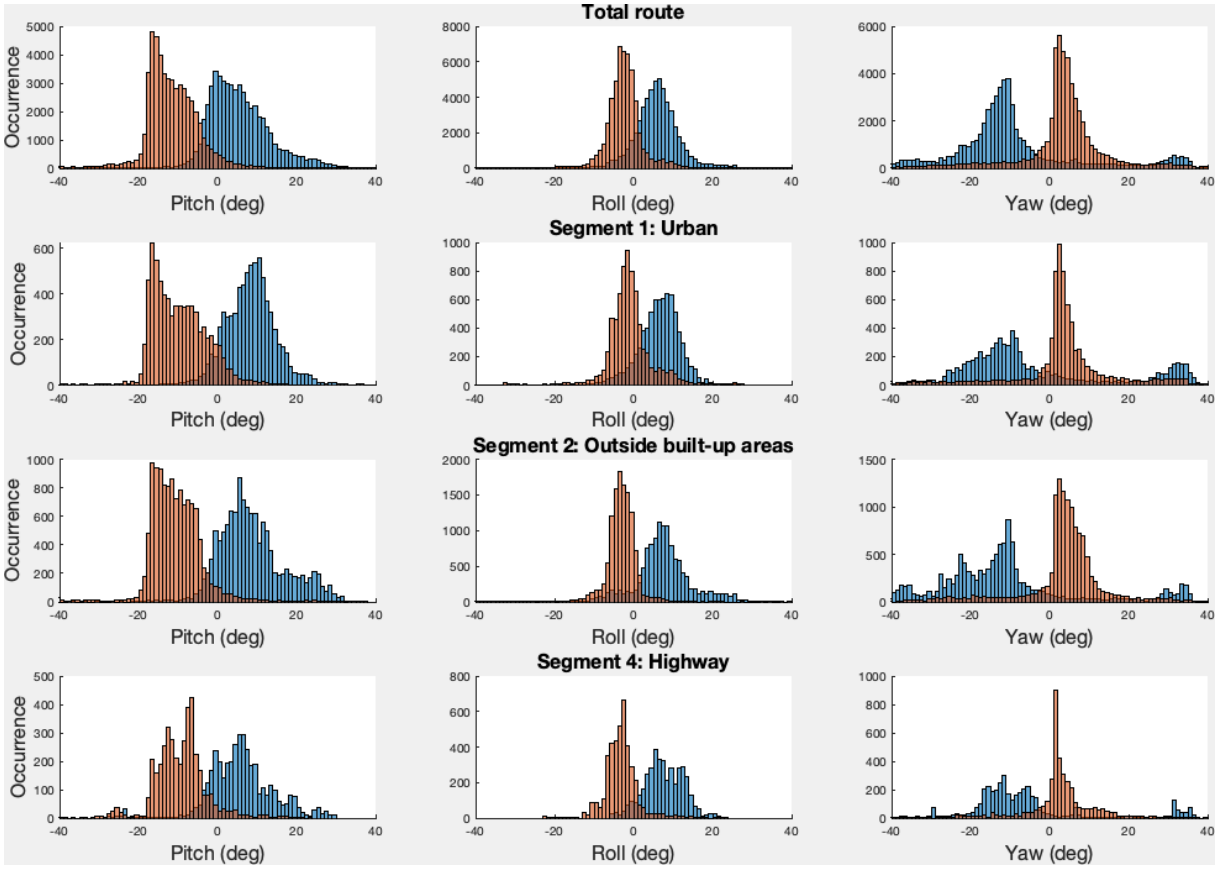
Total route
Occurrence
Pitch (deg)
Roll (deg)
Yaw (deg)
Segment 1: Urban
Segment 2: Outside built-up areas
Segment 4: Highway

E

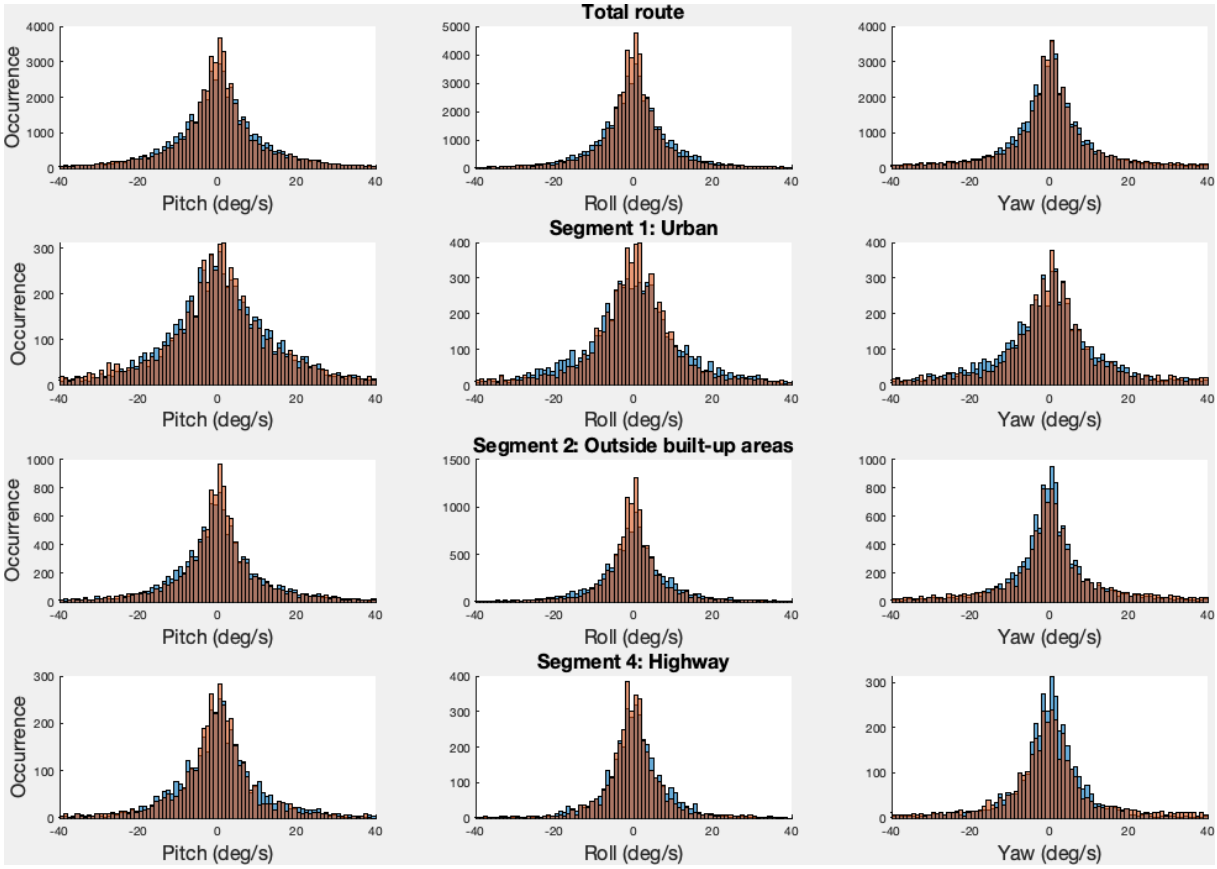
Total route
Occurrence
Pitch (deg/s)
Roll (deg/s)
Yaw (deg/s)
Segment 1: Urban
Segment 2: Outside built-up areas
Segment 4: Highway

Trip 21

D

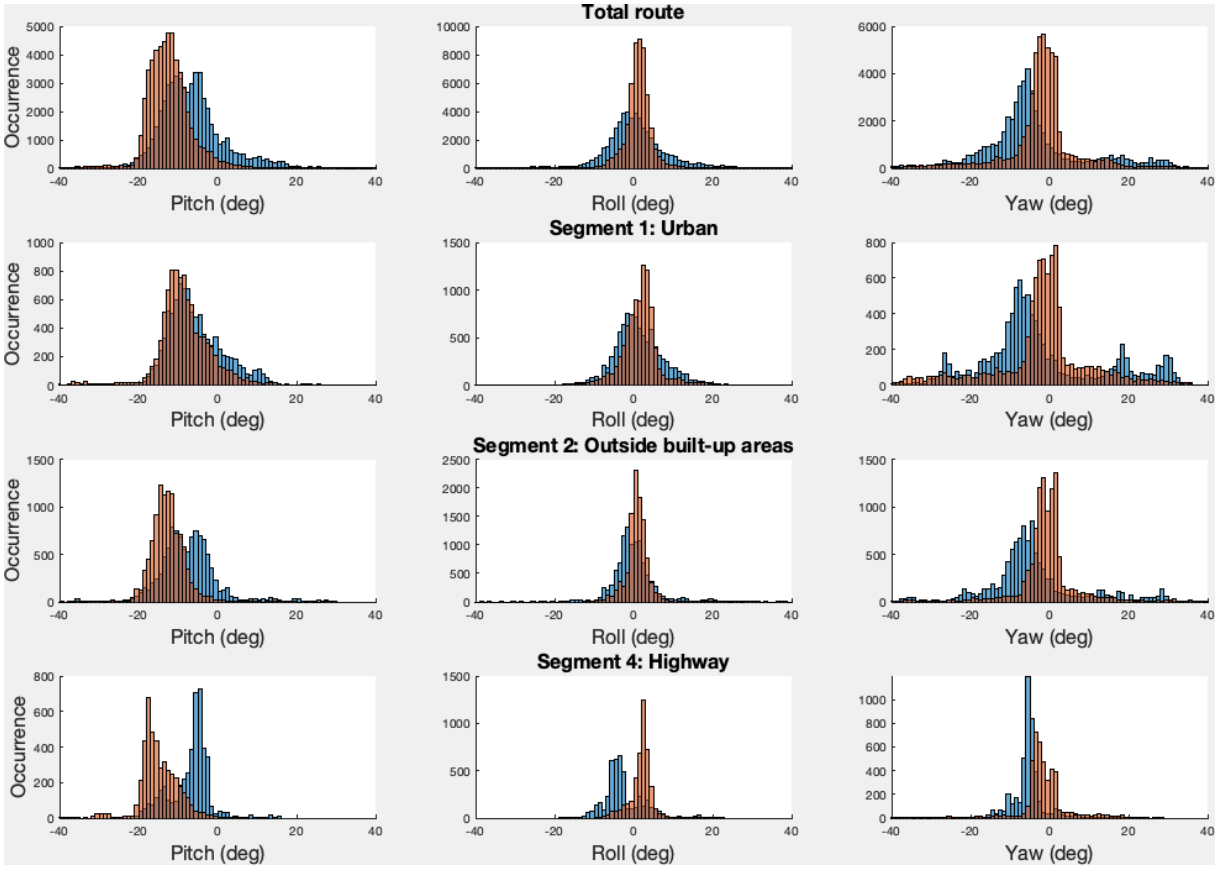
Total route
Occurrence
Pitch (deg)
Roll (deg)
Yaw (deg)
Segment 1: Urban
Segment 2: Outside built-up areas
Segment 4: Highway

E

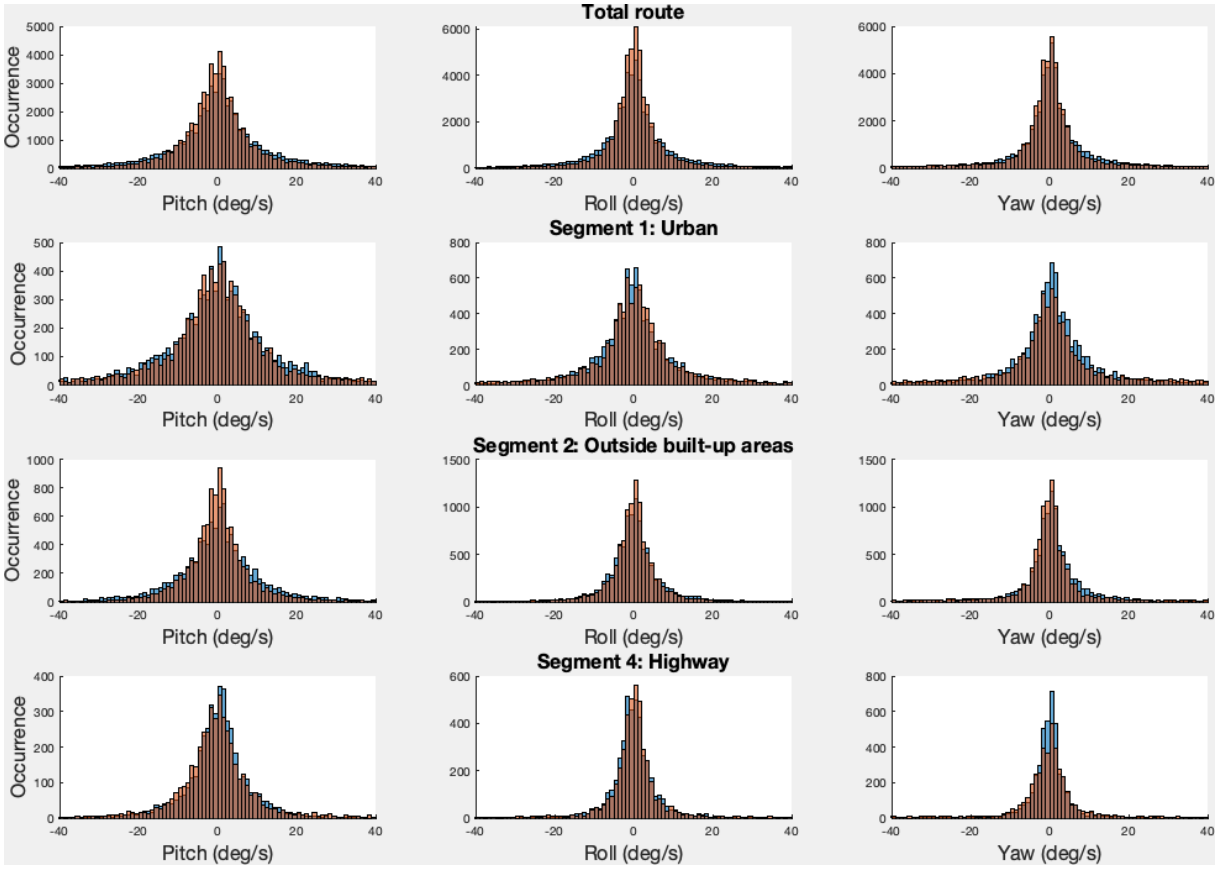
Total route
Occurrence
Pitch (deg/s)
Roll (deg/s)
Yaw (deg/s)
Segment 1: Urban
Segment 2: Outside built-up areas
Segment 4: Highway

Trip 23

D

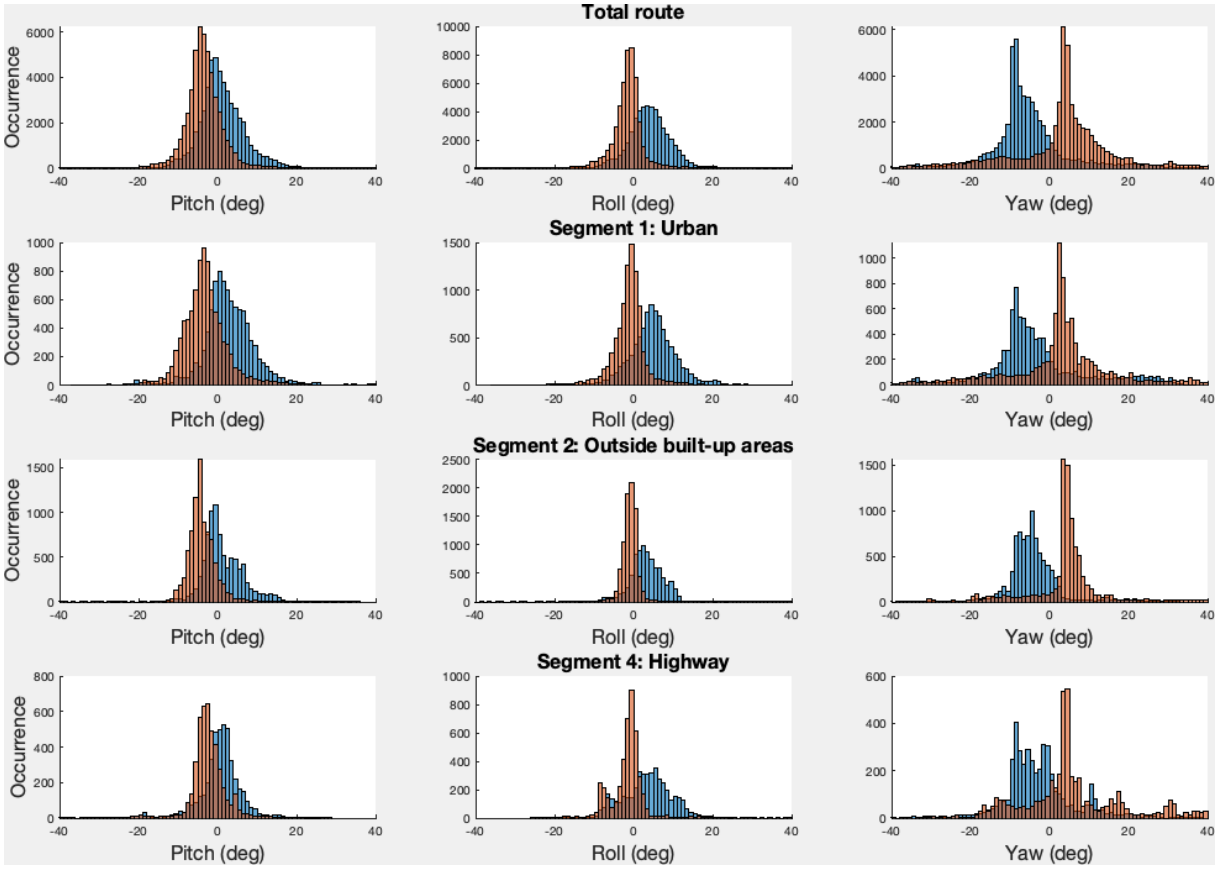
Total route
Occurrence
Pitch (deg)
Roll (deg)
Yaw (deg)
Segment 1: Urban
Segment 2: Outside built-up areas
Segment 4: Highway

E

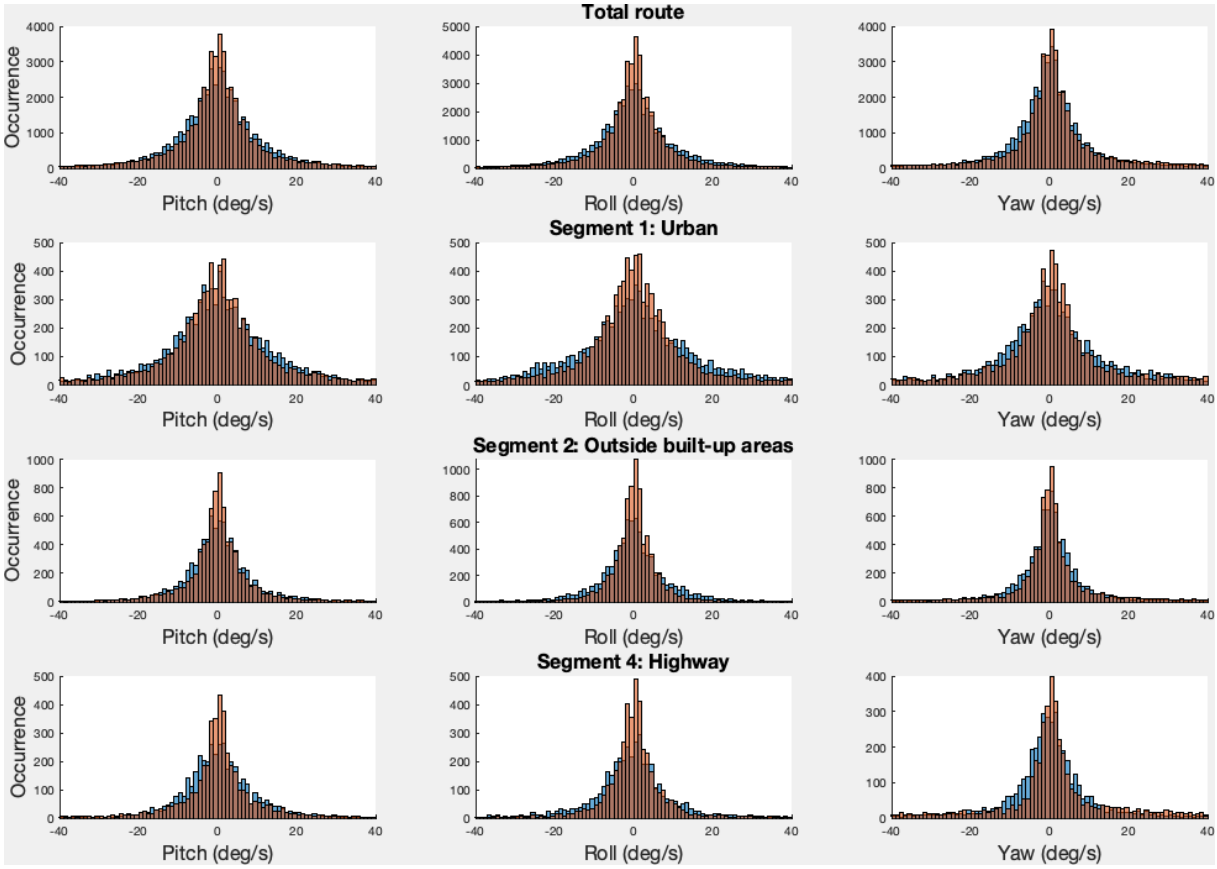
Total route
Occurrence
Pitch (deg/s)
Roll (deg/s)
Yaw (deg/s)
Segment 1: Urban
Segment 2: Outside built-up areas
Segment 4: Highway

Trip 24

D

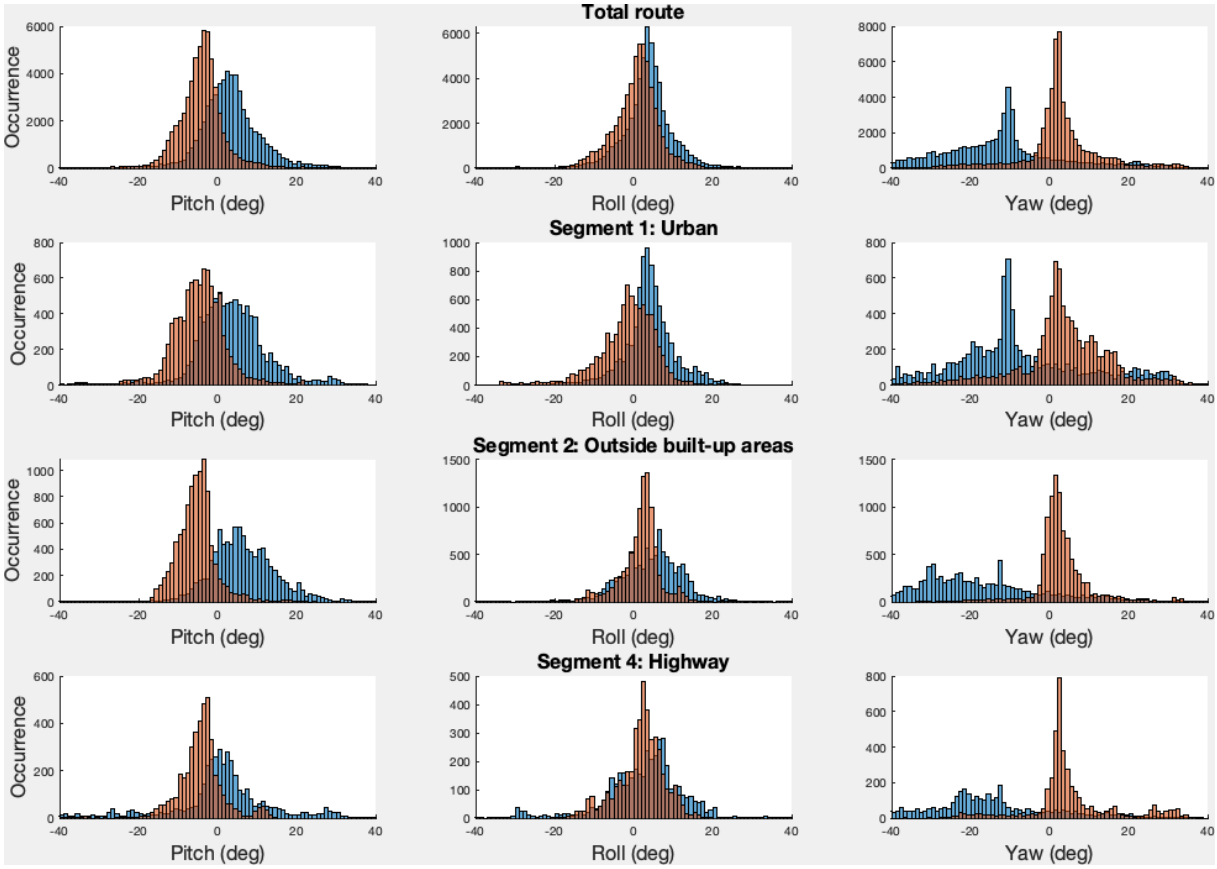
Total route
Occurrence
Pitch (deg)
Roll (deg)
Yaw (deg)
Segment 1: Urban
Segment 2: Outside built-up areas
Segment 4: Highway

E

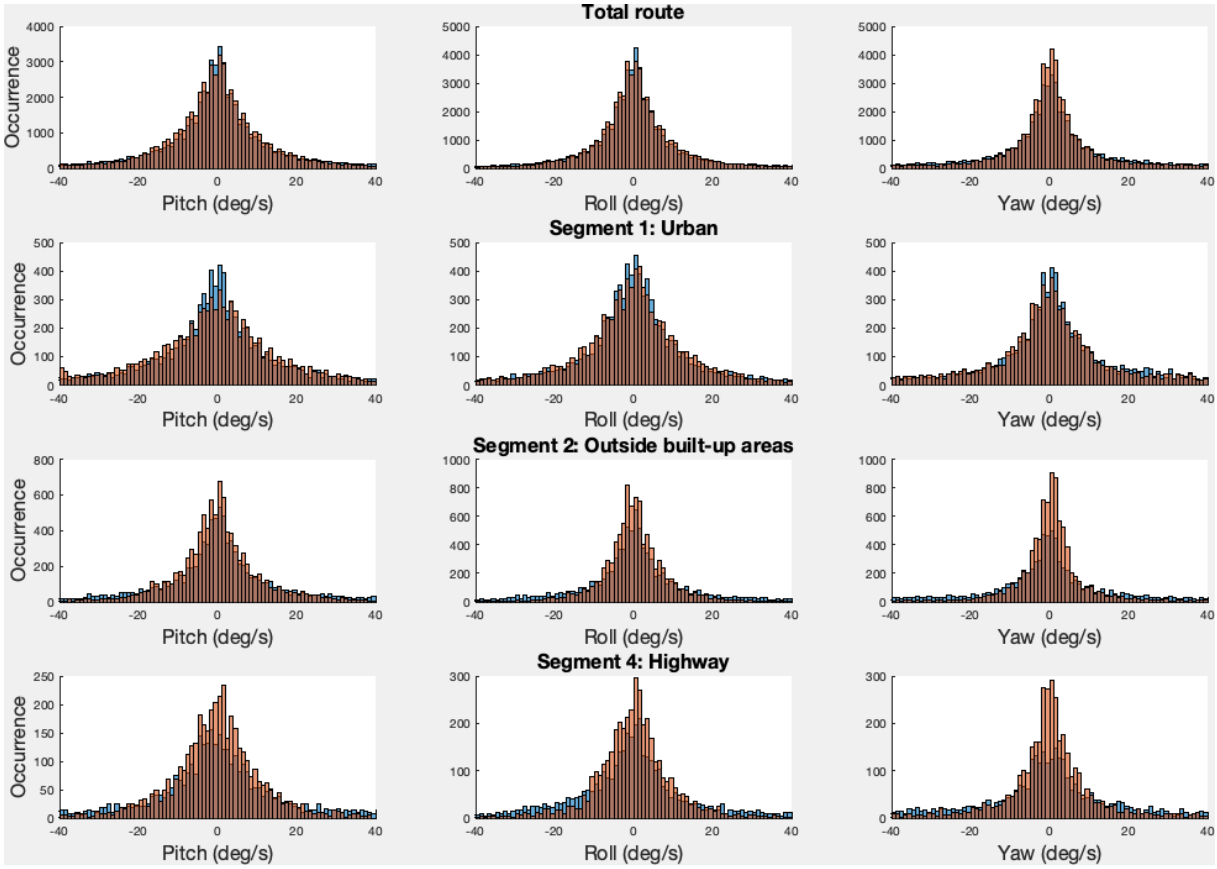
Total route
Occurrence
Pitch (deg/s)
Roll (deg/s)
Yaw (deg/s)
Segment 1: Urban
Segment 2: Outside built-up areas
Segment 4: Highway

Trip 25

D

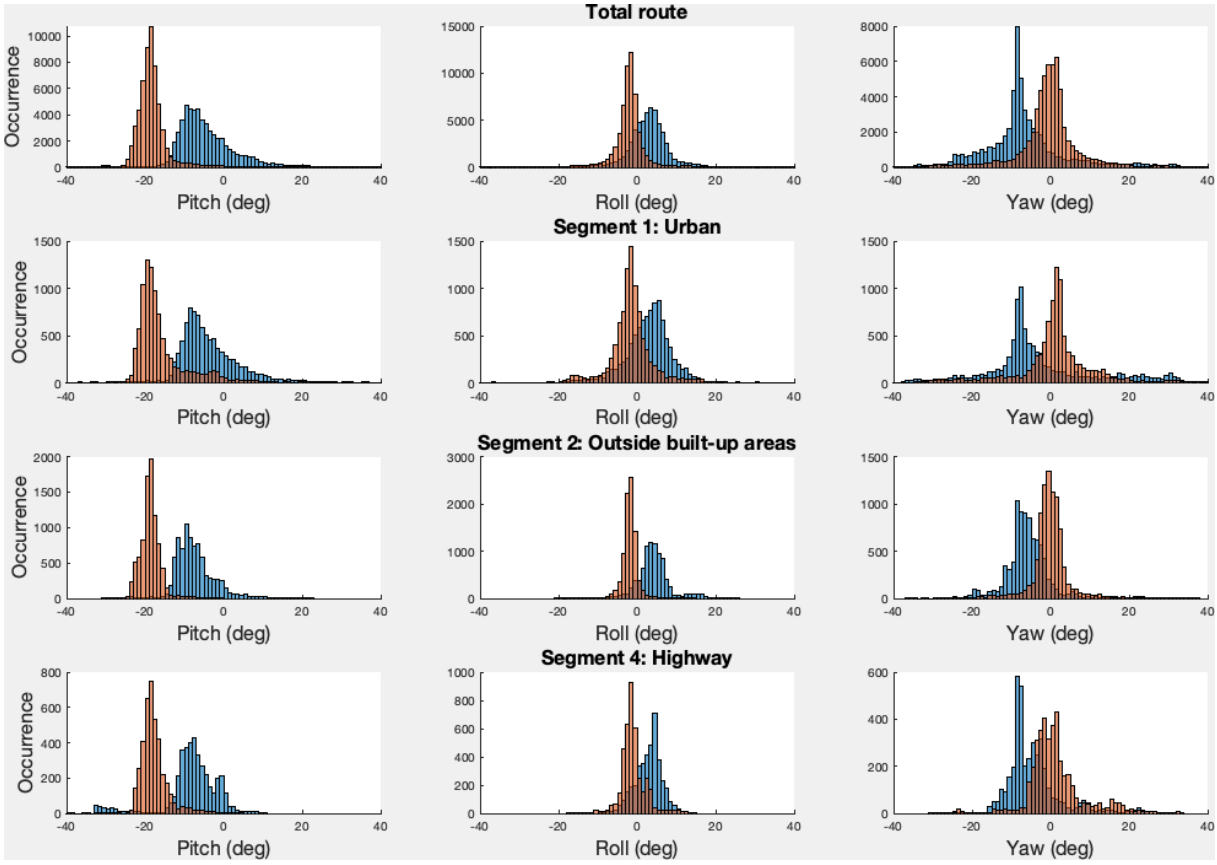
Total route
Occurrence
Pitch (deg)
Roll (deg)
Yaw (deg)
Segment 1: Urban
Segment 2: Outside built-up areas
Segment 4: Highway

E

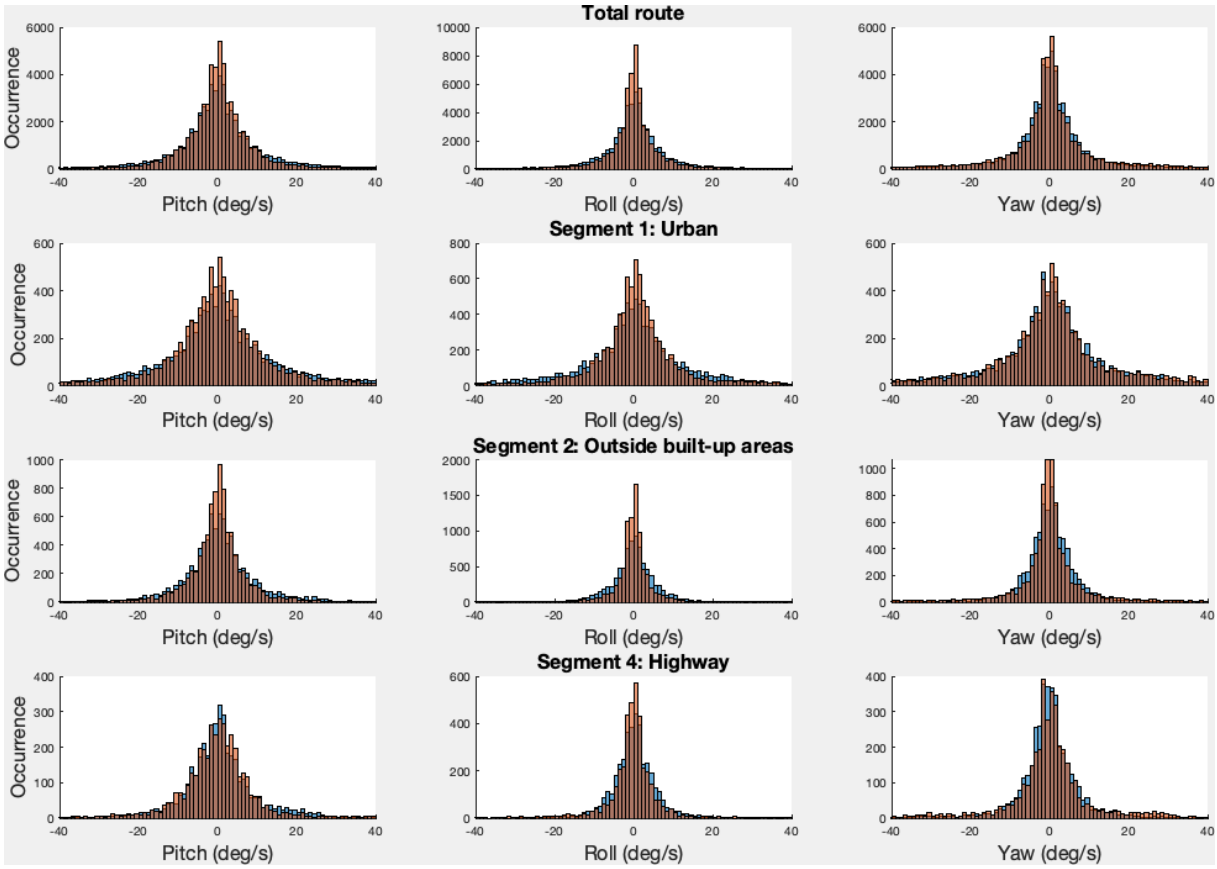
Total route
Occurrence
Pitch (deg/s)
Roll (deg/s)
Yaw (deg/s)
Segment 1: Urban
Segment 2: Outside built-up areas
Segment 4: Highway

Trip 26

D

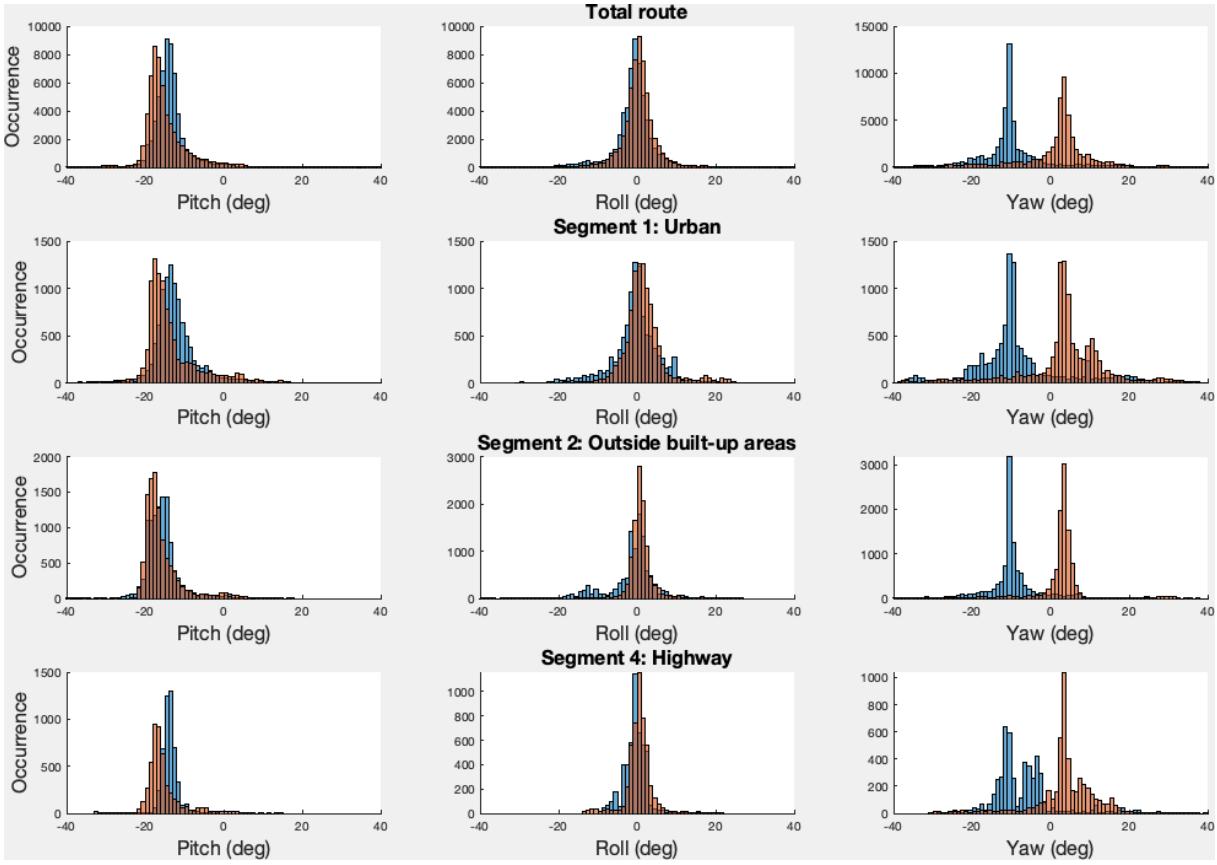
Total route
Occurrence
Pitch (deg)
Roll (deg)
Yaw (deg)
Segment 1: Urban
Occurrence
Pitch (deg)
Roll (deg)
Yaw (deg)
Segment 2: Outside built-up areas
Occurrence
Pitch (deg)
Roll (deg)
Yaw (deg)
Segment 4: Highway
Occurrence
Pitch (deg)
Roll (deg)
Yaw (deg)

E

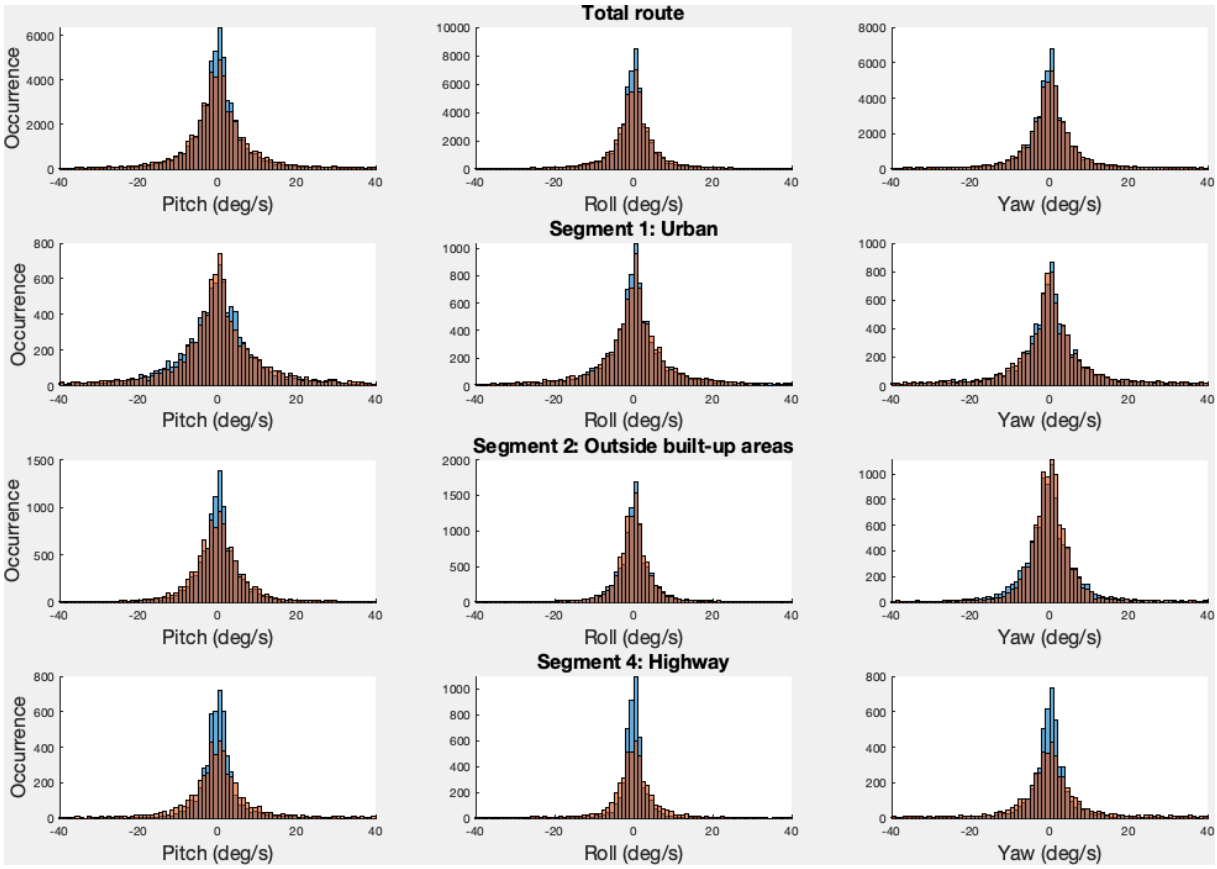
Total route
Occurrence
Pitch (deg/s)
Roll (deg/s)
Yaw (deg/s)
Segment 1: Urban
Occurrence
Pitch (deg/s)
Roll (deg/s)
Yaw (deg/s)
Segment 2: Outside built-up areas
Occurrence
Pitch (deg/s)
Roll (deg/s)
Yaw (deg/s)
Segment 4: Highway
Occurrence
Pitch (deg/s)
Roll (deg/s)
Yaw (deg/s)

Trip 28

D

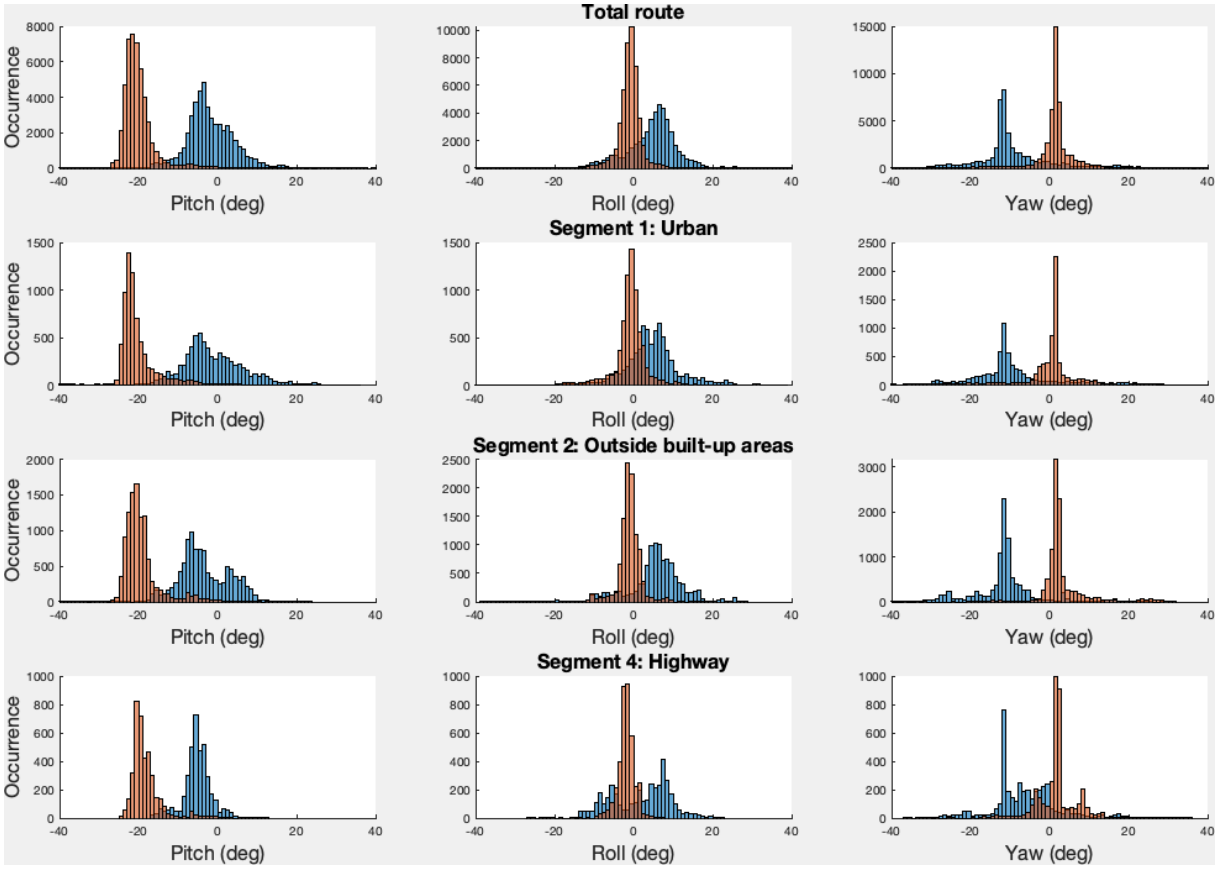
Total route
Occurrence
Pitch (deg)
Roll (deg)
Yaw (deg)
Segment 1: Urban
Segment 2: Outside built-up areas
Segment 4: Highway

E

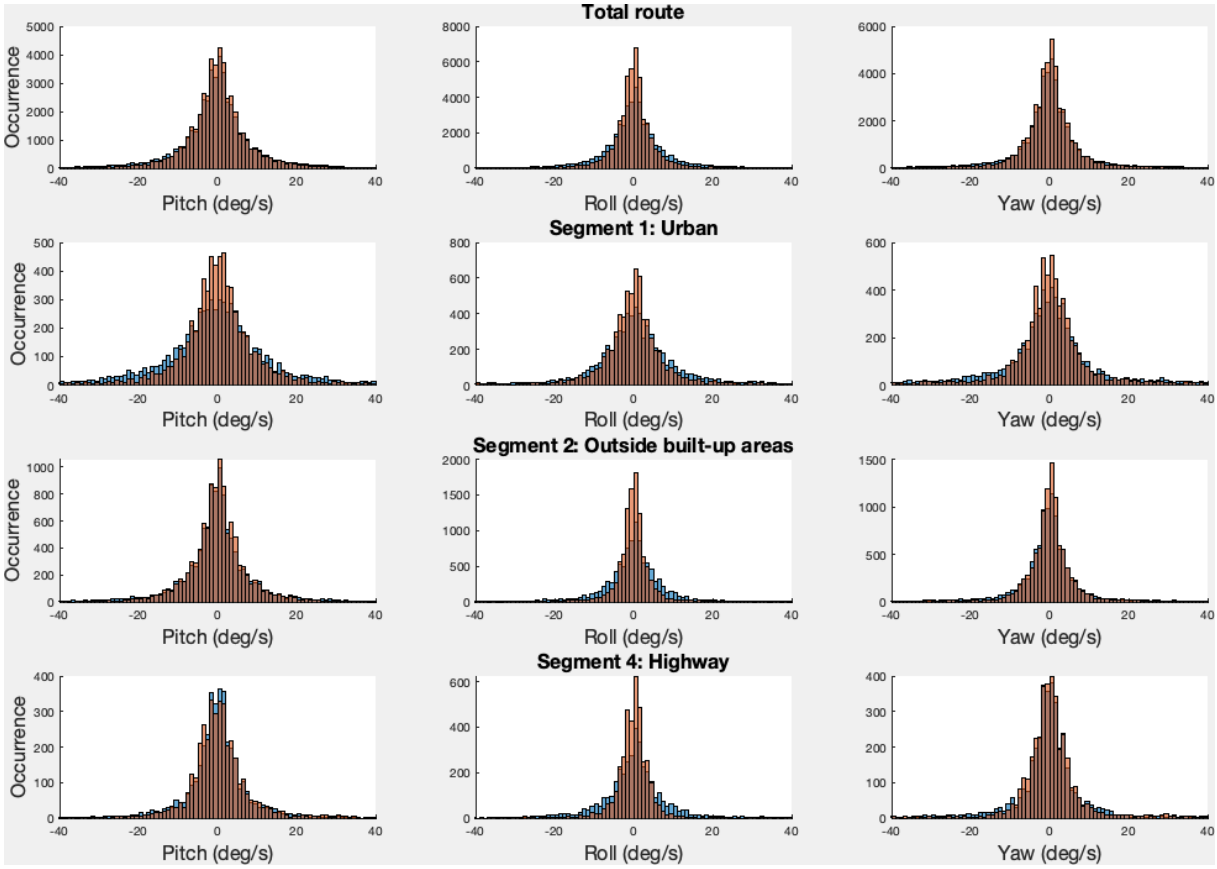
Total route
Occurrence
Pitch (deg/s)
Roll (deg/s)
Yaw (deg/s)
Segment 1: Urban
Segment 2: Outside built-up areas
Segment 4: Highway

Trip 29

D

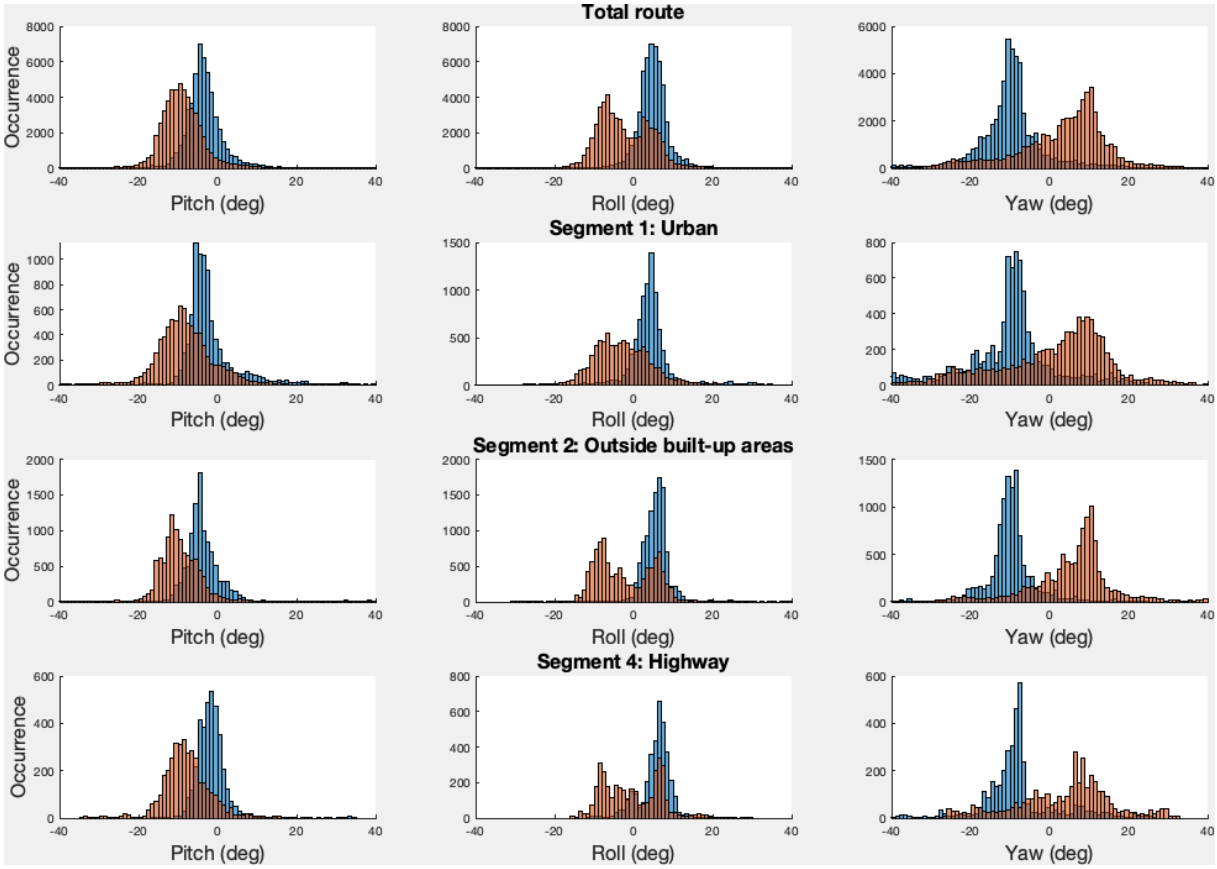
Total route
Segment 1: Urban
Segment 2: Outside built-up areas
Segment 4: Highway
Occurrence
Pitch (deg)
Roll (deg)
Yaw (deg)

E

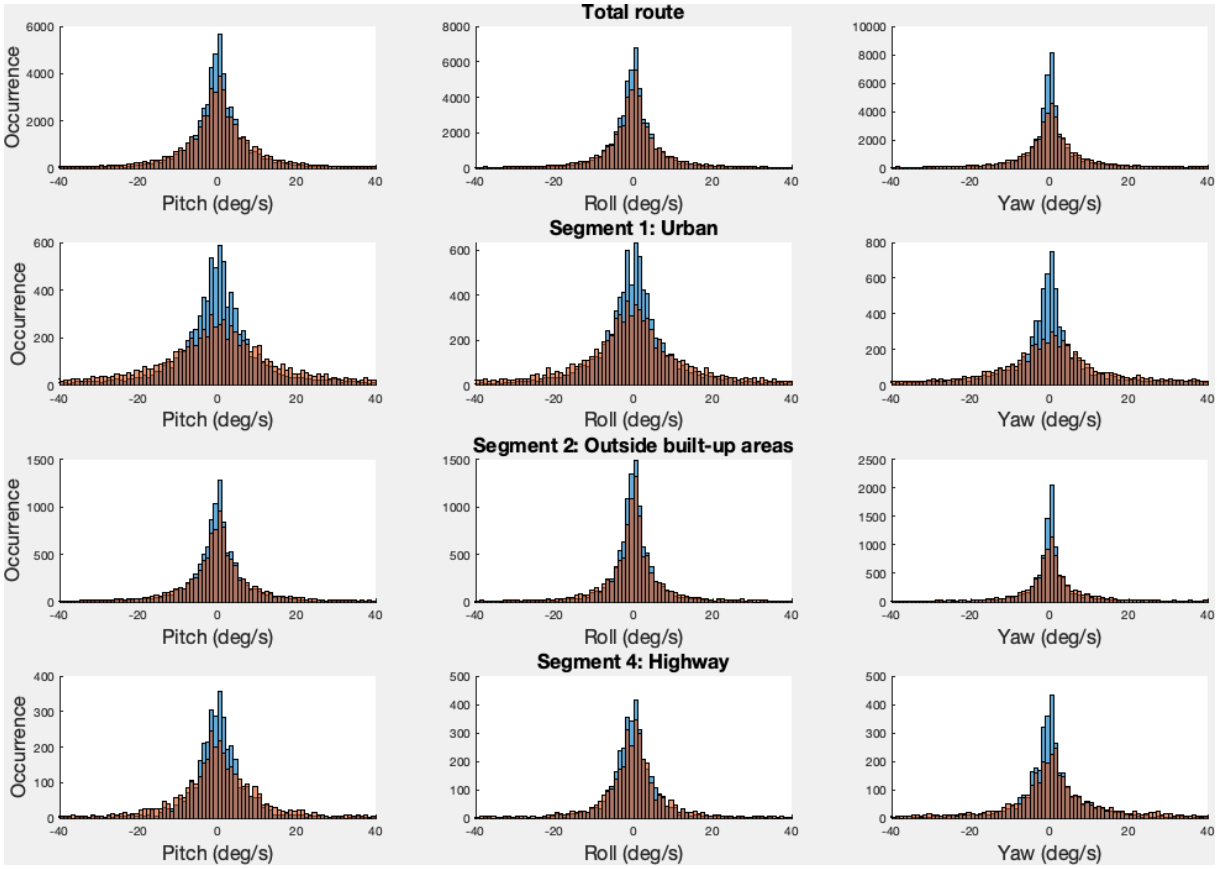
Total route
Segment 1: Urban
Segment 2: Outside built-up areas
Segment 4: Highway
Occurrence
Pitch (deg/s)
Roll (deg/s)
Yaw (deg/s)

Trip 30

D

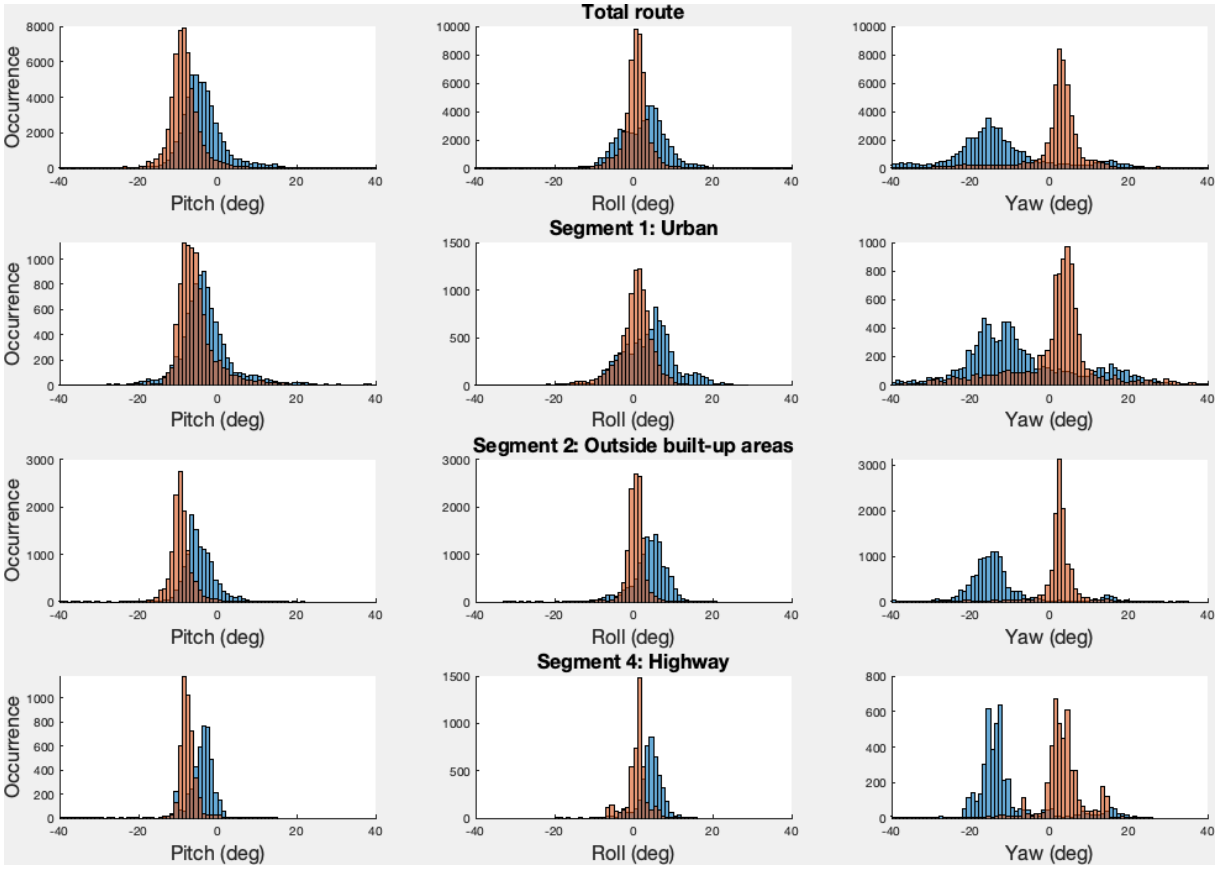
Total route
Segment 1: Urban
Segment 2: Outside built-up areas
Segment 4: Highway
Occurrence
Pitch (deg)
Roll (deg)
Yaw (deg)

E

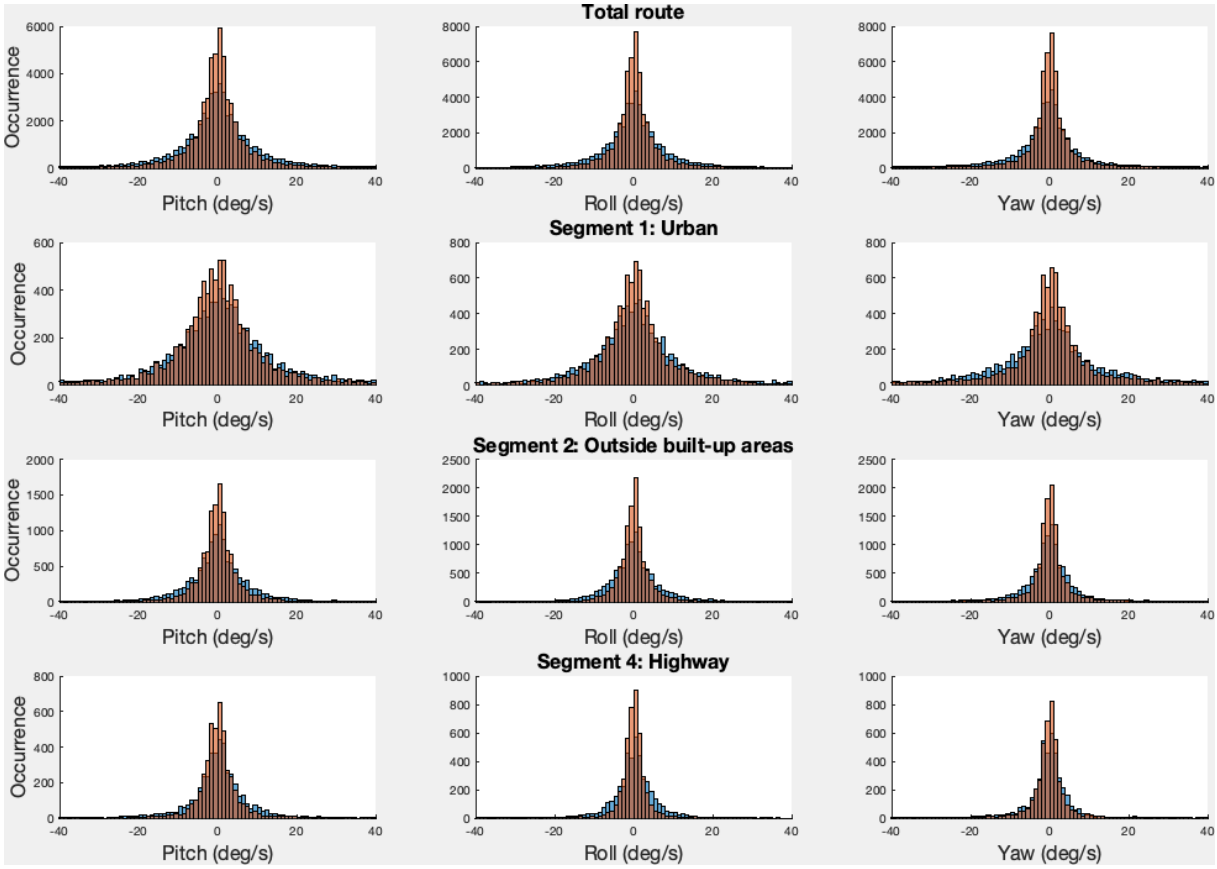
Total route
Segment 1: Urban
Segment 2: Outside built-up areas
Segment 4: Highway
Occurrence
Pitch (deg/s)
Roll (deg/s)
Yaw (deg/s)

Trip 31

D

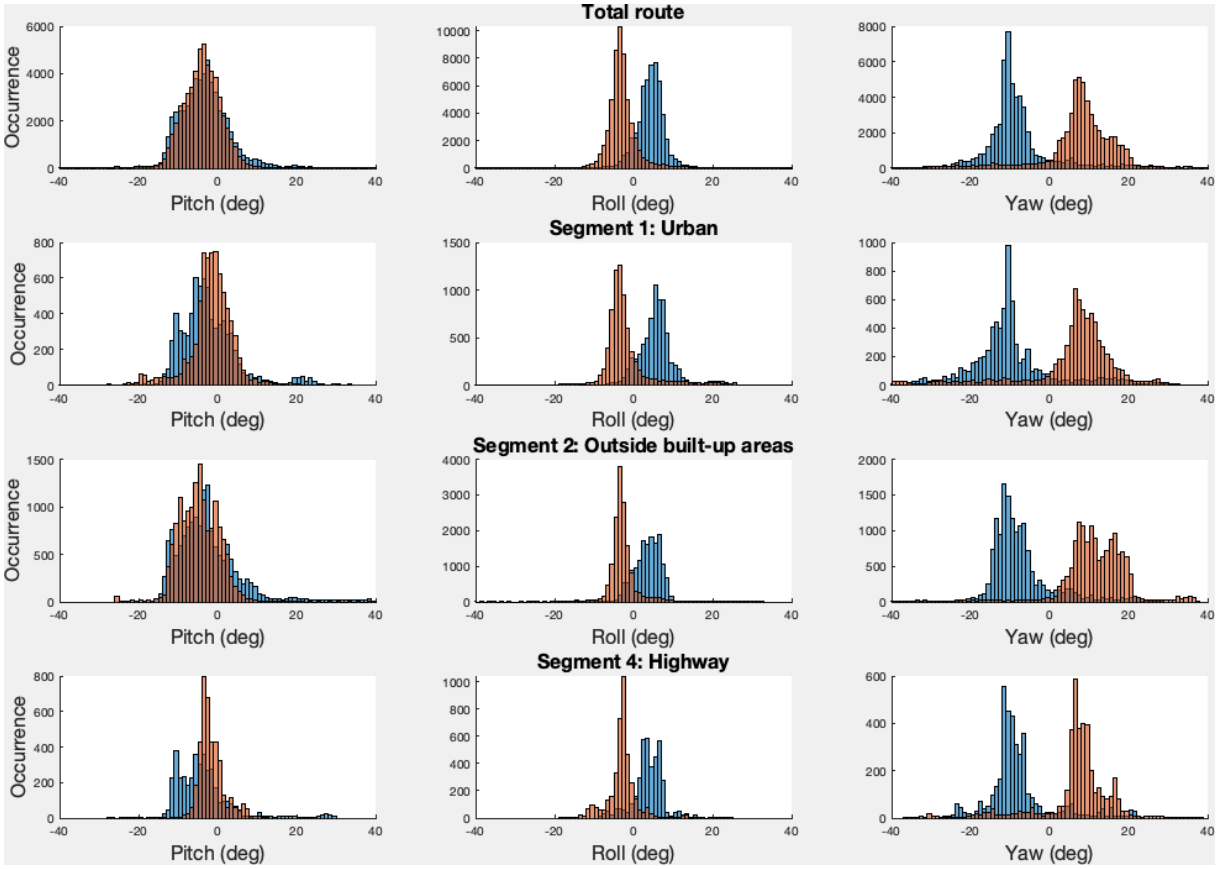
Total route
Segment 1: Urban
Segment 2: Outside built-up areas
Segment 4: Highway
Occurrence
Pitch (deg)
Roll (deg)
Yaw (deg)

E

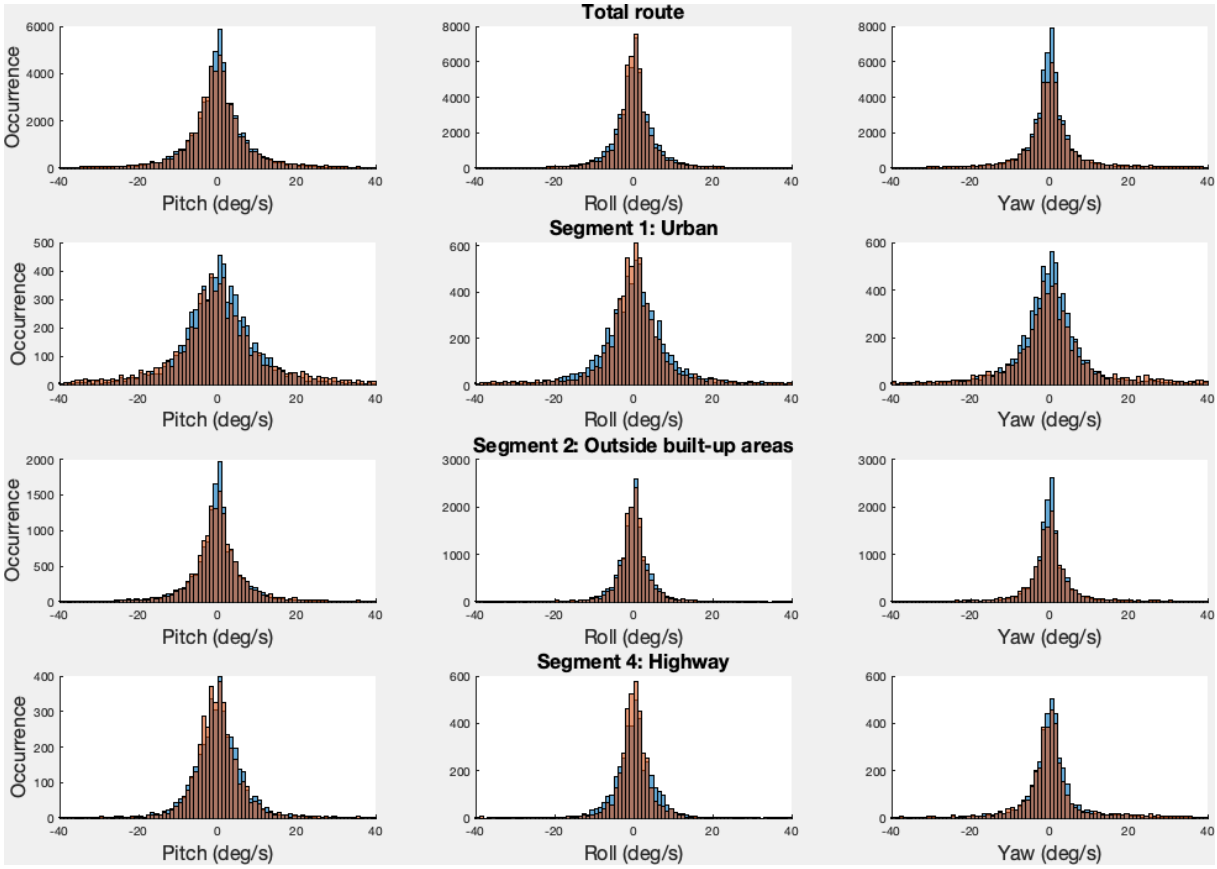
Total route
Segment 1: Urban
Segment 2: Outside built-up areas
Segment 4: Highway
Occurrence
Pitch (deg/s)
Roll (deg/s)
Yaw (deg/s)